GEM, a Generic Ecological Model for estuaries

model documentation

June 1997

T2087

delft hydraulics

GEM, a Generic Ecological Model for estuaries

J.G.C. Smits, M. Bokhorst, A.G. Brinkman,
P.M.J. Herman, P. Ruardij
H.L.A. Sonneveldt, M.W.M. van der Tol

delft hydraulics

delft hydraulics

CLIENT : National Institute for Coastal and Marine Management (RIKZ),
Rijkswaterstaat, Ministry of Public Works

TITLE : GEM, a Generic Ecological Model for estuaries

ABSTRACT : This documentation report describes the mathematical formulations of the model GEM. Following the introduction, which specifies the objectives of the model, an outline of DELWAQ-based GEM is given. The outline provides an overview of the main features of GEM, the processes included and their coherence.

The next chapters each deal with the formulations of a (group of) state variable(s), among which primary producers, primary consumers, detritus, nutrients (N,P,Si), dissolved oxygen and suspended sediment. An additional chapter discusses the numerical algorithms used in specific process modules. Finally, the demo application of GEM for the Western Scheldt is presented and discussed.

REFERENCES: Contract nr. RKZ-329
Letter, RIKZ/OSE/966547 (July 24, 1996)
Assignment in the framework of the Project ESTUARIUM*BOS

Subcontractors:
IBN-DLO, Letters RWM21058/T1058/up (July 22, 1996) and NWPR-AE (August 13, 1996)
NIOZ-DLO, Letters RWM21058/T1058/up (July 22, 1996) and NIOZ (August 12, 1996)
IBN-DLO, Letter RWM21058/T1058/up (July 22, 1996)

REV.	ORIGINATOR		DATE	REMARKS	REVIEWED BY		APPROVED BY	
1	J.G.C. Smits		May 1997	Incl. contributions IBN-DLO, NIOZ, RIKZ & NIOO-CEMO	F.J. Los		P.C.G. Glas	
	M. Bokhorst	MB						
	H.L.A. Sonneveldt	HA.						
2	J.G.C. Smits		June 1997		F.J. Los		P.C.G. Glas	

KEYWORD(S)	CONTENTS	STATUS
ecological model, estuaries, eutrophication, primary production, primary consumption, phytoplankton, detritus, nutrients	TEXT PAGES : 132 TABLES : 5 FIGURES : 24 APPENDICES : -	☐ PRELIMINARY ☐ DRAFT ■ FINAL

Contents

I Introduction

I.I Background

The development of the Generic Ecological Model for estuaries (GEM) started in 1994 as a joint undertaking of RIKZ, WL, NIOO-CEMO, NIOZ en IBN-DLO. RIKZ initiated the model development in order to take away difficulties in management of estuarine water quality and ecosystems, arising from a situation in which several models were being used for management policy analysis (RIKZ, 1993). Models like ECOWASP, Eems-Dollard Model, EMOWAD, ERSEM, moses, SMOES, ECOLUMN and DELWAQ (DBS, SAWES) had been developed separately by the above institutes and are very different regarding objectives, formulations, data requirements and capacities. Consequently, consensus on modelling efforts was generally lacking, which troubled the incorporation of forthcoming conclusions in policy analysis. Moreover, development and maintenance of so many complicated models proofed to be very cumbersome and costly. Objectives and data requirements being so diverse prevented comprehensive yet optimized field monitoring in Dutch estuaries.

Three scientific workshops provided the foundation of the functional design of GEM that was produced in the first stage of the project (WL et al., 1995a). Although consensus could be established among the participants regarding state-of-the-art formulation of many parts of GEM, some differences in scientific judgement remained. These relate to concepts and algorithms for a) primary production and competition of algae species and b) nutrient processes in the sediment. It was therefore decided, to provide GEM with parallel modules for these subjects, from which a user may choose according to his needs and preferences. Although essentially different in approach, the options would have to be tuned in order to allow intercomparison. This implies that formulations must be conceptionally identical, if there are no specific, important reasons for them to be different.

RIKZ committed DELFT HYDRAULICS in 1995 to construct a technical design for GEM on the basis of the functional design, describing functionality, state variables and main starting points and concepts for the formulation of ecological processes and mass transport (WL, 1995b). The technical design makes a distinction between the basis of the model, that would have to be built within the short and mid terms, and extensions, that may be established in the long run.

Processes in GEM are meant to be formulated in a generic way. They can be implemented in any simulation package. For practical reason it had been decided, that DELWAQ would be the modelling framework for GEM. DELWAQ is DELFT HYDRAULICS' simulation package for water and sediment quality (WL, 1995c/d). It has core modules for the calculation of mass transport and mass balances in interacting compartments of a natural aquatic system. Other processes than advection and dispersion that determine water quality and ecosystem components can be added to the model from a so called user-defined process routine library. The process formulations are described in full detail in this report.

The third stage of model development concerned the detailed formulation and programming of a pilot-GEM. Once again a scientific workshop was held on the details of the formulations. Main aim of the meeting was to tune the activities and products of the participants in the project. The activities resulted in the present documentation report. Whenever possible and appropriate, use was made of parts of existing models. Throughout the development of GEM, DELFT HYDRAULICS acted as main contractor for RIKZ, which implied having responsibility for organization of the project. All participating institutes contributed to the elaboration of concepts and formulations. GEM is therefore to be considered a consensus model. However, scientific responsibilities during the formulation stage have for practical reasons been divided among the participating institutes as follows:

- phytoplankton: DELFT HYDRAULICS (optimization of production approach), RIKZ (Monod-type kinetics approach);
- microphytobenthos: NIOO-CEMO;
- detritus: IBN-DLO and DELFT HYDRAULICS;
- primary consumers: DELFT HYDRAULICS;
- nutrient and water quality processes: DELFT HYDRAULICS; and
- nutrient processes in the sediment: NIOZ (estimated gradient approach), DELFT HYDRAULICS (dynamic gradient approach).

RIKZ funded the development of GEM for roughly 75%. NIOZ, NIOO-CEMO, IBN-DLO and WL shared the remaining part of the cost.

1.2 Objectives and scope of application

GEM describes the behaviour of nutrients, organic matter, primary producers and primary consumers in estuaries. Water quality parameters that affect the principle state variables are simulated additionally. GEM's main objectives are:

- providing of a unified and widely accepted ecosystem model for policy analysis of the management of estuaries;
- providing of a platform for further development of consensus modelling of water quality and ecological components in Dutch estuarine systems; and
- invoking of enhanced scientific cooperation between Dutch institutes involved in estuarine research, consultancy and management.

Because of the desired broad applicability of GEM, an estuary is defined in the widest possible way as a brackish or salt water body interfacing land and sea. This definition encompasses:

- river delta water bodies such as the Western Scheldt and the Eems-Dollard;
- sea branches such as the Eastern Scheldt;
- stagnant former sea branches such as Lake Grevelingen and Lake Vere; and
- shallow coastal seas with mudflats such as the Waddensea.

These ecosystems have very diverse features. Applicability of GEM on all of them requires a generic, flexible model structure. Maximal flexibility has been obtained by making the model both input defined and input driven.

Problems which can be addressed with the present version of GEM relate to:

- input, retention and cycling of nutrients and organic matter;
- effects of eutrophication on primary production, algae species composition, and primary consumption;
- effects of disturbances caused by the removal of grazers, turbidity in- or decrease, changes in residence time, salinity, morphology and climate, meteorological variability, etc. on primary production and the comparison of effects in different estuaries;
- structuring and integration of field data;
- estimation of carrying-capacity for higher trophic levels; and
- the model as research object.

1.3 Stage of development

The pilot-GEM has been implemented in DELWAQ as a somewhat simplified first version of the eventual, comprehensive model. According to the functional and technical designs, the effects of the activity of bacteria and oligochaetes are modelled implicitly in the decomposition of organic matter. However, important restrictions of the pilot-GEM compared to the designs are:

- Macrophytes, such as Ulva and Zostera, have not been included.
- Grazers, that is micro- and mesozooplankton and various types of filter feeders, such as coccels and mussels, are not simulated dynamically but included as forcing functions. Age classes can be taken into account by introducing a separate species into the forcing function for each age class. Hyperbenthos is ignored.
- GEMSED, one of the three sediment-water interaction modules and described in this report, has not yet been implemented.
- The model is suitable for 1-DH and 2-DH simulations. Vertical stratification was not taken into account. Moreover, compartments should not run dry. Although technically possible in DELWAQ, process formulations do not apply to that condition.
- The proposed innovative mass transport schemes, in which aggregation over time and space is different between the mass transport module and the ecological module, have not been implemented.

The restrictions with respect to primary producers and consumers implicate that the pilot-GEM is not suitable for analysis of the ecosystem concerning dynamic behaviour of consumers. Moreover, the model is limited in the prediction of shifts in primary production between various functional groups.

Considering mass transport schemes it must be noticed that GEM does not produce water flow patterns by itself. Water flow calculated with a separate hydrodynamical model such as WAQUA or TRISULA has to be made part of the input for GEM (RIKZ, 1996, DELFT HYDRAULICS, 1996a). Aggregation of water flow over space and time in preparing tide-averaged input is possible with a tool called DIDO (DELFT HYDRAULICS, 1996b). In addition to this option, the innovative transport schemes would facilitate intra-tidal computations with a very fine grid for mass transport. Although technically possible for a grid that is equally fine for transport and processes, it is not recommended to perform this type of simulations with the present model. As mentioned above, process formulations have not (yet) been optimized from the viewpoint of intra-tidal computations, and there is virtually no experience with intra-tidal simulations, in which a part of the compartments run dry during low tide.

Moreover, the resulting computational burden may be unacceptably large. It is expected that the above limitations will be taken away in future versions of GEM.

Two examples of the conceptual inappropriateness of the pilot-GEM for intra-tidal simulations are the following. Both benthic and pelagic algae have an ability to take up nutrients during the night and to use them for primary production during the day. This phenomenon would have to be described with Droop-kinetics in stead of the time-averaged growth kinetics used in the pilot-GEM (Droop, 1973). The resuspension of sediment depends on flow velocity peaks during the tidal cycle. These peak values in stead of time-averaged value would have to be used in GEM to describe accurately high suspended solids concentrations affecting primary production through extinction.

1.4 About this report

The documentation report contains a full description of the process formulations and the algorithms implemented in GEM. This is preceded by chapter 2, in which the main features of DELWAQ are summarized, as this modelling package forms the basis of GEM. This chapter also presents an overview of the state variables and the processes simulated in GEM. Given the complex and detailed nature of this documentation report, it is recommended to read this chapter first.

Each of the chapters on process formulations has the same structure. An introductory section summarizes the main assumptions and boundary conditions. At the same time it is illuminated how processes add up to the change of a state variable. The sections that follow the introduction deal with a specific process or a group of closely related processes. In some cases processes have been grouped in previously constructed modules such as BLOOM and SWITCH. All processes give a change of concentration per units of volume and time. Such a change is called a flux, and is invariably indicated with the symbol F. Process fluxes are output of process routines and are delivered to the core routines of DELWAQ.

The chapters on processes have been arranged more or less according to the hierarchy of these processes. Chapter 3 deals with the primary production of phytoplankton and microphytobenthos. Section 3.3 contains only a brief summary of BLOOM. The report refers to the existing literature which contains descriptions in full detail. Algae provide food to grazers, described in chapter 4. The mortality of algae as well as grazing leads to the production of detritus, the production and decomposition of which are illuminated in chapter 5. The cycle of organic matter is accompanied by parallel cycles of nutrients and dissolved oxygen. Chapters 6 and 7 present the formulations for respectively those substances. Chapter 8 deals with the autonomous behaviour of inorganic suspended sediment, which imposes conditions on all the other state variables.

Chapter 9 briefly describes algorithms that have been implemented in DELWAQ and in various modules of GEM. Algorithms have to do with numerical integration, fractional step calculation of fluxes, iteration, optimization, and mass conservation.

Finally, the demo-application of GEM on the Western Scheldt is discussed in chapter 10. Preliminary results of the model are evaluated, which leads to some conclusions on priorities and options for further model development.

This documentation report is not a manual. The user of GEM is referred to the DELWAQ manuals (WL, 1995c/d) for details on:

- structure and contents of input files;
- names of parameters, that have to be used in input files;
- schematization of a water body in space and time;
- formulations regarding the syntax in which they were implemented in process routines; and
- input options and numerical algorithms available in DELWAQ.

The report was composed and edited by J.G.C. Smits. F.J. Los provided expertise knowledge with respect to the phytoplankton modules, BLOOM in particular. The following authors contributed to this documentation report:

- M. Bokhorst (DELWAQ, chapter 2 / section 9.2; phytoplankton, sections 3.3 and 9.1; consumers, chapter 4);
- A.G. Brinkman (detritus, chapter 5);
- P.M.J. Herman (microphytobenthos, section 3.4);
- P. Ruardij (nutrients, section 6.5.1 / 9.2);
- J.G.C. Smits (introduction, chapter 1; nutrients, chapter 6 / section 9.3; demo application, chapter 10);
- H.L.A. Sonneveldt (dissolved oxygen, chapter 7; suspended sediment, chapter 8; demo application, chapter 10); and
- M.W.M. van der Tol (phytoplankton, section 3.2).

The report was reviewed by F.J. Los. However, all authors are responsible for the scientific soundness of their own contributions.

2 Outlines of GEM

2.1 DELWAQ framework

2.1.1 Introduction

GEM is set up as an application of DELWAQ, available for PC's and workstations. Transport of substances is dealt with by the standard DELWAQ software, whereas the water quality and ecological processes are specific for GEM. This section gives an introduction to DELWAQ, a water quality modelling framework with an extensive set of options, features and different modes for usage. Detailed information is provided in the User's Manual, the Technical Reference Manual and the Systems Reference. (DELFT HYDRAULICS, 1995c and 1995d).

2.1.2 Principles and structure

DELWAQ simulates the transport and transformation of substances by numerically solving a set of coupled advection-diffusion equations. The advection-diffusion equations are coupled through source (or sink) terms which describe the transformation of substances due to water quality and/or ecological processes. The total transformation rate of a substance is determined by the sum of fluxes as defined by the various water quality and ecological processes. These fluxes are discussed more in detail in section 2.4 to 2.7. A precise definition of the fluxes is provided in chapters 3 to 8.

The calculation of the concentration patterns as a result of the process and transport fluxes is illustrated by figure 2.1. Figure 2.2 gives an overview of the basic structure of DELWAQ with its input and output files.

2.1.3 Schematisation in space

In order to solve the advection-equation equation numerically the study area must be schematised into computational elements representing finite homogeneous volumes of water containing dissolved and suspended material. The segments (= computational elements) may have any shape and any degree of detail and may expand in any direction. Between the computational elements there is exchange of matter due to advective flow of water or mixing processes. By defining links a segment may exchange matter with any other segment. The DELWAQ segments have a number and each link is defined by a pair of segment numbers.

The DELWAQ segments are characterised by a volume (in m^3), an exchange area (in m^2) and an exchange length (in m). The exchange length is used for the definition of the distances along the links and is used to calculate dispersive transport. The exchange area is used to calculate advective transport.

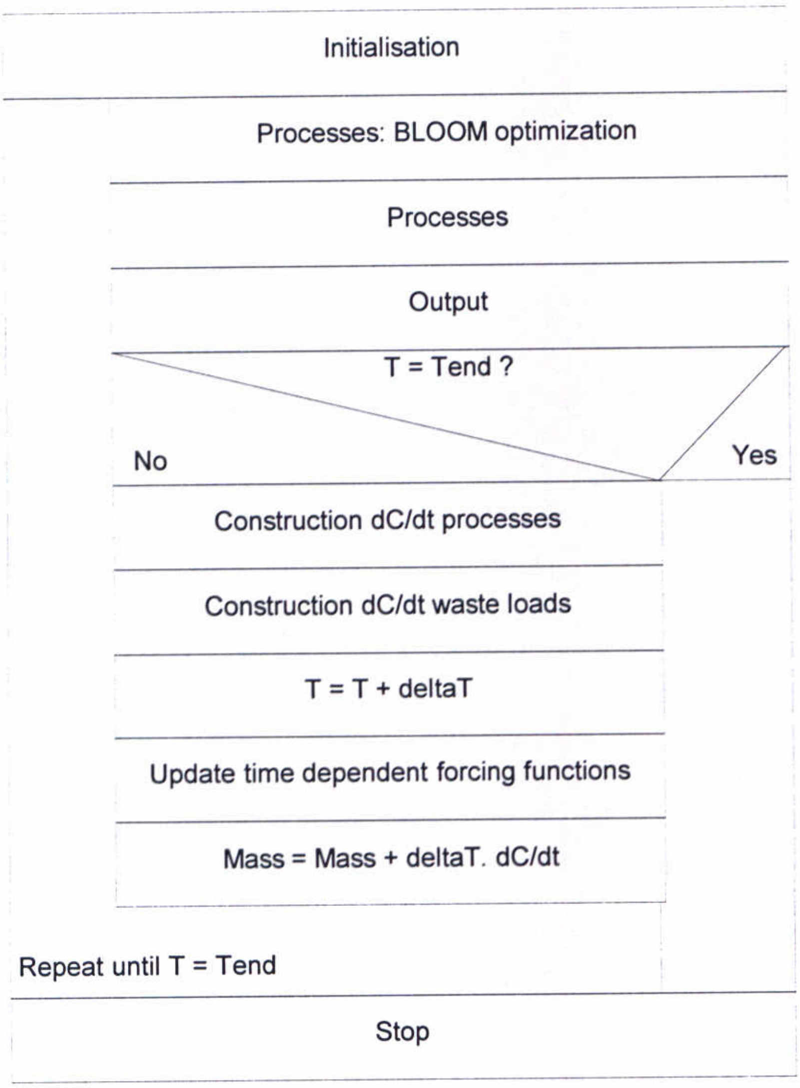

Figure 2.1 The calculation procedure of transport and processes in GEM within the framework of DELWAQ

2.1.4 Important options

Below are some important options that DELWAQ offers:

- The modeller can choose from a list of numerical schemes on the basis of the characteristics of the problem and trade-off considerations like computation time, accuracy and computer resource limitations.
- Flexible interfacing with hydrodynamic models such as WAQUA. Flexible aggregation in time and space of the results of hydrodynamic modelling with the tool DIDO.
- All water quality and ecological processes as defined in GEM are stored in a generic process-library. This process-library allows for the selection of pre-defined processes.
- The modelled processes involve constant, spatially varying, time varying and time and spatially varying parameters. DELWAQ provides a convenient way to import the process-parameters into the model. Time functions are evaluated given time and passed to the water quality and ecological processes.

- To derive information from the model DELWAQ provides tools to retrieve almost any information (including balances) in a flexible way.

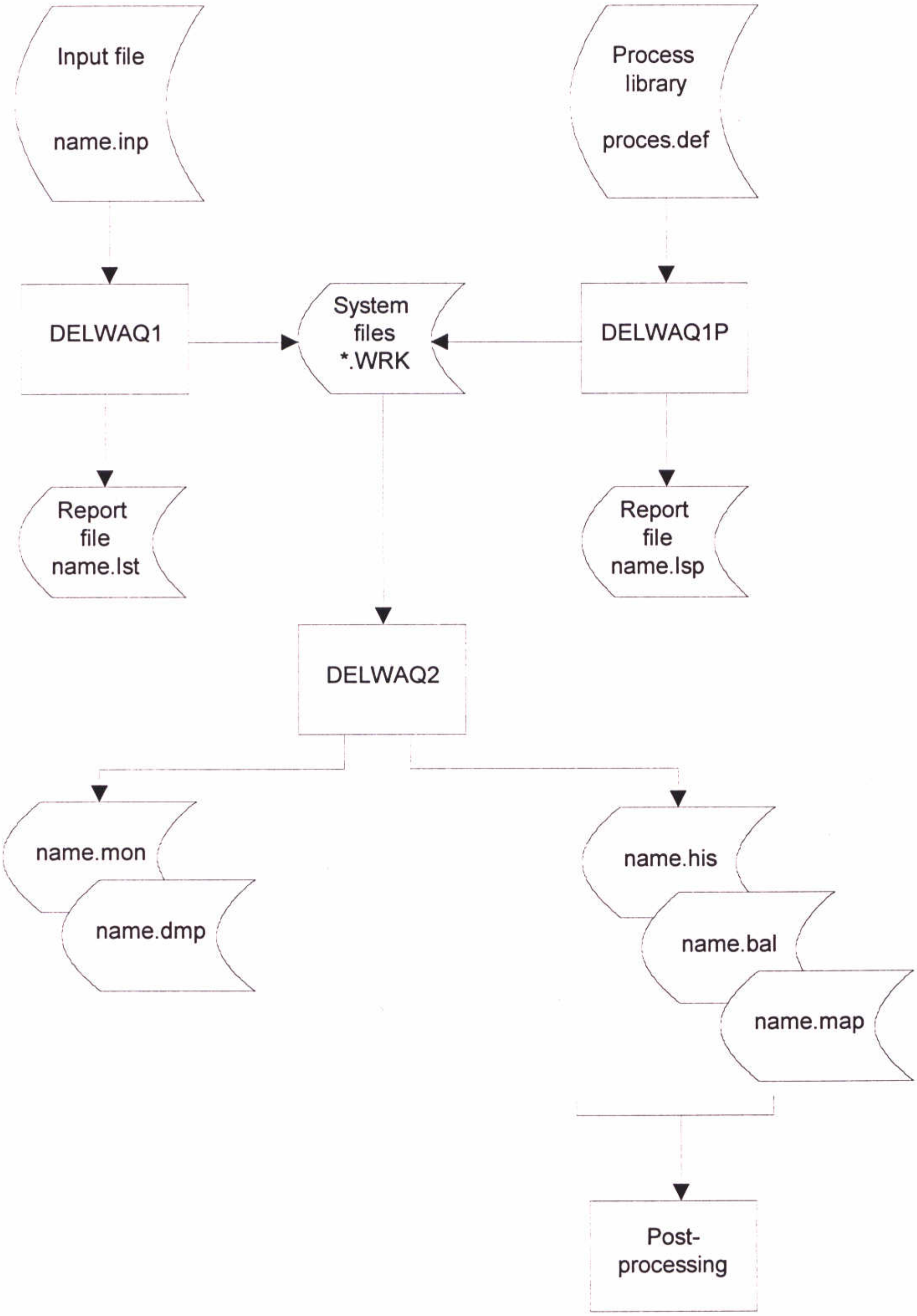

Figure 2.2 Basic structure of DELWAQ including input and output files

2.1.5 Input principles

DELWAQ input is provided in an ASCII file. The input file is divided into 9 sequential input blocks as summarised below:

1. *Identification*
   Specification of the identification of the model and dimensioning of the problem.

2. *Timers and general information*
   Specification of the state variables, selection of an integration options and model-timing.

3. *Schematisation*
   Specification of the number of segments and their volume.

4. *Transport*
   In this block all information related to the exchange area's is specified (flows, exchange area's, dispersion length's etc.) Also a so called "pointer table" must be provided. This table defines the link between segments and exchanges.

5. *Boundary conditions*
   Specification of the boundary conditions.

6. *Loads*
   Specification of the waste loads.

7. *Process parameters*
   There are 4 types of process parameters that may be specified:
   - Constants
     Values that hold for all computational elements and time steps
   - Parameters
     Values that differ for the computational elements but do not vary in time.
   - Functions
     Values that hold for all computational elements but vary in time.
   - Segment functions
     Values that differ for the computational elements and vary in time.

8. *Initial conditions*
   Specification of the initial concentrations.

9. *Output specification*
   Specification of the model output.

Basically the program accepts input through one input file. For larger model area's it may be useful to prepare certain parts of the input file with a separate program. It may also be useful to split the input file in a part that will not change for many subsequent applications (e.g. hydrodynamics) and in a part that will change frequently (e.g. waste loads, process parameters). DELWAQ enables the use of so called "multiple input files" for reasons of convenience. Some of the information can be supplied in binary files (e.g. hydrodynamics, boundary conditions).

2.2 Water flow and mass transport

2.2.1 Advection and dispersion

DELWAQ simulates the transport of substances by solving the advection-diffusion equation numerically:

$$\frac{\partial c}{\partial t}-\frac{\partial}{\partial x}(D_x-u_xc)-\frac{\partial}{\partial y}(D_y-u_yc)-\frac{\partial}{\partial z}(D_z-u_zc)=0 \tag{2.1}$$

DELWAQ does not simulate hydrodynamics. In the GEM framework DELWAQ interfaces with the hydrodynamic models WAQUA and TRISULA. The coupling programs WAQUA-DELWAQ and TRISULA-DELWAQ provides the necessary DELWAQ input, such as flows and volumes (optionally aggregated in time). These input may be aggregated in space using the tool DIDO.

2.2.2 Import and export of substances

Import or export of substances through transport may be due to:

- advective and/or dispersive transport over open boundaries; and
- loadings to the system.

2.3 Water quality and ecological processes

2.3.1 State variables and forcing functions

Embedded in the DELWAQ framework GEM provides a flexible modelling tool. Any state variable can easily be redefined as a forcing function simply by changing it to a constant, parameter, function or segment function in the DELWAQ input file (and vice versa). This allows for a modelling approach whereby gradually the complexity of the model is increased.

Grazing by zooplankton and suspension feeders is standard a forcing function and cannot be modelled dynamically (see chapter 4).

The concentration of the state variables changes due to both transport (as discussed in section 2.2) and transformation processes (water quality and ecological processes). The next section discusses how the transformation processes are embedded within the DELWAQ framework.

In pilot-GEM a distinction is made between the following state variables:

- *Nutrients*
    - ammonium, nitrate and nitrogen in organisms and detritus
    - dissolved phosphate, adsorbed phosphate, precipitated phosphate and phosphate in organisms and detritus
    - dissolved silicate, opal silicate and silicate in organisms

- *Primary producers*
    - marine diatoms
    - marine non-diatoms namely dinoflagellates, other flagellates and *Phaeocystis*
    - fresh water diatoms
    - fresh water non-diatoms namely flagellates
    - microphytobenthos

- *Organic matter*
    - organic matter in the various organisms (per functional group)
    - two decomposable detritus fractions
    - two refractory detritus fractions (particulate and dissolved)

- *Remaining substances*
    - dissolved oxygen
    - suspended matter
    - chloride

Primary consumers are incorporated into the pilot-GEM as forcing functions:

- *Primary consumers*
    - micro- and meso zooplankton
    - suspension feeders

The pilot GEM deals with variable nutrient to carbon ratios for detritus. Therefore every state variable of the functional group detritus is subdivided into three groups (C,N,P).

2.3.2 Processes and parameters

In order to take the transformation of the state variables due to water quality and/or ecological processes into account an extra source (or sink) term is added to the advection-diffusion equation:

$$\frac{\partial c}{\partial t}-\frac{\partial}{\partial x}(D_x-u_x c)-\frac{\partial}{\partial y}(D_y-u_y c)-\frac{\partial}{\partial z}(D_z-u_z c)=F(c,t) \tag{2.2}$$

The transformation rate of a state variable F(c,t) is composed of the fluxes calculated by the water quality or ecological processes involved.

All water quality and ecological processes are stored in a generic process library. It contains process-definition files and generic FORTRAN modules library. Each process uses a module, a generic FORTRAN subroutine, and a process definition file to calculate the process flux. The process definition file defines:

- the link between the process and the appropriate module and
- the process input and output (fluxes).

2.3.3 Important input rules

The principle for the selection of processes is the following: a pre-processor scans the DELWAQ input file for reserved names of state variables that are present in the process-library. If a state variable is recognised, all the processes found in the library acting on that state variable are tagged. If all necessary input for a process is available, the process is actually switched on. The names of the input items are fixed and may be supplied at any location within the DELWAQ-input file (f.i. as a constant or a space and time varying parameter). Detailed information on the process selection mechanism is given in the DELWAQ user's manual.

2.4 Budgets

In the next sections the budgets of carbon, nutrients (N, P and Si), oxygen and suspended sediment as considered in GEM are discussed. The construction of the budgets is illustrated by Figure 2.3 to Figure 2.10. The legend of the figures is given in Table 2.1.

■	statevariable (dissolved)
■	statevariable (particulate)
▱	forcing function (constant, f(place), f(time), f(place,time))
──▶	first order flux
-------▷	transportflux (sedimentation, resuspension, diffusio
─×─▶	flux divided over more than one state variable
─⧗─▶	function determining a process flux
- - -▶	combined transport and (bio)chemical flux
──▶▶	chemical flux (dissolution, precipitation, adsorption)
S	settling
R	resuspension
D	diffusion
B	burial
G	digging

Table 2-1 Legend of Figure 2.3 to Figure 2.10.

2.4.1 The organic carbon budget

The organic carbon budget is affected by the processes related to:

- the primary production of biomass,
- mortality of phytoplankton and microphytobenthos,
- the mineralisation of organic material and
- grazing by primary consumers.

Primary producers

The following processes related to primary producers affect the organic carbon budget (see Figure 2.3):

- *Primary production*
  - Net uptake of nutrients (3)
- *Mortality*
  - production of detritus (1A)
  - release of nutrients (autolysis) (1B)
  - settling and mortality phytoplankton (6)
  - resuspension and mortality microphytobenthos (7)
- *Grazing*
  - Grazing by zooplankton and zoobenthos (5A)

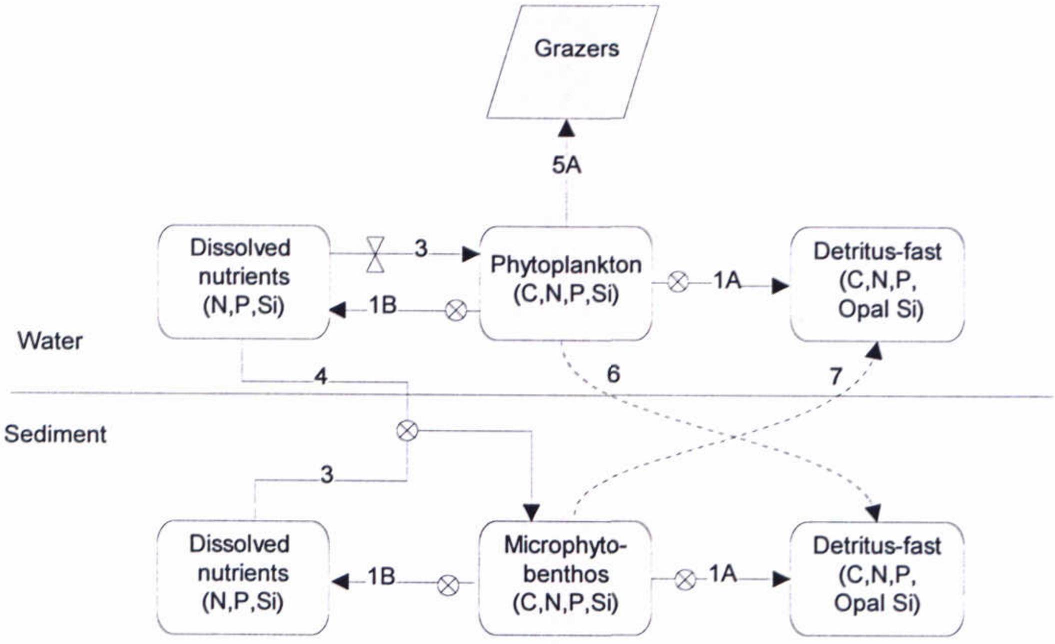

Figure 2.3 Cycling of organic matter: processes related to primary producers.

Detritus

The following processes related to detritus affect the organic carbon budget (see Figure 2.4):

- *Mortality*
  - Production of detritus by mortality of phytoplankton (1A)
  - Production of detritus by mortality of primary consumers (8B)
  - Sedimentation and mortality of phytoplankton (6)
- *Mineralisation*
  - Production of nutrients (2A)
  - Production of particulate organic matter (2B)
  - Production of dissolved organic matter (2C)
- *Grazing*
  - Grazing of detritus (5B)
- *Transport*

  For all particulate detritus:
  - burial in sediment (B)
  - digging from sediment (G)

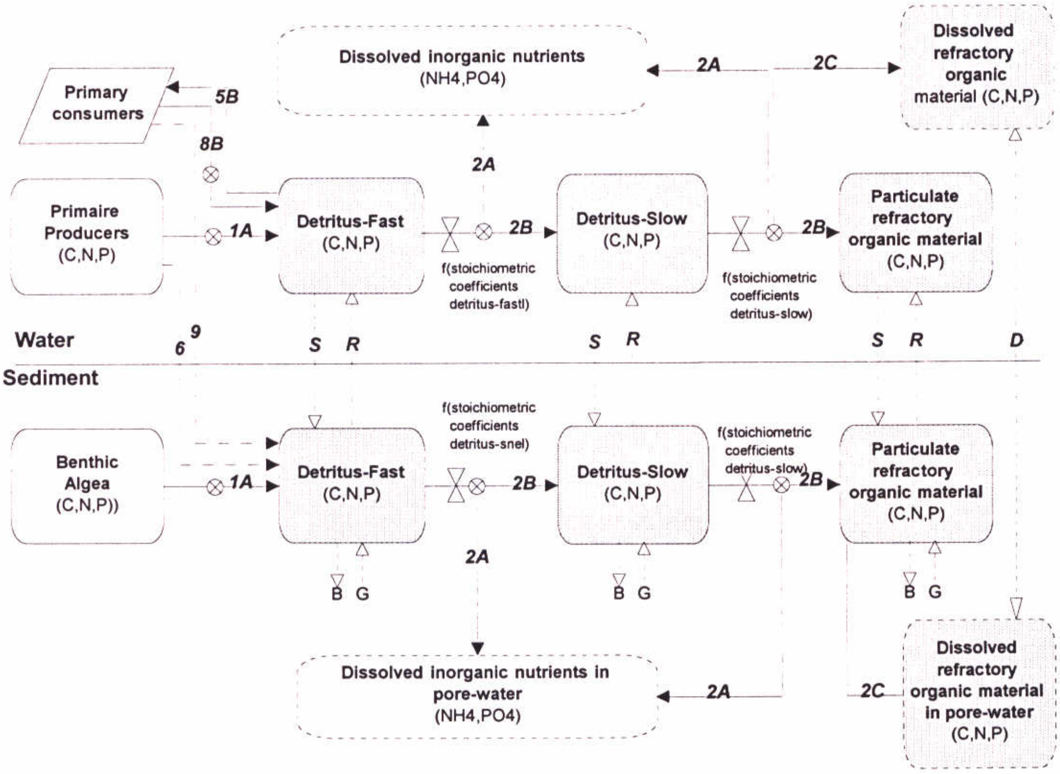

Figure 2.4 Cycling of organic matter: processes related to detritus.

2.4.2 The nutrient budgets

The following processes affect the budgets of both nitrogen, phosphate and silicate (see Figure 2.5):

- *Primary production*
  - Net uptake of nutrients by phytoplankton and microphytobenthos (3)
- *Mortality*
  - Release of nutrients due to mortality of phytoplankton (autolysis) (1B)
  - Release of nutrients due to mortality of microphytobenthos (1B)
  - Release of nutrients due to mortality of primary consumers (8A)
- *Mineralisation*
  - Production of nutrients (2A)

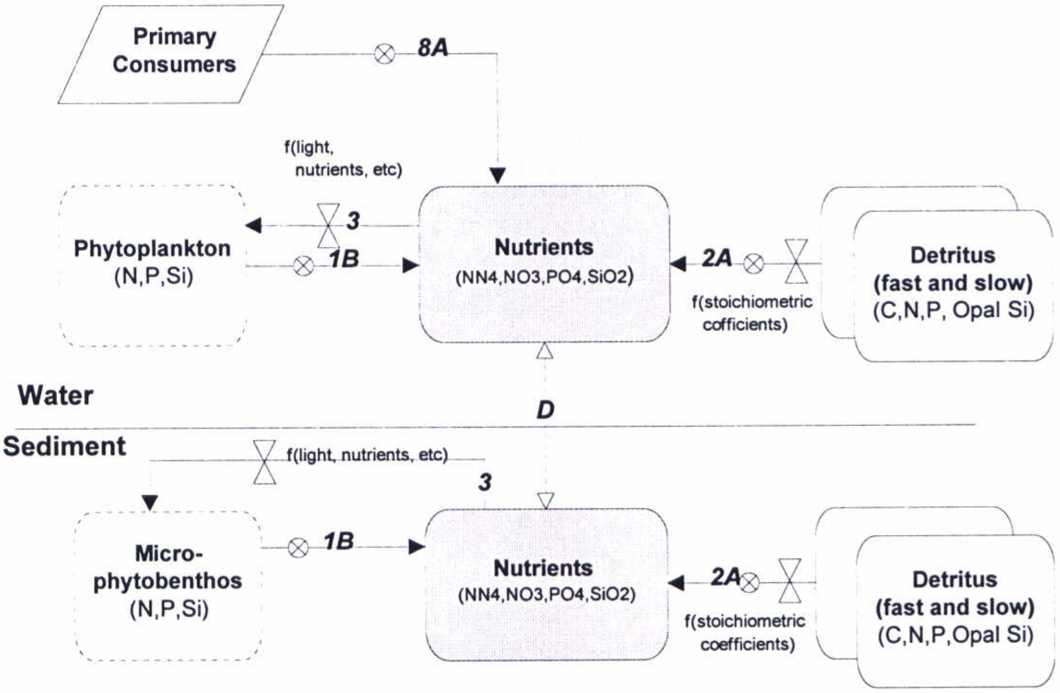

Figure 2.5 Overview of nutrient cycles.

Nitrogen

Additional processes related to the nitrogen budget are (see Figure 2.6):

- *Nitrification*
  - Nitrification in the watercolumn (10A)
  - Nitrification in the sediment (10B)
- *Denitrification*
  - Denitrification in the watercolumn (11A)
  - Denitrification in the sediment (11B)

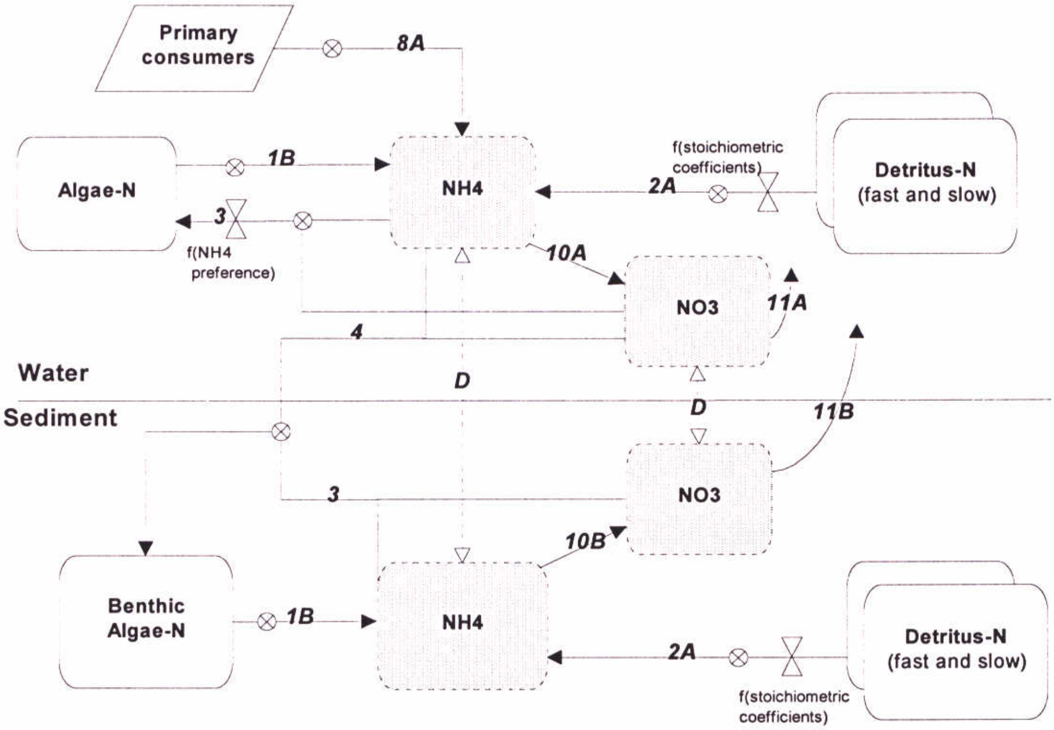

Figure 2.6 Overview of the nitrogen cycle.

Phosphorus

Additional processes related to the phosphate budget are (see Figure 2.7):

- Adsorption and desorption (12)
- Precipitation and dissolution (13)
- Burial (B) and digging (G) of adsorbed and precipitated material

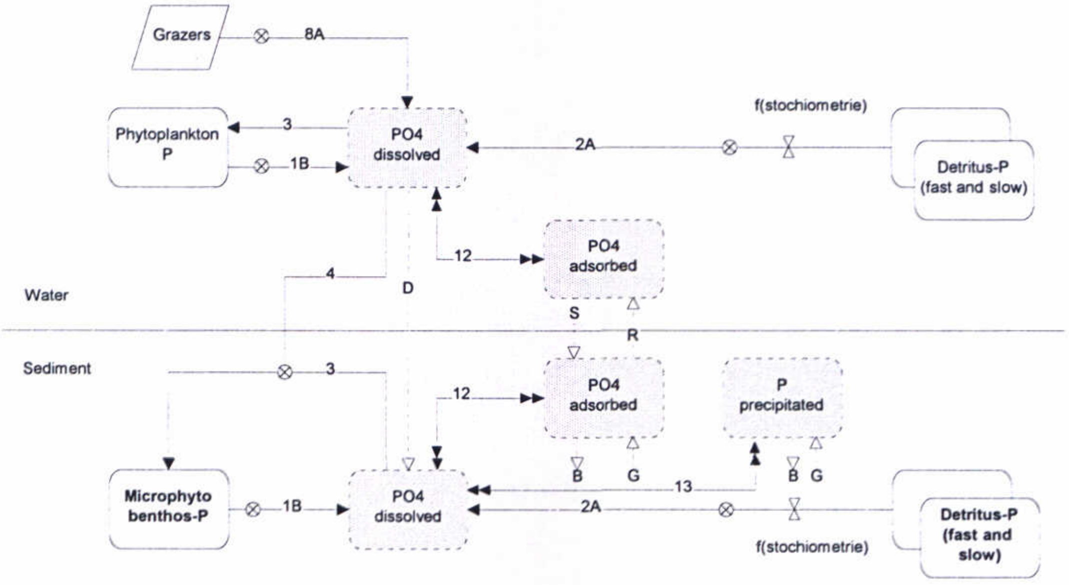

Figure 2.7 Overview of the phosphorus cycle.

Silicon

The silicate budget has one additional process (see Figure 2.8):

- Dissolution opal silicate (14)
- Resuspension (R) and settling (S) opal silicate
- Burial (B) and digging (S) opal silicate

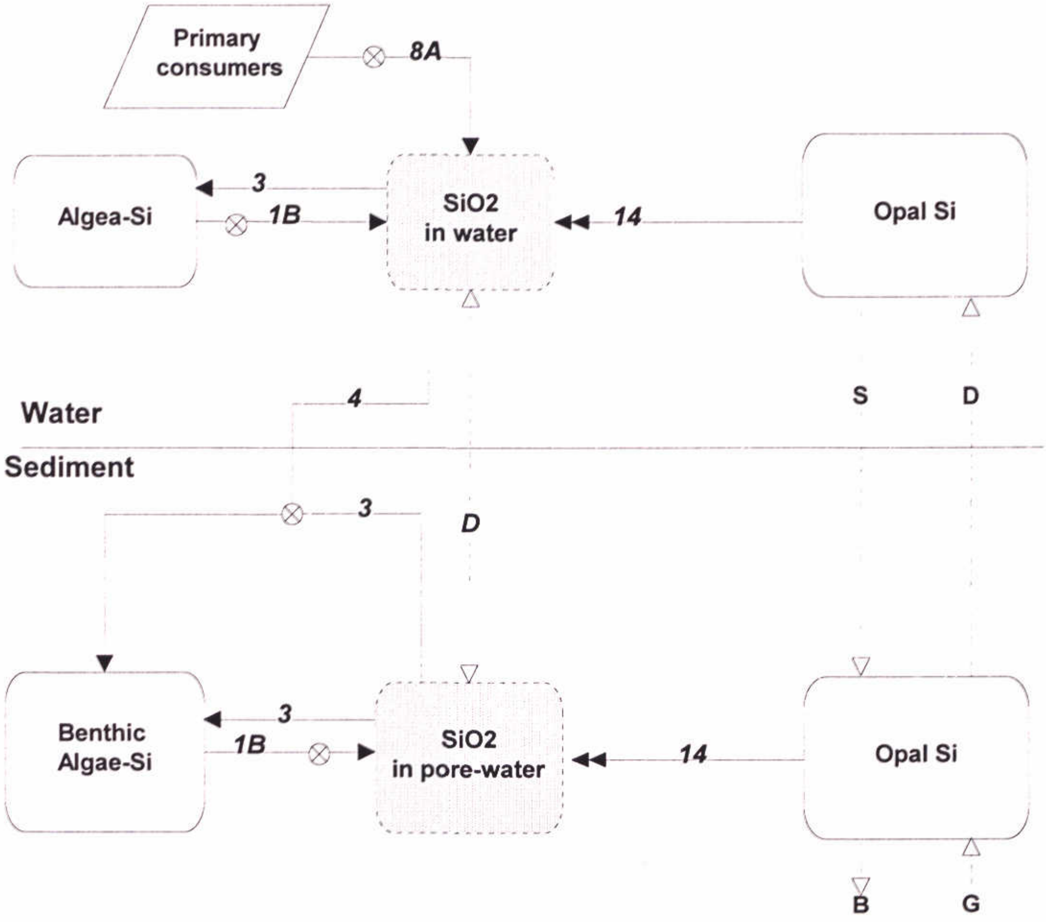

Figure 2.8 Overview of the silicate cycle.

2.4.3 The dissolved oxygen budget

The following processes affect the oxygen budget (see Figure 2.9):

- *Primary production*
  - Production oxygen by phytoplankton and microphytobenthos

- *Mineralisation*
  - Consumption of oxygen in the watercolumn
  - Consumption of oxygen in the sediment

- *Nitrification*
  - Consumption of oxygen in the water column
  - Consumption of oxygen in the sediment

- *Reaeration*
  - Exchange of oxygen over the air-water interface

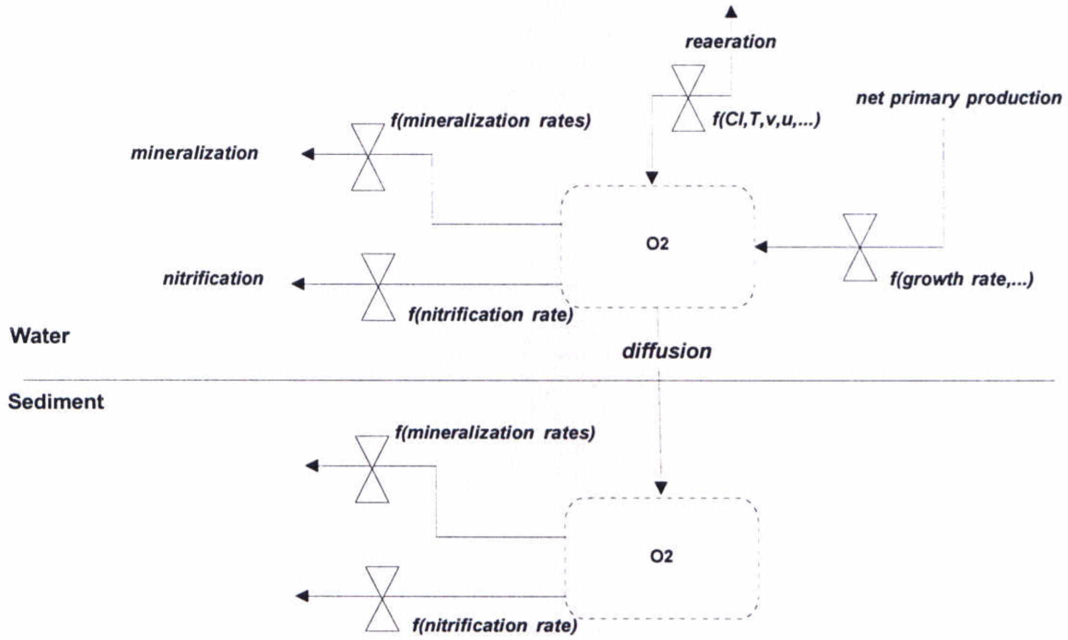

Figure 2.9 Overview of the oxygen cycle.

2.4.4 The sediment budget

The following processes affect the sediment budget (see Figure 2.10):

- Sedimentation
- Resuspension
- Burial
- Digging

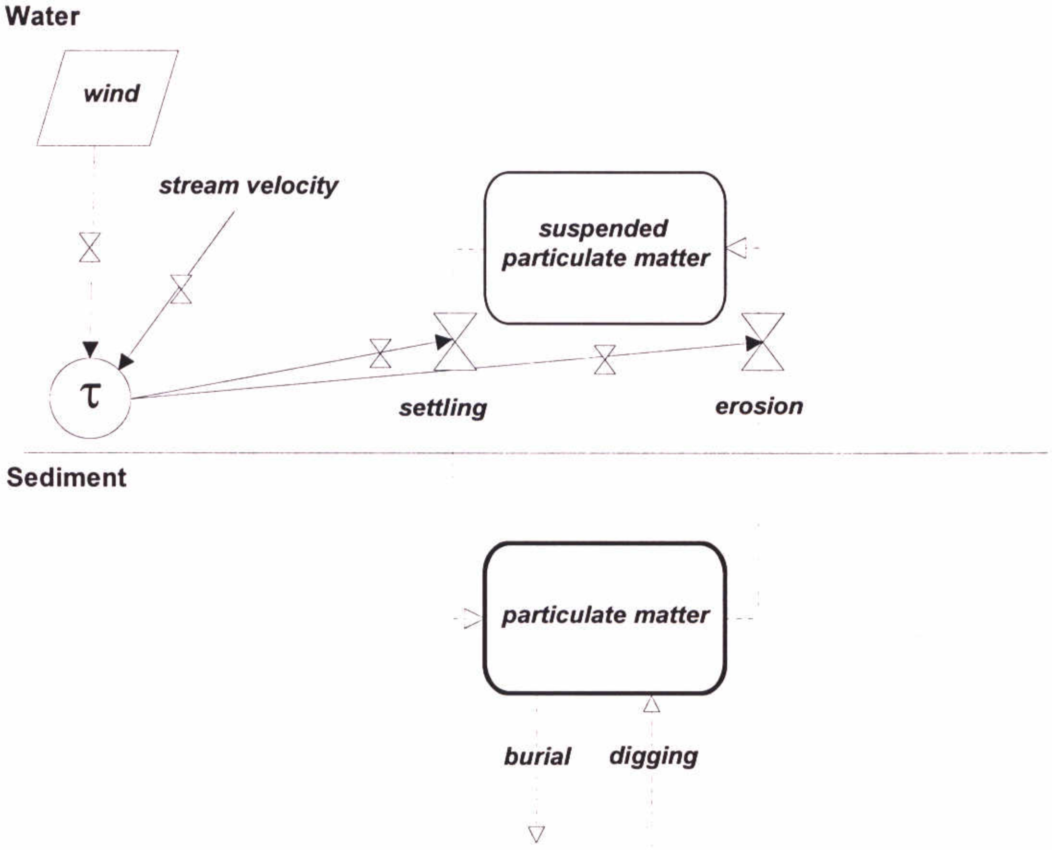

Figure 2.10 Overview of the budget of suspended sediment.

3 Process formulations for primary procedures

3.1 Starting points and coherence

3.1.1 Phytoplankton behaviour

Two different approaches are available in GEM to simulate the primary production by phytoplankton in the water column. In the Monod approach the production is limited by nutrient availability according to Monod-kinetics. For each species it is proportional to the nutrient concentration divided by the sum of this concentration and the concentration at which the rate obtains half its maximal value. The latter is species specific.

The optimization approach according to the phytoplankton module BLOOM takes care that the set of species is selected by which nutrients and energy are used in an optimal way. A linear programming technique is used to find the optimum.

The Monod approach

The Monod type phytoplankton module uses a strictly mechanistic approach to describe algae dynamics. The phytoplankton module presented here is based on a combination of existing phytoplankton modules of ecosystem models (SMOES: Klepper et al, 1994, Scholten & Van der Tol, 1994; moses: NIOO/CEMO, 1993; grewaq: DELFT HYDRAULICS, 1988; DELWAQ 4.2: DELFT HYDRAULICS, 1995; mesocosm: DGW, 1993). A general feature of the MONOD type approach is that algae process rates are multiplicatively limited by environmental factors, like nutrient availability, light availability, and temperature. To describe limitation by nutrients typically Monod functions are applied. More specific features of the MONOD type phytoplankton module are:

- To apply the MONOD type phytoplankton module at least four groups have to be defined. These groups are marine flagellates and diatoms and fresh water flagellates and diatoms. The distinction between a fresh water and a marine water group is made for the reason that in estuaries fresh water species enter the marine environment and subsequently die (or vice versa). Diatoms differ from flagellates by their dependency on dissolved silicon for growth. It is possible to define distinct species or physiological types within these two groups. For each individual species within a group a different set of species specific parameters can be defined.
- Net algal growth within a box depends on the existing concentration of algae, the gross primary production rate, and several loss rates like mortality, settling, respiration and excretion.

- Primary production is a function of light availability (daylength and radiation), available nutrients (N, P and Si (only for diatoms)), temperature (Q10) and a potential maximum production rate. The potential maximum production rate depends on the chlorophyll content of the algae and the chlorophyll specific maximum production rate (Klepper, 1989). Heterotrophy is not (yet) implemented.
- Primary production involves the uptake of nutrients (chapter 6) and the production of dissolved oxygen (chapter 7). The state variables that are simulated with respect to algae in GEM are the organic carbon concentrations of the individual species. The organic nutrient concentrations connected to algae species are derived from the state variables using stoichiometric constants.
- The chlorophyll content of the algae, expressed as the carbon to chlorophyll ratio is a function of light and nutrient availability (Klepper (1989).
- Factors that can limit algal growth are light availability (light and daylength), nutrient availability (N,P,Si) and temperature (Q10). These factors are multiplied to calculate the growth limitation. The effect of oxygen deficiency is not (yet) considered.
- Low nutrient concentrations in the water can limit algal growth. The combined availability of nutrients needed for growth determines the limitation. A MONOD type function is applied to calculate nutrient limitation. Half saturation constants differ between species within the groups.
- There is an optimal daylength for each species within a group. If the daylength is longer than optimal, growth is limited.
- Phytoplankton production is limited, if the light availability in the water column is less than the optimal radiation of a phytoplankton species. Below this optimal radiation light limitation is a linear function of light availability. It is assumed that there is no inhibition if light availability exceeds this optimum. The optimal radiation is temperature dependent.
- The availability of light in the water column depends on the extinction of light. Light extinction is the sum of a background extinction (by water and non-modelled substances) and extinction due to phytoplankton (chlorophyll), detritus and suspended inorganic material.
- The maximal production rate is temperature dependent.
- In the pilot GEM nutrient carbon ratios in algae are constant. Uptake and release of nutrients by algae occurs with constant ratios (C:N:P:Si, Si only for diatoms). Preferential uptake of ammonium over nitrate is included.
- Losses are respiration, excretion and mortality. See chapters 5 and 6 with respect to the resulting nutrient and detritus fluxes.
- Algal respiration consists of maintenance respiration and growth respiration. Maintenance respiration is temperature dependent (Q10). Growth respiration is a function of the net algal production rate. Due to respiration oxygen is consumed. Also excretion is defined for phytoplankton. The excretion is a function of nutrient stress.
- The algal mortality rate consists of grazing by consumers, a temperature dependent mortality, and a salinity stress mortality.
- Due to mortality a fixed fraction of algal nutrients is immediately released to the water column as dissolved components (autolysis). The remaining fraction becomes detritus.
- Grazing by primary consumers is described in chapter 4. See chapters 5 and 6 with respect to the resulting nutrient and detritus fluxes.
- All algal species may settle on the sediment.

- Settling depends on the suspended sediment dynamics. Each algal species has a different fraction of suspended sediment like behaviour. Some algal species are able to control their buoyancy and prevent sedimentation. The buoyancy is modelled as a fraction of the growth respiration. This approach appeared useful to describe sudden collapses of phytoplankton blooms during short periods of light limitations in mesocosm experiments (Van der Tol, unpublished results). Planktonic algae in the sediments will die, nutrients are released and dead organic particulate material is formed (detritus, see also chapter 6).

The optimization approach

Biologically speaking, phytoplankters are relatively primitive organisms. They require considerable amounts of nitrogen, phosphorus, solar energy and sometimes silicon for primary production. In theory each of these factors might become limiting, but the question is where and when.

Natural blooms often consist of assemblages of different phytoplankton species, sometimes belonging to rather distinct groups of species such as diatoms, microflagellates or dinoflagellates. However, groups or even species within a group, often have rather distinct characteristics. Therefore, many of the adverse impacts of eutrophication depend on the dominant (group of) species.

In Monod-type differential equation models competition between phytoplankton species depends on net growth rates, which is expressed as the product of several terms based upon the availability of resources. This approach is straightforward when the total biomass is by far the most important variable in the system (single species model). Differential equation models, however, may deliver problems in describing the competition between a relatively large number of phytoplankton species. Suppose we want to consider 10 different species and 4 potentially limiting factors: nitrogen, phosphorus, silicon and light. So there is a total of 40 interactions to be considered. First of all we must make assumptions on the interactions between the potentially limiting resources. Often the terms for some or even all of these are simply multiplied. As a consequence, competition between different species becomes a fairly complicated function of both limiting and non-limiting resources.

When nutrient levels get low, a single coefficient actually decides the outcome of the competition: the Monod coefficient for the limiting nutrient. Unfortunately these coefficients are not known very accurately, at least not for a large number of species, and therefore reproducing multi-species competition with Monod-type models is traditionally troublesome.

In contrast competition between species in BLOOM II is determined by:

- the net growth rate constant as a measure for the uptake rate of (limiting) resources by each phytoplankton species; and
- the requirements of each species for each resource (as opposed to Monod coefficients, these values are often rather well known).

Occasionally the first term is decisive: a rapidly growing type of phytoplankton can outcompete a slowly growing type even it the latter has a lower requirement for the limiting nutrient. This may happen for example in early spring when potential growth rates of diatoms clearly exceed those of other species. The second term is often of more importance during summer when for example dinoflagellates become dominant under nitrogen limitation even though the potential net growth rates of other species are higher.

3.1.2 Microphytobenthos behaviour

Microphytobenthos can be characterized by the biomass of two groups, one diatom group (silicate requiring) and a non-diatom group. It is assumed that microphytobenthos occurs in a single layer, immediately below the sediment-water interface. Metabolically active microphytobenthos may be found in the upper 3 mm. Below this, it should be considered as detritus.

Daily averaged rates of carbon production, nutrient uptake, etc. is delivered by the microphytobenthos module to GEM. These rates are obtained by integrating production over the day (taking into account the tidal phase) and depth in the sediment, where biomass is assumed to be uniformly distributed over the top 1.5 mm of the sediment. Nutrient uptake is assumed to be a continuous process over the day, whereas in reality it has been shown to be a discontinuous process.

For the integration over the day, the exposure time and the phase of the tide (relative to the daylight cycle) in a compartment is assumed to be known. Incident light on the sediment surface is calculated from incident light on the water surface (if any) and attenuation in the water column. In turbid estuaries, microphytobenthos production is normally limited to ebb and daytime. However, the formulations in GEM are more generic, allowing production over both flood and ebb. The present approach in GEM implies that water height and relative depth distribution in a compartment are known at hourly intervals.

3.2 Monod-type phytoplankton module

The module is implemented for four algal species. Additional species within these four main groups may be implemented. Phytoplankton growth is a function of primary production, respiration, excretion, mortality, grazing and settling. For each algal species an alternative set of parameters can be defined. The overall net process flux for an algae species i is:

$$F_{algi} = F_{algi,gp} - F_{algi,rsp} - F_{algi,ex} - F_{algi,mor} - F_{algi,csgr} - F_{algi,set} \qquad (3.2.1)$$

in which:

F_{algi} = species production [$gC.m^{-3}.d^{-1}$]
$F_{algi,gp}$ = species gross primary production [$g.C.m^{-3}.d^{-1}$]
$F_{algi,rsp}$ = species respiration [$gC.m^{-3}.d^{-1}$]
$F_{algi,ex}$ = species excretion [$gC.m^{-3}.d^{-1}$]
$F_{algi,mor}$ = species mortality [$gC.m^{-3}.d^{-1}$]
$F_{algi,csgr}$ = species grazing [$gC.m^{-3}.d^{-1}$]
$F_{algi,set}$ = species settling [$gC.m^{-3}.d^{-1}$]

3.2.1 Primary production

Primary production is formulated as a temperature dependent first order process limited by light and nutrient availability:

$$F_{algi,gp} = f_{algi,nut} \cdot f_{algi,lt} \cdot f_{algi,tmp} \cdot Pm_{algi,10} \cdot C_{algi} \qquad (3.2.2)$$

in which:

$F_{algi,gp}$ = species primary production flux [gC.m^{-3}.d^{-1}]
C_{algi} = biomass of algal species i [gC.m^{-3}]
$Pm_{algi,10}$ = species maximal gross production rate at 10 °C [d^{-1}]
$f_{algi,lt}$ = species light limitation function [-]
$f_{algi,nut}$ = species nutrient limitation function [-]
$f_{algi,tmp}$ = species temperature function for production [-]

Maximal production

The maximal gross primary production rate depends on the chlorophyll content of the species.

$$Pm_{algi,10} = Pm_{algi,chl10} \cdot C_{algi,chl} \qquad (3.2.3)$$

in which:

$C_{algi,chl}$ = chlorophyll concentration of algal species i [gChl.m^{-3}]
$Pm_{algi,chl10}$ = chlorophyll specific max. prod. rate at 10 °C for species i [m^3.gChl^{-1}.d^{-1}]

$Pm_{algi,chl10}$ is defined at 10 °C. Literature based estimates of this parameter have to be corrected for this temperature.
The chlorophyll content of an individual species is calculated with a variable carbon to chlorophyll ratio. This ratio is modelled with an empirical function of the light and nutrient limitation function (Klepper, 1989).

$$C_{algi,chl} = C_{algi} / a_{algi,chl} \qquad (3.2.4)$$

$$a_{algi,chl} = am_{algi,chl} / (f_{algi,nut} \cdot (1 - f_{algi,lt} \cdot f_{algi,nut}))^{b_{algi,chl}} \qquad (3.2.5)$$

$$C_{chl} = \Sigma_i \, C_{algi,chl} \qquad (3.2.6)$$

in which:

$a_{algi,chl}$ = species carbon to chlorophyll ratio [gC.gChl^{-1}]
$am_{algi,chl}$ = species minimal carbon to chlorophyll ratio [gC.gChl^{-1}]
$b_{algi,chl}$ = species scaling exponent for growth limitation effect C/Chl ratio [-]
C_{chl} = total chlorophyll concentration [gChl.m^{-3}]

Temperature dependency

The temperature function is:

$$f_{algi,tmp} = kt_{gp}^{(T-10)} \tag{3.2.7}$$

in which:

kt_{gp} = temperature coefficient for gross production [-]

T = water temperature [°C]

Nutrient limitation

Nutrient limitation is described by means of Monod-functions. In most models Liebig's law of the minimum is applied to calculate the overall nutrient limitation. Here the additive model described by O'Neill et al. (1989) is proposed. This additive model assumes that more than one nutrient can be limiting.

Due to the silicate demand of diatoms, the diatom limitation function is slightly different from the flagellate limitation function. Phytoplankters can use two inorganic sources of nitrogen. The nitrogen limitation depends on both the availability and saturation constants of ammonium and nitrate.

$$f_{algi,am} = C_{am} \cdot C_{pho} \cdot C_{si} / \\ (K_{algi,am} \cdot C_{pho} \cdot C_{si} + C_{am} \cdot K_{algi,pho} \cdot C_{si} + C_{am} \cdot C_{pho} \cdot K_{algi,si} + C_{am} \cdot C_{pho} \cdot C_{si}) \tag{3.2.8}$$

$$f_{algi,ni} = C_{ni} \cdot C_{pho} \cdot C_{si} / \\ (K_{algi,ni} \cdot C_{pho} \cdot C_{si} + C_{ni} \cdot K_{algi,pho} \cdot C_{si} + C_{ni} \cdot C_{pho} \cdot K_{algi,si} + C_{ni} \cdot C_{pho} \cdot C_{si}) \tag{3.2.9}$$

$$f_{algi,nut} = f_{algi,am} + (1 - f_{algi,am}) \cdot f_{algi,ni} \tag{3.2.10}$$

in which:

$f_{algi,am}$ = species ammonium based limitation function [-]

$f_{algi,ni}$ = species nitrate based limitation function [-]

$f_{algi,nut}$ = species nutrient limitation function [-]

C_{am} = ammonium concentration [gN.m^{-3}]

C_{ni} = nitrate + nitrite concentration [gN.m^{-3}]

C_{pho} = phosphate concentration [gP.m^{-3}]

C_{si} = dissolved inorganic silicate concentration [gSi.m^{-3}]

$K_{algi,ni}$ = species half saturation constant for nitrate [gN.m^{-3}]

$K_{algi,am}$ = species half saturation constant for ammonium [gN.m^{-3}]

$K_{algi,pho}$ = species half saturation constant for phosphate [gP.m^{-3}]

$K_{algi,si}$ = species half saturation constant for dissolved silicate [gSi.m^{-3}]

Default values for the nutrients and saturation constants are respectively 1.0 and 0.0. If the default values for a nutrient are applied, the nutrient will not contribute to the final limitation. If no distinction is made between ammonium and nitrate the equations for ammonium and nitrate limitation are not used. $f_{algi,am}$ together with f_{nut} is used to calculate the preference for ammonium uptake. Algae have a preferential uptake for ammonium (McCarthy et al., 1977). The ratio between the growth limitation function with ammonium as the single dissolved nitrogen source and the nutrient limitation function, defines the ammonium uptake fraction. Equations 3.2.8-10 have not yet been tested in an existing model application.

Light limitation

Light limitation depends on a functional relationship between in situ light intensity and primary production. This function is integrated over time and depth to get a daily and surface averaged depth integrated primary production rate.

$$f_{algi,lt} = (1/24)\,.\,(1/zmax)\,.\,\Sigma_h^{24}\,\Sigma_z^{zmax}\,(A_{rel}(z)\,.\,P_{algi,rel}(z)\,.\,dz) \qquad (3.2.11)$$

in which:

$A_{rel}(z)$ = surface of box at depth z relative to surface of box at depth 0 [-]

dz = integration step for z [m]

$P_{algi,rel}(z)$ = production rate at depth z, relative to max production rate [-]

$zmax$ = max depth [m]

Where $P_{algi,rel}(z)$ is 0 outside the light hours.
There are several alternatives to describe the influence of radiation on algal production rate. Most alternatives describe this influence by a saturation curve (e.g. Steele, 1962). Some alternatives include light inhibition also (e.g. Eilers & Peeters, 1988). In GEM the Eilers & Peeters model is applied.

$$P_{algi,rel}(z) = G_{rrad}(z)\,.\,(W+2)\,/\,(G_{rrad}(z)^2 + (W.G_{rrad}(z)) + 1) \qquad (3.2.12)$$

and

$P_{algi,rel}(z) = P_{algi}(z)\,/\,Pm_{algi}$

$G_{rrad}(z) = G_{rad}(z)\,/\,G_{orad}$

$W = G_{orad}\,/\,(f_{algi,tmp}.\,Pm_{algi,10}/a_{algi}) - 2$

in which:

$P_{algi,rel}(z)$ = production rate at depth z, relative to max production rate [-]

$Pm_{algi}(z)$ = production rate at depth z [d^{-1}]

G_{orad} = optimal light intensity at which $P = Pm_{algi}$ [$W.m^{-2}$]

$G_{rrad}(z)$ = light intensity at depth z, relative to optimal light intensity [-]

$G_{rad}(z)$ = light intensity at depth z

W = shape parameter of production function [-]

a_{algi} = initial slope of production function [$W^{-1}.m^2.d^{-1}$]

The optimal light intensity depends on temperature.

$$G_{orad} = G_{orad10} \cdot f_{algi,tmp} \qquad (3.2.13)$$

in which:

G_{orad10} = optimal light intensity connected with Pm_{algi} at 10°C [W.m-2]

Light extinction is usually modelled as an empirical function of the sum of a background extinction (water) and a first order dependency on suspended materials. These functions are system dependent. In the following equation chlorophyll, detritus and suspended sediment are included:

$$e_{tot} = e_{back} + (e_{chl} \cdot C_{chl}) + (e_{dt} \cdot C_{dt}) + (e_{ss} \cdot C_{ss}) \qquad (3.2.14)$$

in which:

C_{ss} = concentration of suspended sediment [$gDW.m^{-3}$]
C_{chl} = chlorophyll concentration [$gChl.m^{-3}$]
C_{dt} = detritus concentration [$gC.m^{-3}$], the sum of four components (chapter 5)
e_{tot} = total extinction coefficient [m^{-1}]
e_{back} = background extinction [m^{-1}]
e_{chl} = chlorophyll specific extinction [$g\ Chl^{-1}\ m^3\ m^{-1}$]
e_{dt} = detritus specific extinction [$g\ C^{-1}\ m^3\ m^{-1}$]
e_{ss} = suspended sediment specific extinction [$gDW^{-1}\ m^3\ m^{-1}$]

Typically, suspended matter is not distributed homogeneously over the vertical in estuarine waters. Higher concentrations are usually found near the bottom, and the pattern can often be well described with a logarithmic profile. Empirical data were used to describe the vertical distribution of suspended matter over the vertical from campaigns in Elbe, Gironde and Scheldt performed in the framework of the EU-project MATURE (Pfeiffer, 1995). Light attenuation was measured directly by light transmissometry (optical path length 10 cm), with a high vertical resolution. Depth (z) was transformed into relative depth by division by the maximum depth (z_{max}) from CTD pressure data. For a total of 255 vertical profiles, ln(e(z)) was regressed versus z/z_{max}. In general, the regressions gave an excellent fit. Since in principle a 2DH modelling provides average suspended matter concentrations, slopes and intercepts of the regressions were analysed for a relation with depth-averaged extinction (e_{tot}). Slopes were not significantly related to e_{tot} nor to estuary or other measured factors; the average slope for the depth-dependence was 0.890. It is most practical to express the intercepts as a function of e_{tot}. These values allow the estimation of the vertical profile of the extinction coefficient as a function of e_{tot}.

$$e(z) = e_{tot} \cdot (0.890/(\exp(0.89)-1)) \cdot \exp(0.89\ z/zmax) \qquad (3.2.15)$$

in which:

$e(z)$ = extinction at depth z [m^{-1}]

Light intensity at depth z can now be obtained by integrating the Lambert-Beer equation with variable attenuation coefficient:

$$G_{rad}(z) = G_{rad}(0) \, . \, \exp[0.7 \, e_{tot} \, . \, zmax \, . \, (1 - \exp(0.89 \, z/zmax))] \qquad (3.2.16)$$

Although this formulation is closer to field measurements, in practice it rarely makes a difference in light intensity at a particular depth of more than a few %, compared with a description using a fixed attenuation coefficient (e_{tot}). An option to omit the depth-dependent formulation of e_{tot} has been incorporated into GEM.

$G_{rad}(0)$ (surface incident irradiance in $W.m^{-2}$) is the daily averaged Photosynthetic Active Radiance (400-700nm). Field data are often provided in $J.cm^{-2}.h^{-1}$ or $Wh.m^{-2}$ in PAR. The conversion factor from $J.cm^{-2}.h^{-1}$ to $W.m^{-2}$ is 1/0.36. Often only data of global irradiance are available. The conversion factor from global irradiance to PAR is equal to values between 0.37 and 0.51. Colijn (1983) applies a value of 0.45, while unpublished data of RIKZ reveal a conversion factor of 0.37 (+/- 0.04). Other references are Szeics (1974) 0.47-0.51, and Luning (1981) 0.45. The modeller should be careful to use the correct transformations. If for the modelled year, an hourly time series of incident radiation is available, it is advisable to use this time series. If it is unavailable, a 'synthetic' time series with - as much as possible - the statistical properties of incident light in the Netherlands is to be used. In order to derive the statistical properties of this time series, a one-year long time series of hourly averaged incident radiation in Yerseke was analysed. Light-hours were defined as hours with (on average) more than 1 $\mu E.m^{-2}.s^{-1}$. Daylength was defined as the total numbers of light-hours in a day. It is predicted by:

$$DL = 13.22 + 4.25 \sin(2\pi t/365 - 1.396) \qquad (3.2.17)$$

in which:
DL = daylength [hr]
t = time [day]

Average light intensity over a day was defined as the average of the light intensity measurements during the light-hours. It can be modelled by a deterministic and a (multiplicative) autoregressive error term. The deterministic part of the model is given as:

$$G_{arad}(0) = 405.0657 + 267.3135 \sin(2\pi t/365 - 1.396) \qquad (3.2.18)$$

in which:
$G_{arad}(0)$ = long term average surface light intensity over a day [$W.m^{-2}$]

The model for the error, which takes care of the autocorrelation in the series, is given as:

$$[(G_{drad}(0) - G_{arad}(0))/G_{arad}(0)]_t = 0.266 \, [(G_{drad}(0) - G_{arad}(0))/G_{arad}(0)]_{t-1} + 0.358 \, N[0.1] \qquad (3.2.19)$$

in which:
$N[0,1]$ = normally distributed error with mean 0 and variance 1.
$G_{drad}(0)$ = average surface light intensity over a day [$W.m^{-2}$]

Within a day, the time course of light intensity can again be given by a deterministic and a (multiplicative) autoregressive term. Light intensity is expressed relative to the average over the daylength. Time within the light part of the day is rescaled as t'=(t-tm)/DL, where tm is the morning time (midpoint of the first 'light' hour). All times then scale between 0 and 1. The deterministic part of the model contains a sine and a sine squared in the following expression:

$$G_{hrad}(0)/G_{drad}(0) = 0.405 \sin(2\pi t') + 1.493 \sin^2(2\pi t') \qquad (3.2.20)$$

in which:

$G_{hrad}(0)$ = average surface light intensity as a function of time of the day [$W.m^{-2}$]

The model for the error is:

$$[(G_{rad}(0) - G_{hrad}(0))/G_{hrad}(0)]_t = 0.567\,[(G_{rad}(0) - G_{hrad}(0))/G_{hrad}(0)]_{t-1} + 0.312\,N[0.1] \qquad (3.2.21)$$

In which:

Grad(0) = actual surface light intensity as a function of time of the day [$W.m^{-2}$]

The formulas given can be used either for an off-line calculation of a light time series, or for one-line calculation within the simulation loop. In the latter case, a new random series can be generated for every simulation.

If compartments are relatively large in surface, it cannot be assumed that depth within the compartment is homogeneous. In particular for non-linear, essentially surface dependent processes like pelagic primary production, it could be erroneous not to take into account the depth distribution. It is therefore assumed that, from the bathymetry underlying the hydrodynamic model, depth distributions are derived for all compartments:

$$A_{rel}(z) = A(z)/A(0) \qquad (3.2.22)$$

A negative exponential relationship for A(z) is often applied, so:

$$A_{rel}(z) = \exp(-a_{surf} \cdot z) \qquad (3.2.23)$$

in which:

$A(z)$ = surface at depth z [m^2]

a_{surf} = coefficient for surface depth relationship [-]

3.2.2 Respiration

Total respiration is divided in a growth respiration (a fraction of the nutrient and light limited production) part and a maintenance respiration. The maintenance respiration is a first order temperature dependent process.

$$F_{algi,rsp} = r_{algi,mt} \cdot C_{algi} + r_{algi,pr} \cdot F_{algi,gp} \qquad (3.2.24)$$

$$r_{algi,mt} = r_{algi,mt10} \cdot rt_{algi}^{(T-10)} \qquad (3.2.25)$$

in which:

$F_{alg,rsp}$ = species respiration flux [gC.m^{-3}.d^{-1}]

$r_{algi,pr}$ = species growth respiration fraction [-]

$r_{algi,mt}$ = species maintenance respiration rate [d^{-1}]

$r_{algi,mt10}$ = species maintenance respiration rate at 10 °C [d^{-1}]

rt_{algi} = species temperature coefficient for respiration [-]

3.2.3 Excretion

Excretion is a function of nutrient limitation (Klepper, 1989). Excretion increases with increasing nutrient limitations. It is modelled as a fraction of the primary production. Excreted products are allocated to the detritus pool.

$$F_{algi,ex} = b_{algi,ex} \cdot (1 - f_{algi,nut}) \cdot F_{algi,gp} \qquad (3.2.26)$$

in which:

$F_{algi,ex}$ = species excretion flux [gC.m^{-3}.d^{-1}]

$b_{algi,ex}$ = species max excretion fraction [-]

3.2.4 Mortality

Fresh water algal species enter estuaries, as they are carried along by rivers. These species will die due to high salinity stress. On the other hand marine algal species may die when they are dispersed into a brackish or fresh environment. Mortality is modelled as a first order temperature and salinity dependent process.

$$F_{algi,mor} = (m_{algi,tmp} + m_{algi,chl}) \cdot C_{algi} \qquad (3.2.27)$$

$$m_{algi,tmp} = m_{algi,tmp10} \cdot mt_{algi}^{(T-10)} \qquad (3.2.28)$$

$$m_{algi,chl} = 1 / (1 + e^{(b1algi.Ccl + b2algi)}) \qquad \text{for fresh algae} \qquad (3.2.29)$$

$$m_{algi,chl} = 1 - 1 / (1 + e^{(b1algi.Ccl + b2algi)}) \qquad \text{for brackish/marine algae}$$

in which:

$b1_{algi}$ = species coefficient 1 of salinity stress function $[(^{o}/_{oo})^{-1}]$

$b2_{algi}$ = species coefficient2 of salinity stress function [-]

C_{cl} = chloride concentration, chlorinity $[^{o}/_{oo}]$

$F_{algi,mor}$ = species mortality flux $[gC.m^{-3}.d^{-1}]$

$m_{algi,tmp}$ = species temperature driven mortality rate $[d^{-1}]$

$m_{algi,tmp10}$ = species temperature driven mortality rate at 10 °C $[d^{-1}]$

$m_{algi,chl}$ = species salinity stress mortality rate $[d^{-1}]$

mt_{algi} = species temperature coefficient for mortality [-]

The salinity stress formulation of the moses model is applied, in which mortality is attributed a sigmoidal function of chlorinity. Coefficient 'b1' gives the offset of the steep part, coefficient 'b2' stands for the degree of steepness of this part.

3.2.5 Consumption

Phytoplankton is consumed by grazers, such zooplankton and benthic filter feeders. Grazing processes are described in chapter 4. The consumption flux for an algae species i is the sum of the fluxes for the various grazer species:

$$F_{algi,csgr} = \Sigma_j F_{algi,csgrj} \tag{3.2.30}$$

in which:

$F_{algi,csgr}$ = species consumption flux from grazing $[gC.m^{-3}.d^{-1}]$

$F_{algi,csgrj}$ = species consumption flux from grazer j $[gC.m^{-3}.d^{-1}]$

3.2.6 Settling

Settling of algae is related to some extent with the settling of suspended sediment. It is assumed that algae show partly dissolved like behaviour and a suspended sediment behaviour (Klepper, 1989). The fraction of suspended sediment behaviour determines the sedimentation rate. Moreover algae are able to control their buoyancy. It is assumed that this buoyancy control is a function of growth respiration. If growth respiration (energy expenditure) increases, the settling velocity decreases. This assumption is based on observations in the RIKZ mesocosm experiments.

$$F_{algi,set} = \mathrm{Max}\,(v_{ss} \,.\, b_{algi,ss} \,.\, C_{algi} / H - b_{algi,buoy} \,.\, r_{algi,pr} \,.\, F_{algi,gp} , 0.0) \tag{3.2.31}$$

with:

$F_{algi,set}$ = species settling flux $[gC.m^{-3}.d^{-1}]$

v_{ss} = settling velocity of suspended sediment $[m.d^{-1}]$

$b_{algi,ss}$ = species fraction of suspended sediment behaviour [-]

$b_{algi,buoy}$ = buoyancy fraction of growth respiration [-]

Settled algae are instantaneously converted to fast decomposing detritus, as it is assumed that they are not able to survive in sediment (chapter 5).

3.3 BLOOM II phytoplankton module

3.3.1 Introduction

BLOOM II uses an optimization technique called linear programming to maximize the total net production, or optionally the total biomass[1], of several phytoplankton species in a certain time period consistent with the environmental conditions and the existing biomass levels.

The general linear programming problem is to find a set of variables x_j maximizing or minimizing a linear objective function subject to a set of linear constraints. In BLOOM II the basic variables are the biomasses of the individual phytoplankton types (the difference between 'types' and 'species' is explained in the next paragraph). The objective function is the mathematical expression for maximizing the total net production or the total biomass of the system. The incorporation of both principles into the model is straightforward. The hardest part of the model is setting up a set of linear equations, which take all the environmental conditions and the existing species composition at the previous time step into account. Using linear equations for nutrients is fairly straightforward; they follow directly from the mass balance equations, which are linear too. For the potential production and mortality it takes more ingenuity to derive linear equations. Once these problems are solved, however, the linear programming technique provides a way to distribute all available resources in an optimal way among all phytoplankton types.

For each time step and computational element the model sets up a new set of equations, computes new coefficients for the objective function and computes a new optimal composition of phytoplankton types.

In the next paragraphs we shall give some more details on the actual formulations of this module. A detailed description of the model, including all equations and default coefficient values can be found in Los (1991).

3.3.2 Phytoplankton kinetics

Typically BLOOM II considers between three and ten representative phytoplankton species. Besides river algae species , we have selected four (groups of) species for the pilot version of GEM:

- Diatoms
- Microflagellates
- Dinoflagellates
- *Phaeocystis*

---

[1] *This alternative objective is sometimes selected for worst case analysis.*

Each species is further divided into three types, so we include a total of twelve phytoplankton types. For each type we specify its requirements for nitrogen, phosphorus and silicon (only used by diatoms). Other stochiometric coefficients included in BLOOM II are the carbon to dry weight and carbon to chlorophyll ratios. The rate of production of each phytoplankton type depends on:

- temperature (an exponential or optionally linear function);
- light intensity (a numerical integration of the growth versus light curve with an average intensity distribution for a normalized day); and
- day length (numerical approximation of actual curve).

Losses occur due to the following processes:

- respiration (exponential temperature function); and
- natural mortality (exponential temperature function).

Notice that grazing is not included in BLOOM II, but it is included as a forcing function (See chapter 4).

3.3.3 Adaptation: selection of phytoplankton types

Most species of phytoplankton adapt rapidly to changes in their external environment. Individuals of a single species can therefore display a significant range of variation. To incorporate this phenomenon each species of BLOOM II is represented by several (pheno)types. Each type is representative for a species under either nutrient or energy limitation. For most waters it is sufficient to consider three types for:

- conditions of abundant nutrients and hence ultimately energy limitation (E type);
- nitrogen limitation (N type); and
- phosphorus limitation (P type).

The number of types and their characteristics are inputs to the model, so they can be easily adjusted for different kinds of water systems. They may also reflect different phenotypes such as colonies.

Types are the actual variables of the model. After the model has computed the optimum composition of phytoplankton types, the biomasses of the individual types of each species are summed up to compute the total biomass of each species. In theory all of the types of a species can be present at the same time.

Because adaptation is such a rapid process[2] transitions between phytoplankton types **within** a species can occur in a single time-step of the model (order of one day). So for example an E-type dinoflagellate might be completely replaced by an N-type as soon as nitrogen is depleted. Of course this does not hold for transitions **between** species. If in the previous example a type of another species e.g. the *Phaeocystis* N-type is the best adapted species, dinoflagellates disappear due to mortality (a comparatively slow process) and are thus **gradually** replaced by this *Phaeocystis* N-type.

---

[2] *Adaptation occurs when a cell divides, which means that its characteristic time is the same as for the gross growth rate (order of a day or even less)*

All properties by which the species are characterized in the model are included in the optimization scheme and can be varied[3]. Hence the model not only adjusts the internal level of some nutrient or its growth rate, but also the levels of other nutrients, the mortality rate, the carbon to chlorophyll ratio etc.

3.3.4 Environmental constraints

To compute values for the environmental constraints, BLOOM II needs information on the concentrations of total available nutrients, temperature, the influx of solar radiation and certain site specific characteristics (depth and background turbidity). Some of these conditions are determined directly or indirectly from measurements. Others (notably nutrients) can either be determined from measurements or from the results of other modules. In combination with DELWAQ the latter provides the total available amount of nutrients.

Nutrient constraints

The solution for the phytoplankton should satisfy the following set of nutrient balances:

$$\Sigma_k (a_{i,k} \cdot x_k) + e_i = b_i \quad \text{and} \quad x_k > 0 \quad \text{and} \quad e_i > 0 \tag{3.3.1}$$

in which:

k = type k (-)
$a_{i,k}$ = fraction of nutrient i in type k (-)
x_k = biomass of type k (gdry·m^{-3})
e_i = amount of dissolved nutrient i (g·m^{-3})
b_i = total available amount of nutrient i (g·m^{-3})

Energy limitation

Energy becomes limiting through self-shading when the total extinction exceeds the maximum at which primary production is just balanced by respiration and mortality. For each type there exists a specific value $Kmax_k$ at which this is the case.

On the other hand the light intensity can also be too high, which means the total extinction is too low (photo-inhibition). Hence the total extinction should satisfy the following condition:

---

[3] *In practice some coefficients are usually kept the same for several or for all types, for example because we do not have information on the differences in maximum growth rate constants of a nitrogen and a phosphorus type. This is not a limitation of the model, however. Except for the light dependency, all other coefficients can be varied for each individual type.*

$$Kmin_k \leq \Sigma_k (K_k \cdot x_k) < Kmax_k \tag{3.3.2}$$

in which:

$Kmin_k$ = $Umin_k - K_b - K_d$ (m^{-1})

$Umin_k$ = minimum extinction at which the net production of type k is positive. In other words the lower limit for photo-inhibition (m^{-1})

$Kmax_k$ = $Umax_k - K_b - K_d$ (m^{-1})

$Umax_k$ = maximum extinction coefficient at which the net production of type k is positive. In other words the limit for energy limitation (m^{-1})

K_b = background extinction coefficient (water plus contribution of suspended matter (m^{-1})

K_d = extinction due to detritus (m^{-1})

$\Sigma_k(K_k \cdot x_k)$ = extinction due to live phytoplankton (m^{-1})

x_k = biomass of type k ($gdry \cdot m^{-3}$)

K_k = specific extinction type k ($m^2 \cdot gdry^{-1}$)

Growth limitation

It may or may not be possible for a phytoplankton species to achieve its energy limited upperbound within a single time-step of the model. Whether or not this is the case depends on:

- the initial biomass and
- the net growth rate.

To simplify the formulation we consider a single growth constraint for all types (k) within each species (j) considered by the model. We use the maximum growth rate of the energy type. Furthermore since rapidly growing species have a low mortality rate, we ignore the mortality in the computation of the growth constraint. Thus we include the next set of constraints:

$$x_{max,j} = x_j \cdot e^{(Pg_{max,j} \cdot E_{avg,j} - R_j)\Delta t} \tag{3.3.3}$$

in which:

$x_{max,j}$ = maximum possible biomass of species j at the end of the time interval Δt ($gdry \cdot m^{-3}$)

x_j = biomass of species j at the beginning of interval Δt ($gdry \cdot m^{-3}$)

$Pg_{max,j}$ = maximum gross production rate of species j (E-type) (d^{-1})

$E_{avg,j}$ = time and depth averaged production efficiency (-)

R_j = respiration rate constant species j (d^{-1})

Δt = time interval (d)

Note: for each species a base level is defined in the model for xj. If the actual biomass is lower, this base level is used instead. This is to enable the growth of new species in a particular environment.

Mortality limitation

As in the case of growth the mortality of each phytoplankton species is also constrained within the model to prevent a complete removal within a single time-step. The minimum biomass value of a species is obtained when there is no production, but only mortality. This minimum biomass depends on:

- initial biomass; and
- mortality rate.

This minimum value is computed for each individual phytoplankton type, but the model takes the summation of all types within a species. This way the maximum possible mortality cannot be exceeded, but transitions between types remain possible. Thus we include the following equation:

$$x_{k,t+\Delta t} = x_{k,t} \cdot e^{-M_k \cdot \Delta t} \tag{3.3.4}$$

in which:

$x_{k,t+-t}$ = minimum biomass of type *k* at the end of time interval Δt ($\mathrm{gdry \cdot m^{-3}}$)
$x_{k,t}$ = biomass of type k at the beginning of Δt ($\mathrm{gdry \cdot m^{-3}}$)
M_k = specific mortality rate constant of type *k* ($\mathrm{d^{-1}}$)

The actual value for the mortality constraint of BLOOM II is:

$$x_{min,j} = \Sigma_j (x_{j,t+\Delta t}) \tag{3.3.5}$$

in which:
x_{minj} = minimum biomass of species *j* at the end of time interval Δt ($\mathrm{gdry \cdot m^{-3}}$)

As mortality is computed according to a negative exponential function, the minimum biomass level is always positive, in other words a species can never disappear completely. For numerical reasons, however, a base level is included in the model. When the minimum biomass of a species drops below this base level we make it zero.

3.3.5 An illustration of linear programming.

The general purpose of a linear programming problem is to find a set of variables $x_j \geq 0$ satisfying a number of linear constraints such that some linear combination of these variables is either maximal or minimal[4].

In the case of BLOOM II the variables are the phytoplankton types, the linear constraints are the boundaries imposed on the phytoplankton community by the environment and the objective is to maximize the net production rate of all phytoplankton types.

Figure 3.1 shows a very simple illustration for only two types of phytoplankton with biomasses x_1 and x_2 and two nutrients: N and P. At the straight line denoted by N this nutrient is exhausted. Each combination of x_1 and x_2 at this line or to the left of it satisfies the N constraint. Similarly the area to the left of the P line represents all feasible combinations of x_1 and x_2, at which the P constraint is satisfied. Notice that type 1 is a more efficient user of nitrogen because the distance between the point where the N line intercepts the x_1 axis as larger than the distance along the x_2 axis. In other words more biomass can be created of type 1 compared to type two with the same limiting amount of nitrogen. In contrast type 2 is a more efficient user of phosphorus.

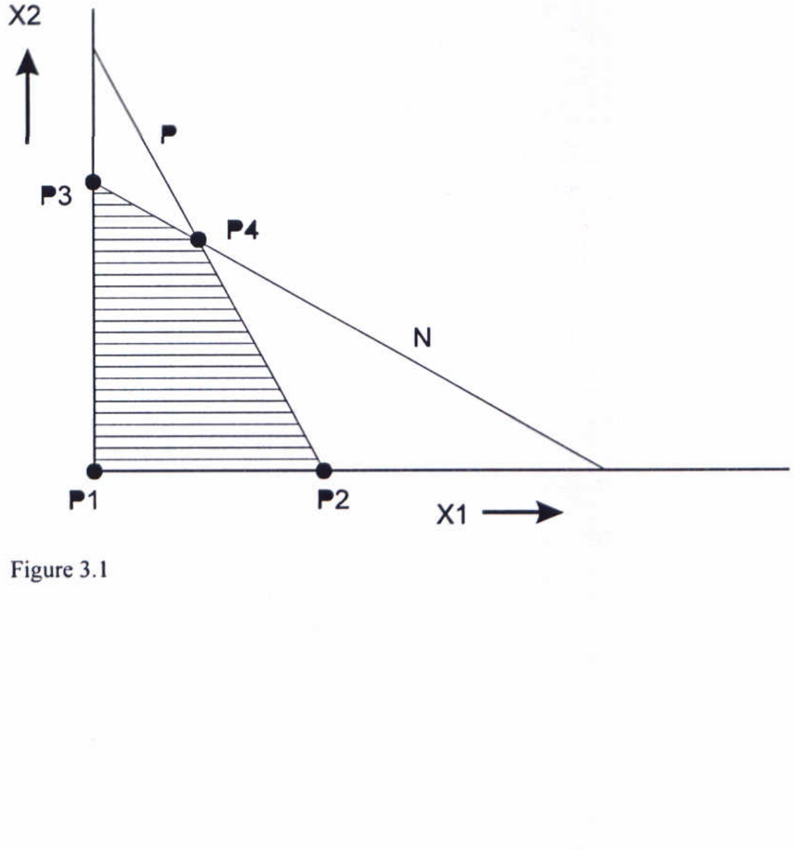

Figure 3.1

---

[4] *It can be shown that each maximization problem can also be formulated as a minimization problem of an opposite objective ("goal") function (Danzig, 1963). The solution of both problems are identical. Thus many problems can be formulated both in terms of minimizing some costs as well as maximizing profits.*

Within the hatched area **both** constraints are satisfied simultaneously. It has been shown that the optimal solution of a linear programming problem is **always** at the interception of lines (Danzig, 1963). Hence we can now easily verify that there are only four points to consider in this case: P1 (the origin), P2, P3 and P4. P1 is obviously not the best possible solution either since both x_1 and x_2 are zero and in all other points at least one type has a positive biomass. Notice that two interesting solutions: type 1 limited by N, type 2 is zero or type 2 limited by P and type 1 is zero are now ruled out as they are not within the area in which both constraints are satisfied.

The linear programming algorithm will thus consider only P2, P3 and P4 and it will pick the one in which the production function

$$Pn_1 \cdot x_1 + Pn_2 \cdot x_2$$

in which:

Pn_k = the net production rate constant of type k (k=1,2) (d^{-1})
x_k = the biomass of type k (k=1,2) ($gC.m^{-3}$)

is maximal.

Suppose that this is the case in P4. We have now found the optimal solution: both type 1 and type 2 occur, both N and P are limiting. Notice the P4 has the largest distance from the origin, which means it also has the highest possible biomass of all three points considered. So in this case maximizing the total biomass would have given us exactly the same solution as maximizing the total net production. This is not always the case, of course. If the net production of type 2 would have been much larger than the net production of type 1, than P3 would have been the optimal solution selected by BLOOM II.

Another important property of linear programming is also obvious from Figure 3.1 the amount of non-zero variables is always equal to the amount of limiting constraints. Hence in point P3 only N is limiting and only type 2 is present and similarly in point P2 only P is limiting and only type 1 is present.

In the previous example we have only considered two environmental conditions. In the next example we introduce four additional constraints: the growth and mortality constraints of both types. These are denoted by M1, M2, G1 and G2 respectively (Figure 3.2). Notice that the N and P lines have not changed. The growth and mortality constraints can be represented by four additional lines on a 90° angle to the biomass axis. The area, in which all six constraints are satisfied is this example is much smaller than in the previous one. Again only the extremes have to be taken into account so there are four possible solutions: P1, P2, P3 and P4. Notice that the original optimal solution of example 1 (point P4) is **not** within the hatched area so it is an infeasible solution here. The same holds for the origin. This is important in case we consider some additional phytoplankton types: a minimum amount of both type 1 and type 2 should always be present (point P1). If the net production rates are the same as in the previous example, than P4 is the optimal solution of this example. Here type 1 is limited by phosphorus and type 2 is growth limited.

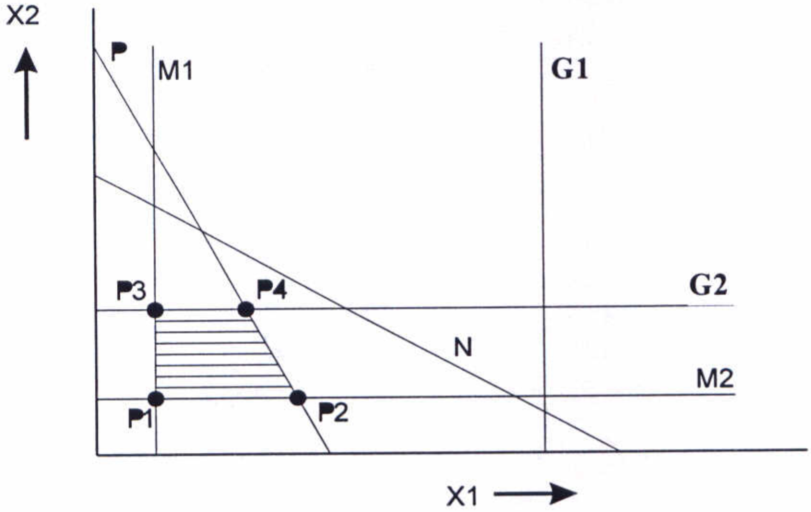

Figure 3.2

Notice that the available amount of nitrogen, which was also limiting in the previous example, is no longer depleted. So nitrogen is not a limiting factor anymore, but it may still become one in the future if the environmental constraints remain (more or less) the same because the P2 line will be moved further along the x_2 axis as the initial biomass of x_2 gets larger each time-step. In contrast x_1 is now larger than in the previous example: although it is a less efficient phosphorus user than type 1, it can take up more of this nutrient than in the previous example because type 2 is growth limited. After a while this growth constraint exceeds P4 and now P4 becomes optimal again; any further changes in growth or mortality constraints no longer affect the optimal solution.

The actual optimization problems considered by BLOOM II are more complicated because they involve more environmental constraints and more types of phytoplankton. Hence the problems can no longer be represented within simple 2-dimensional drawings. However, the same general mathematical principles still hold so there is always a finite number of possible solutions to be considered: the interception points of constraint lines. Only they should now be considered within a n-dimensional space.

3.4 Microphytobenthos

Microphytobenthos growth is a function of primary production, respiration, excretion, mortality (due to non-grazing, non resuspension events), grazing and (net) resuspension. For each of the two groups an alternative set of parameters can be defined. The overall net process flux for a microphytobenthos group i is:

$$F_{mfbi} = F_{mfbi,gp} - F_{mfbi,rsp} - F_{mfbi,ex} - F_{mfbi,mor} - F_{mbfi,res} \qquad (3.4.1)$$

in which:

F_{mfbi} = species production [$gC.m^{-3}.d^{-1}$]

$F_{mfbi,gp}$ = species gross primary production [$gC.m^{-3}.d^{-1}$]

$F_{mfbi,rsp}$ = species respiration [$gC.m^{-3}.d^{-1}$]

$F_{mfbi,ex}$ = species excretion [$gC.m^{-3}.d^{-1}$]

$F_{mfbi,mor}$ = species mortality [$gC.m^{-3}.d^{-1}$]

$F_{mfbi,res}$ = species net resuspension [$gC.m^{-3}.d^{-1}$]

3.4.1 Primary production

Primary production is formulated as a temperature dependent first order process limited by light, nutrient and inorganic carbon availability:

$$F_{mfbi,gp} = f_{mfbi,nut} \cdot f_{mfbi,lt+ic} \cdot f_{mfbi,tmp} \cdot Pm_{mfbi,10} \cdot C_{mfbi} \tag{3.4.2}$$

in which:

$F_{mfbi,gp}$ = species gross primary production [$gC.m^{-3}.d^{-1}$]
C_{mfbi} = species biomass [$gC.m^{-3}$]
$Pm_{mfbi,10}$ = species maximal gross production rate at 10 °C [d^{-1}]
$f_{mfbi,lt+ic}$ = species light limitation function [-]
$f_{mfbi,nut}$ = species nutrient limitation function [-]
$f_{mfbi,tmp}$ = species temperature function for production [-]

Maximal production

The maximal gross primary production rate per day depends on the chlorophyll content of the algae. The effect of day length and time of emersion for intertidal sites is incorporated into the light limitation function.

$$Pm_{mfbi,10} = Pm_{mfbi,chl10} \cdot C_{mfbi,chl} \tag{3.4.3}$$

in which:

$Pm_{mfbi,10}$ = species maximal gross production rate at 10 °C [d^{-1}]
$C_{mfbi,chl}$ = chlorophyll concentration of species i [$gChl.m^{-3}$]
$Pm_{mfbi,chl10}$ = species specific max. gross prod. rate at 10 °C [$gChl^{-1}.m^{3}d^{-1}$]

Inorganic carbon limitation

Due to high production rates in very small volumes, diffusional transport of inorganic carbon to microphytobenthic algae may be a limiting factor. Simulations with a detailed diagenetic model showed that this process can be described by a zero-order limitation term. Instantaneous production cannot exceed a limit ICLIM set by the sum of the depth-integrated CO_2 production (by mineralization) plus the maximum CO_2 transfer over the air-sediment or water-sediment interface, which is in the order of 2.7 $gC\ m^{-2}.d^{-1}$ (instantaneous value). Since instantaneous values for production are needed to evaluate this factor, it is most easily incorporated into the light limitation function.

Light limitation

Microphytobenthos typically shows a hyperbolic reaction of production with incident light. Photoinhibition is typically not observed (McIntyre & Cullen, 1995 and references therein; Barranguet, pers. comm.). McIntyre & Cullen studied P/I curves at different stations and at a 1 mm depth scale. Maximal production and initial slope both decrease with depth in the sediment; this is most probably caused by dark adaptation after long periods of burial. In the surface sediments (most active algae) little difference between stations is observed. The formulation of Webb et al. (1974), as fitted by McIntyre & Cullen (1995) is a good basis for description of the production-light relation:

$$f_{mfb,lt+ic} = \frac{1}{z_{\max}} \frac{1}{t_1} \int_{t=0}^{t_1} \min(IC_{rel}, \int_{z=0}^{z=z_{\max}} (1 - e^{\frac{-\alpha I}{P_m}}) fbiom(z)\, dz)\, dt \tag{3.4.4}$$

in which:

t_1 = 1 day [d]

IC_{rel} = ICLIM / ($f_{mfbi,tmp}$ * $Pm_{mfbi,10}$ * C_{mfbi} / z_{max}) [-]

ICLIM = limit of depth-integrated production by Inorganic carbon transfer [gC.m^{-2}.d^{-1}]

fbiom(z) = relative density function of biomass over depth z [-]

P_m = maximum rate of photosynthesis [gC (g Chl)$^{-1}$$d^{-1}$]

α = initial slope of the PI curve [gC (g Chl)$^{-1}$$h^{-1}$ (μE.m^{-2}.s^{-1})$^{-1}$].

I = light intensity at depth z and time t [μE.m^{-2}.s^{-1}]

Typical values (for surface algae) are:

$P_m \sim 240$ (gC (g Chl)$^{-1}$$d^{-1}$)

$\alpha \sim 1.5$ [gC (g Chl)$^{-1}$$d^{-1}$ (μE.m^{-2}.s^{-1})$^{-1}$]

Integration is over the day and over the depth of the microphytobenthos containing layer. fbiom(z) can be assumed to be a step function, with no biomass below 1.5 mm, and a uniform distribution in the top layer. More complicated functions can also be used. For simple biomass distribution functions, the integral over depth may be solved analytically, thus simplifying the calculations. However, to preserve generality, the integration is performed numerically by splitting up depth in m and time in n small intervals, where light intensity I_{ij} is calculated for each depth and time interval midpoint:

$$f_{mfb,lt+ic} = \frac{\Delta t}{1} \sum_{i=1}^{n} \min(IC_{rel}, \sum_{j=1}^{m} (1 - e^{\frac{-\alpha I_{i,j}}{P_m}}) f_{biom_j} \frac{\Delta z}{z_{max}}) \tag{3.4.5}$$

The light climate in sediments is complicated due to the scattering and absorption processes by the sediment particles and algae (Kühl & Jorgensen, 1994; Kühl et al., 1994). It is difficult to derive a general formulation from the scattered measurements. As a first approximation, it can be assumed that scalar irradiance at the sediment surface is appr. 120-200 % of incident radiation, depending on the grain size and the diatom biomass; attenuation coefficients also depend on grain size and diatom abundance, in a typical range of 2-6 mm^{-1}. More detailed literature research is needed to evaluate the relations between biomass and optical characteristics. Over the daytime downwelling incident light at the sediment surface varies due to variation in the sunlight, depth of the water column and attenuation in the water column. Formulations for I_0 can be derived from the formulations used for phytoplankton by taking into account an enhancement factor. Ambient scalar light at time t and depth z is then given by:

$$I = I_{0,d}(t) \cdot a_{enh} \cdot \exp(-k_{sed} \cdot z) \qquad (3.4.6)$$

in which:

I = time and depth dependent ambient scalar irradiance [$\mu E.m^{-2}.s^{-1}$]

$I_{0,d}(t)$ = time dependent incident downwelling light at the sediment surface [$\mu E.m^{-2}.s^{-1}$] (as calculated in the phytoplankton routine, section 3.2)

a_{enh} = enhancement factor of scalar irradiance due to scattering by sediment grains [-]

k_{sed} = sediment attenuation coefficient [m^{-1}]

z = depth in the sediment [m]

Nutrient limitation

Nutrient limitation of microphytobenthic algae is potentially very important, again because of possible diffusion transport limitation to the concentrated sites of nutrient uptake. It is assumed that nutrients can be taken up during the whole day and night periods, both at low and high tide. If the upper sediment layer, actually simulated in GEM with respect to the nutrients, is approximately equal to the physical size of the layer containing microphytobenthos under field conditions (i.e. 1.5-3 mm), than local concentrations in this layer, subject to diffusional transport, can directly be used in the limitation functions. A correction factor is needed when substantially thicker or thinner sediment layers are considered. Monod-type nutrient limitation functions, similar to the ones used for phytoplankton, are applied. However, the equations have been corrected in a simplified way for diffusive nutrient limitation, and consequently look as follows:

$$f_{mfbi,am} = (z_{mfb}/z_{sed}) \cdot C_{am} \cdot C_{pho} \cdot C_{si} / (K_{mfbi,am} \cdot C_{pho} \cdot C_{si} + C_{am} \cdot K_{mfbi,pho} \cdot C_{si} + C_{am} \cdot C_{pho} \cdot K_{mfbi,si} + C_{am} \cdot C_{pho} \cdot C_{si}) \qquad (3.4.7)$$

$$f_{mfbi,ni} = (z_{mfb}/z_{sed}) \cdot C_{ni} \cdot C_{pho} \cdot C_{si} / (K_{mfbi,ni} \cdot C_{pho} \cdot C_{si} + C_{ni} \cdot K_{mfbi,pho} \cdot C_{si} + C_{ni} \cdot C_{pho} \cdot K_{mfbi,si} + C_{ni} \cdot C_{pho} \cdot C_{si}) \qquad (3.4.8)$$

$$f_{mfbi,nut} = (f_{mfbi,am} + (1 - f_{mfbi,am}) \cdot f_{mfbi,ni}) \qquad (3.4.9)$$

in which:

$f_{mfbi,am}$ = species ammonium based limitation function [-]
$f_{mfbi,ni}$ = species nitrate based limitation function [-]
$f_{mfbi,nut}$ = species nutrient limitation function [-]
C_{am} = ammonium concentration [$gN.m^{-3}$]
C_{ni} = nitrate + nitrite concentration [$gN.m^{-3}$]
C_{pho} = phosphate concentration [$gP.m^{-3}$]
C_{si} = dissolved inorganic silicate concentration [$gSi.m^{-3}$]
$K_{mfbi,ni}$ = species half saturation constant for nitrate [$gN.m^{-3}$]
$K_{mfbi,am}$ = species half saturation constant for ammonium [$gN.m^{-3}$]
$K_{mfbi,pho}$ = species half saturation constant for phosphate [$gP.m^{-3}$]
$K_{mfbi,si}$ = species half saturation constant for dissolved silicate [$gSi.m^{-3}$]
z_{mfb} = penetration depth of microphytobenthos into the sediment [m]
z_{sed} = thickness of the upper sediment layer [0.0015-0.003 m]

By keeping the nutrient limitation functions out of the integration over depth and day (as for light and inorganic carbon limitation), in fact the average nutrient uptake over the whole day (and therefore independence of instantaneous concentrations) is effective.

For taking deviation of the top sediment layer from the microfytobenthos penetration depth into account more realistically, a parameterization of the transport processes into the production layer is called for. In this case, average concentrations in the upper layer cannot be used directly in the limitation functions. Moreover, the presence of microphytobenthos will fysically affect the sediment-water fluxes. The average concentration in the thick top layer can be higher than the concentration in the overlying water, suggesting a flux out of the sediment into the water, whereas in reality the flux can be from the water and the underlying sediment into the microphytobenthos. In GEMSED the problem is solved in principle by specifying an analytical form for the concentration profile within each layer. A solution for microphytobenthos presence may be found along this line. In other sediment modules, this within-layer formulation is not present. Parameterization should be based on extensive sensitivity analysis with fine resolution models, which still has to be done. The alternative is never to use thick top layers for the sediment whenever microphytobenthos is present.

3.4.2 Respiration

Respiration is expressed in the same way as phytoplankton respiration, as a sum of a growth respiration and a maintenance respiration. Maintenance respiration is a first order temperature dependent process.

$$F_{mfbi,rsp} = r_{mfbi,mt} \cdot C_{mfbi} + r_{mfbi,pr} \cdot F_{mfbi,gp} \tag{3.4.10}$$

$$r_{mfbi,mt} = r_{mfbi,mt10} \cdot rt_{mfbi}^{(T-10)}$$

in which:
$F_{mfbi,rsp}$ = species respiration flux [gC.m^{-3}.d^{-1}]
$r_{mfbi,pr}$ = species growth respiration fraction [-]
$r_{mfbi,mt}$ = species maintenance respiration rate [d^{-1}]
$r_{mfbi,mt10}$ = species maintenance respiration rate at 10°C [d^{-1}]
rt_{mfbi} = species temperature coefficient for respiration [-]

3.4.3 Excretion

Like respiration, excretion is also expressed in exactly the same way as for phytoplankton.

$$F_{mfbi,ex} = b_{mfbi,ex} \cdot (1 - f_{mfbi,nut}) \cdot F_{mfbi,gp} \qquad (3.4.11)$$

in which:
$F_{mfbi,ex}$ = species excretion flux [gC.m^{-3}.d^{-1}]
$b_{mfbi,ex}$ = species maximum excretion fraction [-]

3.4.4 Mortality

Due to the absence of explicitly modelled sediment grazers, a distinction between physiological and grazing mortality cannot be made for microphytobenthos. A general formulation is used, incorporating first-order mortality (as typical for physiological mortality) and a second-order term, which may be more typical for grazing mortality. However, as all mortality adds to the detritus flux into the sediment, the real mechanisms behind the different terms are not of crucial importance for the model.

$$F_{mfbi,mor} = mt_{mfbi}^{(T-10)} \cdot C_{mfbi} \cdot (m_{mfbi,tmp10} + m_{mfbi,gr10} \cdot C_{mfbi}) \qquad (3.4.12)$$

in which:
$F_{mfbi,mor}$ = species natural mortality and grazing flux [gC.m^{-3}.d^{-1}]
$m_{mfbi,tmp10}$ = species first-order natural mortality coefficient at 10 °C [d^{-1}]
$m_{mfbi,gr10}$ = species second-order grazing mortality coefficient at 10 °C [d^{-1} .gC^{-1}.m^{3}]
mt_{mfbi} = species temperature coefficient for mortality [-]

Mortality adds to the detritus flux into the sediment.

3.4.5 Resuspension

Resuspension of microphytobenthos is a first order process depending on the bottom shear stress and a critical bottom shear stress, according to eq. (8.6). Since microphytobenthos biomass is not defined in the water column segments, resuspension is modelled as a net process, adding to the detritus in the water column. Any cells that are temporarily suspended into the water column, but resettle at a different phase of the tide are not incorporated into the resuspension. The parameters of the microphytobenthos (net) resuspension are consequently different from the ones used for bulk sediment. Net resuspension adds to the detritus pools in the water column (which may subsequently settle on the bottom).

4 Process formulations for primary consumers

4.1 Starting points and coherence

In GEM grazing by zooplankton and suspension feeders is a forcing function. The biomass densities of the zooplankton and the suspension feeders community are supplied to the model (time dependent). Given these densities and accompanying filtration and food uptake rates the effect on the phytoplankton biomass is calculated.

4.2 Zooplankton and suspension feeders

At high densities of phytoplankton and detritus the uptake of food is determined by Φ_{uptake}:

$$\Phi_{uptake} = \theta_{uptake} \cdot \Phi_{uptake,max} \tag{4.1}$$

$$\theta_{uptake} = e^{0.04(T-20)} \tag{4.2}$$

In which:

Φ_{uptake} = rate of food uptake [gC ·gC prim cons^{-1}·d^{-1}]

$\Phi_{\text{uptake, max}}$ = maximum rate of food uptake [gC ·gC prim cons^{-1}·d^{-1}]

Π_{uptake} = temperature correction food uptake [-]

At low densities of phytoplankton and detritus the uptake of food is determined by $\Phi_{\text{filtration}}$:

$$\Phi_{filtration} = \theta_{filtration} \cdot \Phi_{filtration,max} \tag{4.3}$$

$$\theta_{filtration} = e^{0.04(T-20)} \tag{4.4}$$

In which:

$\Phi_{\text{filtration}}$ = filtration rate [m^3·gC prim cons^{-1}·d^{-1}]

$\Phi_{\text{filtration, max}}$ = maximum rate of filtration [m^3·gC prim cons^{-1}·d^{-1}]

$\Pi_{\text{filtration}}$ = temperature correction filtration [-]

The level of food at which the uptake is balanced is calculated by:

$$c_{critical} = \frac{\Phi_{uptake}}{\Phi_{filtration}} \tag{4.5}$$

In which:

$c_{critical}$ = sustainable food level [$gC \cdot m^{-3}$]

The amount of food available to grazing is determined by:

$$c_{available} = \sum_{i=1}^{n_{det}} (p_{det,i} \cdot c_{det,i}) + \sum_{i=1}^{n_{phyt}} (p_{phyt,i} \cdot c_{phyt,i}) \qquad (4.6)$$

In which:

$c_{available}$ = available food level [$gC \cdot m^{-3}$]
n_{det} = number of detritus fractions [-]
$c_{det,\,i}$ = detritus concentration fraction i [$gC \cdot m^{-3}$]
p_{det} = preference for detritus fraction i [-]
n_{phyt} = number of phytoplankton species [-]
$c_{phyt,\,i}$ = phytoplankton concentration species i [$gC \cdot m^{-3}$]
p_{phyt} = preference for phytoplankton species i [-]

In case $c_{available} < c_{critical}$ the grazing rate is calculated by:

$$k_{primcons} = c_{primcons} \cdot \Phi_{filtration} \frac{c_{available}}{c_{available} + K_{available}} \qquad (4.7)$$

In which:

$c_{prim\,cons}$ = biomass primary consumers [$gC \cdot m^{-3}$]
$K_{available}$ = half saturation constant [$gC \cdot m^{-3}$]
$k_{prim\,cons}$ = grazing rate primary consumers [d^{-1}]

In case $c_{available} > c_{critical}$ the grazing rate is calculated by:

$$k_{primcons} = c_{primcons} \cdot \Phi_{uptake} \cdot \frac{1}{c_{available}} \qquad (4.8)$$

The uptake of detritus and phytoplankton is calculated by:

$$F_{det,i} = \sum_{i=1}^{n_{det}} (k_{primcons} \cdot p_{det,i} \cdot c_{det,i}) \qquad (4.9)$$

$$F_{phyt,i} = \sum_{i=1}^{n_{phyt}} (k_{primcons} \cdot p_{phyt,i} \cdot c_{phyt,i}) \qquad (4.10)$$

In which:

$F_{det,\,i}$ = grazing flux detritus fraction i [$gC \cdot m^{-3} \cdot d^{-1}$]
$F_{phyt,\,i}$ = grazing flux phytoplankton fraction i [$gC \cdot m^{-3} \cdot d^{-1}$]

5 Process formulations for detritus

5.1 Starting points and coherence

Detritus is defined as all non-living organic components: dead algae, dead animals, faecal products from animals, excretion products and biochemical breakdown products. Detrital matter may be solid as well as dissolved. The incorporation of detritus in an ecological model is necessary for a number of reasons:

- Detritus serves as a pool of unavailable nutrients, because the mineralization of detrital components is slow. The degradation rate determines the rate at which nutrients become available again for primary production (chapters 3 and 6).
- Detritus is a food source for grazers (chapter 4).
- The microbial degradation of detritus requires dissolved oxygen (chapter 7). Low oxygen concentrations affect a number of water quality and ecological processes (chapter 6).
- In the sediment, the bacterial breakdown of detrital material causes depletion of oxygen and the consumption of other electron acceptors such as iron(III). Through this, the sorption characteristics of sediment with respect to phosphorus are influenced (chapter 6).
- Detritus may be a relatively important part of suspended matter in the water column and it may determine light attenuation for a large part (chapter 3).

It will be clear that not only decomposition rates have to be known, but also decomposition pathways and elemental composition of detrital compounds. It is a problem, however, that degradation pathways and rates hardly can be measured or quantified. "Detritus" is a collective noun for a mixture of very different types of organic matter. It is hardly possible to separate detritus components; it is even difficult to separate algae and detrital matter. Based on counts and pigment analysis, a distinction can be made, but a physical separation is impossible. A further distinction of detrital components is only possible based on overall elemental analysis and reactivity. That means that detritus is characterised by its composition and its decomposition rate. The only check is the total amount of detrital matter, the overall reactivity (often measured as oxygen consumption) and the overall stoichiometry. There is some information on the composition of humic and fulvic matter (Schnitzer & Kahn, 1972, 1978), and on the stoichiometry of algae. Using that information, the composition of the intermediate detrital products can be estimated.

Important processes considered in GEM are:

- Production/conversion: Detritus is basically produced by phytoplankton and microphytobenthos via mortality, by animal organisms as faecal pellets or excretion products and via mortality. Moreover, detritus components are converted into each other as a result of the microbial degradation process.
- Decomposition: Through biochemical processes performed by bacteria or through biochemical autolysis detritus is partly converted into the inorganic components, from which it was made.

- Consumption: Detritus is used as food by zooplankton and benthic filter feeders. A part of the food is respired, another part is stored as body tissue. The remaining part is excreted in the form of faecal pellets.
- Settling/resuspension: Detritus settles to the sediment and may be resuspended through the action of waves, currents or bioturbating animals.
- Vertical dispersion: Organisms in the sediment cause the mixing of sediment by body movement and by ingestion.
- Burial/digging: Once incorporated in sediment, detritus may be removed from the active sediment layer in the model through sediment accretion. Digging is the reverse process, which proceeds because of the erosion of sediment at the sediment-water interface.

After dying of algae, some components are decomposed rapidly (e.g. proteins or sugars), others may be decomposed slowly (e.g. cell walls that may contain lignin or chitin). Gradually, the relatively readily degradable material is converted into refractory organic matter. This material is composed of particulate humic substances and dissolved humic and fulvic acids. Decomposition of these substances is very slow and dependent on the availability of oxygen.

GEM distinguishes four detritus components to cover the complete range of degrading rates. This is in accordance with several model descriptions (EMOWAD, Baretta & Ruardij, 1988; EcoWasp, Brinkman, 1993). These components are fast decomposing detritus, slow decomposing detritus and particulate and dissolved refractory detritus. The refractory components arise from the slow decomposing component, and are decomposed extremely slow.

Furthermore, GEM uses separate state variables to describe the various elements in detritus. The elements are carbon, nitrogen and phosphorus. Silicate is treated differently, as opal frustules produced from dead algae are not decomposed microbially. Opal silicate dissolves in silicate undersaturated water. See chapter 6 for the formulations regarding silicate, section 6.4 in particular. Consequently, GEM has twelve state variables regarding detritus next to opal silicate (table 5.1). Their pathways are outlined in Fig. 5.1.

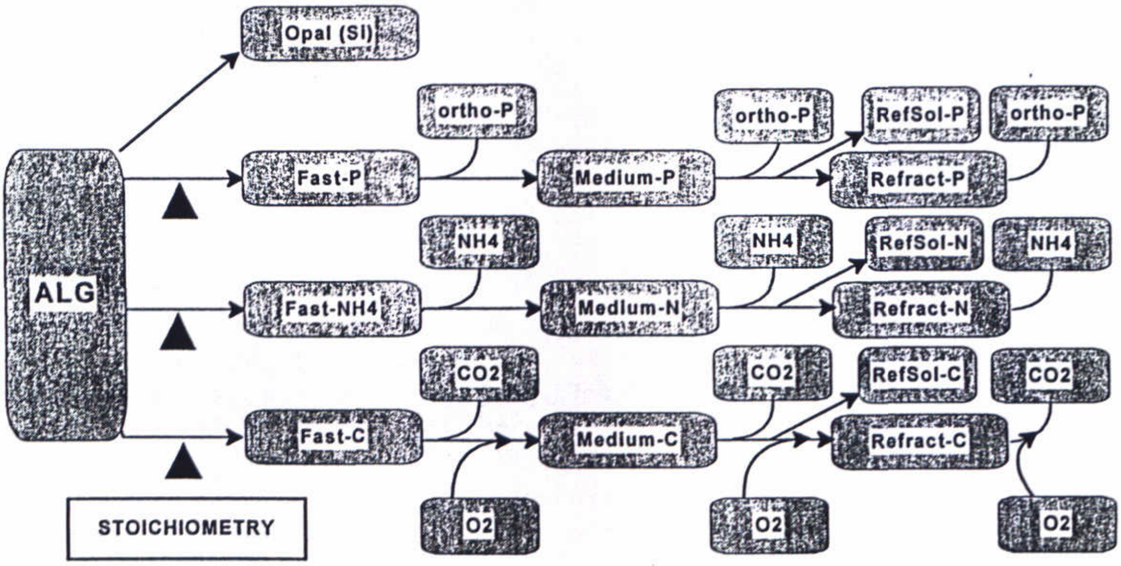

Figure 5.1 The detritus components and their pathways.

Table 5.1 Detritus state variables in GEM

type/nutrient	P	N	C	Si
fast	P-fast	N-fast	C-fast	
slow	P-slow	N-slow	C-slow	Opal
part. refractory	P-part. refrac.	N-part. refrac.	C-part. refrac.	
diss. refractory	P-diss. refrac.	N-diss. refrac.	C-diss. refrac.	

Considering the processes in GEM, the overall net process flux for each of the components is in its most general form equal to the sum of nine process fluxes:

$$F_{dt,npf} = F_{dt,pr} - F_{dt,con} - F_{dt,dec} - F_{dt,cs} - F_{dt,set} - F_{dt,bur} + F_{dt,dig} + F_{dt,res} \tag{5.1}$$

The index dt stands for the carbon components of fast decomposing detritus (dcf), slow decomposing detritus (dcs), particulate refractory detritus (dcpr), dissolved refractory detritus (dcdr) and the concurrent nitrogen and phosphorus components (dnf, dpf, dns, dps, dnpr, dppr, dndr and dpdr).

Obviously, the burial, digging and dispersion fluxes are removed from equation 5.1, when considering detritus components in the water column. The grazing flux is removed when dealing with detritus components in sediment layers. Settling and resuspension only relate to the top sediment layer. Phytoplankton that settles on the sediment and microphytobenthos that dies are incorporated in the top sediment layer as detritus.

Fast decomposing detritus components are produced directly proportional to the algae stoichiometry. The apparent stoichiometry of all detritus components would be a delayed reflection of the algae stoichiometry. In order to establish a more realistic nutrient-poor stochiometry in the refractory organic matter, the organic nutrients are decomposed more rapidly than organic carbon. The stoichiometry of humic matter is taken as a reference point in determining the rates.

The individual process fluxes are described in the next sections. Formulations are given in the most general form for the four components. So, the indexes dtf, dts, dtpr and dtdr stand for the more specific indices referring to carbon (dcf, etc.), nitrogen (dnf, etc.) and phosphorus (dpf, etc.). Deviations from this form that apply to specific elements are indicated. The specific indexes are used in other chapters.

5.2 Production

The production flux for fast decomposing detritus is derived from the mortality and excretion fluxes of algae (chapter 3) and the faeces production flux of grazers (chapter 4). No distinction has been made for phytoplankton and microphytobenthos. The production fluxes of the other components are merely conversion fluxes.

This results in:

$$F_{dtf,pr} = \Sigma_i \left(a_{algi} \cdot (F_{algi,mor} + F_{algi,ex})\right) + \Sigma_j \left(d_j \cdot (F_{dtf,csgrj} + F_{dts,csgrj})\right) \tag{5.2}$$

$$F_{dts,pr} = b_{dts} \cdot F_{dtf,dec} / f_{dtf,sto} \tag{5.3}$$

$$F_{dtpr,pr} = b_{dtpr} \cdot F_{dts,dec} / f_{dts,sto} \tag{5.4}$$

$$F_{dtdr,pr} = b_{dtdr} \cdot F_{dts,dec} / f_{dts,sto} \tag{5.5}$$

in which:
a_{algi} = stoichiometric constant for C/N/P in algae species i ($gC/N/P.gC^{1}$)
b_{dts} = fraction fast decomposing detritus converted into slow decomposing detritus(-)
b_{dtpr} = fraction slow decomposing detritus converted into part. refractory detritus (-)
b_{dtdr} = fraction slow decomposing detritus converted into diss. refractory detritus (-)
d_j = fraction of ingested detritus that is excreted for grazer species j (-)
$f_{dtf,sto}$ = acceleration factor for stoichiometry of fast decomposing detritus (-)
$f_{dts,sto}$ = acceleration factor for stoichiometry of slow decomposing detritus (-)
$F_{algi,mor}$ = mortality flux of algae species i ($gC.m^{-3}.day^{-1}$)
$F_{algi,ex}$ = excretion flux of algae species i ($gC.m^{-3}.day^{-1}$)
$F_{dtf,dec}$ = decomposition flux of fast decomposing detritus ($gC/N/P.m^{-3}.day^{-1}$)
$F_{dts,dec}$ = decomposition flux of slow decomposing detritus ($gC/N/P.m^{-3}.day^{-1}$)
$F_{dtf,csgrj}$ = grazing flux of fast decomp. detritus for grazer species j ($gC/N/P.m^{-3}.day^{-1}$)
$F_{dts,csgrj}$ = grazing flux of slow decomp. detritus for grazer species j ($gC/N/P.m^{-3}.day^{-1}$)
$F_{dtf,pr}$ = production flux of fast decomposing detritus ($gC/N/P.m^{-3}.day^{-1}$)
$F_{dts,pr}$ = production flux of slow decomposing detritus nitrogen ($gC/N/P.m^{-3}.day^{-1}$)
$F_{dtpr,pr}$ = production flux of particulate refractory detritus nitrogen ($gC/N/P.m^{-3}.day^{-1}$)
$F_{dtdr,pr}$ = production flux of dissolved refractory detritus nitrogen ($gC/N/P.m^{-3}.day^{-1}$)

The decomposition fluxes are dealt with in section 5.4. Indicatives values for the conversion fractions are as follows: b_{dts} from 0.05 to 0.1, b_{dtpr} from 0.2 to 0.4, and b_{dtdr} from 0.02 to 0.04. The acceleration factors $f_{dtf,sto}$ and $f_{dts,sto}$ are explained in section 5.4. They appear in the above equations, because the surplus mineralization of nutrients relative to carbon must not affect detritus production.

Notice that the stoichiometric constant for carbon in algae a_{algi} is equal to 1. The fraction of detritus that is excreted by grazers is only dependent on the grazer species, not on the ingested detritus components. It is assumed that only fast and slow detritus are effectively used by grazers.

Equation 5.2 is extended with the settling flux of phytoplankton ($\Sigma_i\, a_{algi} \cdot F_{algi,set}$) in case it applies to the top sediment layer. See chapter 3 for this settling flux.

5.3 Conversion

Fast decomposing detritus is converted into slow decomposing detritus. In its turn this component is converted into refractory detritus. See the previous section. The concurrent fluxes are:

$$F_{dtf,con} = F_{dts,pr} \tag{5.6}$$

$$F_{dts,con} = F_{dtpr,pr} + F_{dtdr,pr} \tag{5.7}$$

in which:

$F_{dtf,con}$ = conversion flux fast decomp. detr. into slow decomp. detr. ($gC/N/P.m^{-3}.day^{-1}$)

$F_{dts,con}$ = conversion flux slow decomp. detr. into refractory detr. ($gC/N/P.m^{-3}.day^{-1}$)

5.4 Decomposition

The decomposition of detritus leads to the release of inorganic nutrients (chapter 6) next to the conversion into other detritus components, described in the previous section. The decomposition flux of fast decomposing detritus components is formulated as follows:

$$F_{dtf,dec} = f_{acc} \cdot f_{dtf,sto} \cdot k_{dtf,dec} \cdot C_{dtf} \tag{5.8}$$

$$f_{dtf,sto} = 1.0 + (C_{dtf} / C_{dcf} - a_{dtpr}) / a_{dtpr}) \tag{5.9}$$

$$k_{dtf,dec} = k_{dtf,dec20} \cdot kt_{dec}^{(T-20)} \tag{5.10}$$

in which:

a_{dtpr} = stoichiometric constant for C/N/P in refractory detritus ($gC/N/P.gC^{-1}$)

C_{dcf} = concentration of fast decomposing detritus carbon ($gC.m^{-3}$)

C_{dtf} = concentration of fast decomposing detritus ($gC/N/P.m^{-3}$)

C_{ni} = concentration of nitrate ($gN.m^{-3}$)

C_{ox} = concentration of dissolved oxygen ($gO_2.m^{-3}$)

$F_{dtf,dec}$ = decomposition flux of fast decomposing detritus ($gC/N/P.m^{-3}.day^{-1}$)

f_{acc} = limiting function for electron acceptors (-)

$f_{dtf,sto}$ = acceleration factor for the stoichiometry of fast decomposing detritus (-)

$k_{dtf,dec}$ = first order decomposition rate for fast decomposing detritus (day^{-1})

$k_{dtf,dec20}$ = first order decomposition rate for fast decomposing detritus at 20 °C (day^{-1})

kt_{dec} = temperature coefficient for detritus decomposition (-)

T = temperature (°C)

The temperature function is similar to a Q_{10}-equation. The temperature coefficient kt would be equal to 1.07 in case the Q_{10} value is 2.0. The degradation of organic matter is carried out by many different species of bacteria. Species adapted to low temperatures cause the temperature dependency to be weaker. It has been shown in many model applications that a coefficient of 1.047 applies to the degradation of detritus under natural conditions.

DELWAQ also considers a zero order rate, taking over below a critical temperature. This rate has a default value of zero, and is ignored in GEM. Formulations similar to equations 5.6-8 exist in GEM for the other detritus components. The rate constant decreases more than a factor 100, going from fast decomposing detritus to refractory detritus. Notice that the acceleration factors for stoichiometry are equal to 1.0 for the carbon detritus components. The formulation of the limiting function for electron acceptors is identical for all components:

$$f_{acc} = 1.0 \qquad \text{if } C_{ox} > 0.0 \tag{5.11}$$

$$f_{acc} = b_{ni} \qquad \text{if } C_{ox} < 0.0 \text{ and } C_{ni} > 0.0$$

$$f_{acc} = b_{su} \qquad \text{if } C_{ox} < 0.0 \text{ and } C_{ni} < 0.0$$

in which:

b_{ni} = attenuation factor in case nitrate is the electron acceptor (-)

b_{su} = attenuation factor in case sulphate and iron are electron acceptors (-)

This limiting function describes the relative mineralization rate when not oxygen but nitrate or other substances are being used as electron acceptor. No distinction is made for sulphate, manganese (IV), iron (III) and organic matter. The attenuation factors have a positive value smaller than 1.0. Indicative values are 0.9 for b_{ni} and 0.6 for b_{su}.

The decomposition rate is dependent on the nutrient stoichiometry of detritus, as bacteria need a supply of nutrients that is proportional to the supply of organic carbon. The nutrient dependency in GEM implies the definition of upper and lower limits for both the rate and the stoichiometry. For intermediate stoichiometry the rate is interpolated linearly between the limits. The formulations for fast decomposing detritus are the following:

$\text{if } (C_{dnf}/C_{dcf}) > au_{dnf} \text{ and } (C_{dpf}/C_{dcf}) > au_{dpf}$:

$$k1_{dtf,dec20} = ku_{dtf,dec20} \tag{5.12}$$

$\text{if } (C_{dnf}/C_{dcf}) < al_{dnf} \text{ or } (C_{dpf}/C_{dcf}) > al_{dpf}$:

$$k1_{dtf,dec20} = kl_{dtf,dec20} + f_{nut} \cdot (ku_{dtf,dec20} - kl_{dtf,dec20})$$

$\text{if } k1_{dtf,dec20} < k1min_{dtf,dec20}$:

$$k1_{dtf,dec20} = kl_{dtf,dec20}$$

$$f_{nut} = \min \{((C_{dnf} / C_{dcf}) - al_{dnf}) / (au_{dnf} - al_{dnf}) , (C_{dpf} / C_{dcf}) - al_{dpf}) / (au_{dpf} - al_{dpf}) \tag{5.13}$$

in which:

al_{dnf} = lower limit stoichiometric constant for N in fast decomposing detritus ($gN.gC^{-1}$)
al_{dpf} = lower limit stoichiometric constant for P in fast decomposing detritus ($gP.gC^{-1}$)
au_{dnf} = upper limit stoichiometric constant for N in fast decomposing detritus ($gN.gC^{-1}$)
au_{dpf} = upper limit stoichiometric constant for P in fast decomposing detritus ($gP.gC^{-1}$)
C_{dnf} = concentration of fast decomposing detritus nitrogen ($gN.m^{-3}$)
C_{dpf} = concentration of fast decomposing detritus phosphorus ($gN.m^{-3}$)
f_{nut} = function for relative nutrient availability (-)
$kl_{dtf,dec20}$ = lower limit first order decomp. rate for fast decomp. detritus at 20 °C (day^{-1})
$ku_{dtf,dec20}$ = upper limit first order decomp. rate for fast decomp. detritus at 20 °C (day^{-1})

Similar equations are used for the other detritus components.

5.5 Consumption

Grazers do not only produce detritus by means of faeces excretion, but also consume detrital material for their own food supply. The ingestion fluxes of fast decomposing detritus and slow decomposing detritus follow from the consumption fluxes described in chapter 4:

$$F_{dtf,cs} = \Sigma_j \, (F_{dtf,csgrj}) \tag{5.14}$$

$$F_{dts,cs} = \Sigma_j \, (F_{dts,csgrj}) \tag{5.15}$$

in which:

$F_{dtf,cs}$ = consumption of fast decomposing detritus ($gC/N/P.m^{-3}.day^{-1}$)
$F_{dts,cs}$ = consumption of slow decomposing detritus ($gC/N/P.m^{-3}.day^{-1}$)
$F_{dtf,csgrj}$ = consumption of fast decomposing detritus by grazer j ($gC/N/P.m^{-3}.day^{-1}$)
$F_{dts,csgrj}$ = consumption of slow decomposing detritus by grazer j ($gC/N/P.m^{-3}.day^{-1}$)

5.6 Settling and resuspension

The principles of settling and resuspension are dealt with in chapter 8, where these processes are formulated for sediment. No distinction exists in GEM with respect to the settling and resuspension of the various detritus components. The settling flux of detritus $F_{dt,set}$ is formulated in the same shear stress dependent way as settling of suspended sediment. However, the settling velocity $v_{dt,set20}$ at 20 °C and the critical shearstress $\tau c_{dt,set}$ are detritus specific. The resuspension flux of detritus is proportional to that of sediment:

$$F_{dt,res} = F_{ss,res} \, . \, (C_{dt} \, / \, C_{ss}) \tag{5.16}$$

in which:

C_{dt} = concentration of a detr. component in the top sediment layer ($gC/N/P.m^{-3}.day^{-1}$)
C_{ss} = sediment concentration in the top sediment layer ($gDW.m^{-3}.day^{-1}$)
$F_{dt,res}$ = resuspension flux of a detritus component ($gC/N/P.m^{-3}.day^{-1}$)
$F_{ss,res}$ = sediment resuspension flux ($gDW.m^{-3}.day^{-1}$)

5.7 Vertical dispersion

Dispersion of detritus in sediment layers and across the sediment-water interface (dissolved components!) is caused by the mixing of water and sediment by organisms through movement and ingestion. The bio-irrigation flux of dissolved refractory detritus and the bioturbation flux of particulate detritus components are formulated on the basis of the discrete version of Fick's law:

$$F_{dtdr,dis} = p_{ij} \cdot (D_{dtdrm} + D_{ir}) \cdot (C_{dtdrj} - C_{dtdri}) / (L_{ij} \cdot L_i) \quad (5.17)$$

$$F_{dt,dis} = D_b \cdot (C_{dtj} - C_{dti}) / (L_{ij} \cdot L_i) \quad (5.18)$$

in which:

C_{dti} = concentration of a particulate detritus component in layer i ($gC/N/P.m^{-3}$)
C_{dtj} = concentration of a part. detritus component in adjacent layer j ($gC/N/P.m^{-3}$)
C_{dtdri} = concentration of dissolved refractory detritus in layer i ($gC/N/P.m^{-3}$)
C_{dtdrj} = concentration of dissolved refractory detritus in adjacent layer j ($gC/N/P.m^{-3}$)
D_b = bioturbation dispersion coefficient ($m^2.day$)
D_{dtdrm} = molecular diffusion of dissolved refractory detritus ($m^2.day$)
D_{ir} = bio-irrigation dispersion coefficient ($m^2.day$)
$F_{dt,dis}$ = vertical dispersion flux of a particulate detritus component ($gC/N/P.m^{-3}.day^{-1}$)
$F_{dtdr,dis}$ = vertical dispersion flux of dissolved refractory detritus ($gC/N/P.m^{-3}.day^{-1}$)
L_i = thickness of the layer (m)
L_{ij} = mixing distance between two adjacent layers (m)
p_{ij} = smallest porosity of adjacent layers i and j (-)

Sections 6.2.6 and 6.3.7 provide details on the temperature dependency of the dispersion coefficients and on the mixing distance.

5.8 Burial and digging

Burial and digging fluxes of particulate detritus components for a sediment layer are formulated as being proportional to sediment accretion and erosion:

$$F_{dt,bur} = F_{ss,ac} \cdot (C_{dt} / C_{ss}) \quad (5.19)$$

$$F_{dt,dig} = F_{ss,er} \cdot (C_{dt} / C_{ss}) \quad (5.20)$$

in which:

$F_{dt,bur}$ = burial flux of a particulate detritus component (gC/N/P.m^{-3}.day^{-1})
$F_{dt,dig}$ = digging flux of a particulate detritus component (gC/N/P.m^{-3}.day^{-1})
$F_{ss,ac}$ = sediment accretion flux (gDW.m^{-3}.day^{-1})
$F_{ss,er}$ = sediment erosion flux (gDW.m^{-3}.day^{-1})

See section 8.4 for formulation of the sediment fluxes.

6 Process formulations for nutrients

6.1 Starting points and coherence

The formulation of the processes that determine the fate and behaviour of inorganic nutrient in GEM is subject to the following starting points:

- Sediment layers are basically dealt with in the same way as the watercolumn. Consequently, the same formulations are used for these compartments. Differences is process rates are established by local conditions and different input parameter values.
- All process rates have been formulated in a temperature dependent fashion. The user of GEM may decide to ignore temperature dependency for specific processes by providing the value 1.0 to the respective temperature coefficients.
- Microphytoplankton reside at the sediment, that is in the top sediment layer. They withdraw their nutrients only from this sediment layer. In contrast with this, benthic grazers excrete nutrients into the water column. The provisions in GEM for this routing have not been made explicit in the formulations given below.
- Algae in GEM may reduce the nutrient concentrations to zero, whereas in reality very small threshold quantities will remain in solution. Thresholds are ignored as they are ill quantified and would cause only a small reduction of primary production within the accuracy range of the model.
- Supersaturation of dissolved silicate might occur with respect to aluminum silicates. The precipitation is slow, does hardly affect dissolved silicate concentrations and is therefore ignored in GEM.
- The burial of dissolved nutrients is ignored in GEM. The model does not keep track of the nutrients and organic matter stored in the deeper sediment through burial below the lower sediment layer. In connection with this, it is assumed that concentrations are equal at both sides of the lower sediment boundary.
- In a number of cases it is necessary to correct concentrations with the porosity as GEM basically follows DELWAQ's rule to work with overall volumetric concentrations in mass balances. However, (pore) water concentrations are often required in process flux formulations.
- Two existing modules for sediment-water interaction with respect to nutrients, organic matter and dissolved oxygen have been included in GEM. They can be used as more sophisticated and more accurate alternatives for the simplified sediment approach which is implicitly described in the formulations of the individual processes in sections 6.2-4.

The inorganic nutrient state variables that are simulated in GEM are ammonium (am), nitrate (ni), dissolved phosphate (pho), adsorbed phosphate (phoa), precipitated phosphate (phop), dissolved silicate (si) and opal silicate (sip). Each of these substances is subjected to a number of processes in GEM, some of which are specific. The net process flux $F_{sv,npf}$ of a state variable is the change of concentrations over time resulting from all individual processes except advection and horizontal dispersion. Mass transport is separately dealt with in the core routines of DELWAQ (chapter 2).

The water quality and ecological processes considered with respect to nutrients are:

- mineralization (min);
- uptake by algae (up) and mortality of algae (mor);
- excretion by grazers (exgr);
- nitrification (nit) and denitrification (den);
- sorption (sor), precipitation (pr) and dissolution (sol); and
- settling (set), resuspension (res), vertical dispersion (dis), burial (bur) and digging (dig).

The net process fluxes for the 7 inorganic nutrient state variables are the following sums of fluxes:

$$F_{am,npf} = F_{am,min} - F_{am,nit} - F_{am,up} + F_{am,exgr} + F_{am,dis} \tag{6.1}$$

$$F_{ni,npf} = F_{ni,nit} - F_{ni,den} - F_{ni,up} + F_{ni,dis} \tag{6.2}$$

$$F_{pho,npf} = F_{pho,min} - F_{pho,sor} - F_{pho,pr} + F_{pho,sol} + F_{pho,exgr} + F_{pho,dis} \tag{6.3}$$

$$F_{phoa,npf} = F_{phoa,sor} - F_{phoa,set} + F_{phoa,res} + F_{phoa,dis} - F_{phoa,bur} + F_{phoa,dig} \tag{6.4}$$

$$F_{phop,npf} = F_{phop,pr} - F_{phop,sol} - F_{phop,set} + F_{phop,res} + F_{phop,dis} - F_{phop,bur} + F_{phop,dig} \tag{6.5}$$

$$F_{si,npf} = F_{si,sol} - F_{si,up} + F_{si,dis} \tag{6.6}$$

$$F_{sip,npf} = F_{sip,mor} - F_{sip,sol} - F_{sip,set} + F_{sip,res} + F_{sip,dis} - F_{sip,bur} + F_{sip,dig} \tag{6.7}$$

Consequently, nutrient concentrations and algae affect each other mutually (chapter 3). The inorganic nutrients have relations with detritus (chapter 5) and grazers (chapter 4). Moreover, nitrification, denitrification, sorption, precipitation and dissolution are dependent on dissolved oxygen (chapter 8).

The formulations of the various fluxes are presented and explained in the next sections. Explanation of the specific sediment-water interaction modules GEMSED and SWITCH follows in sections 6.5-6.

6.2 Nitrogen components

6.2.1 Mineralization of detritus

As appears from chapter 5, detritus nitrogen is present in four components. The total mineralization flux of ammonium is the sum of the decomposition fluxes of these components:

$$F_{am,min} = F_{dnf,dec} + F_{dns,dec} + F_{dnpr,dec} + F_{dndr,dec} \tag{6.8}$$

in which:

$F_{am,min}$ = ammonium release resulting from mineralization of detritus ($gN.m^{-3}.day^{-1}$)

$F_{dnf,dec}$ = decomposition of fast decomposing detritus nitrogen ($gN.m^{-3}.day^{-1}$)
$F_{dns,dec}$ = decomposition of slow decomposing detritus nitrogen ($gN.m^{-3}.day^{-1}$)
$F_{dnpr,dec}$ = decomposition of particulate refractory detritus nitrogen ($gN.m^{-3}.day^{-1}$)
$F_{dndr,dec}$ = decomposition of dissolved refractory detritus nitrogen ($gN.m^{-3}.day^{-1}$)

See section 5.3 for formulation of the decomposition fluxes.

6.2.2 Nitrification

Nitrification is the microbial, stepwise oxidation of ammonium into nitrate, which requires the presence of dissolved oxygen. Several intermediate oxidation products are formed, but the final step from nitrite to nitrate is considered rate limiting. The accumulation of the intermediate product including nitrite is neglectable in systems with residence times longer than a few days.

Nitrification is highly sensitive to temperature. In contrast with the decomposition of detritus, which may occur at a slow but measurable rate below 4 °C, nitrification nearly comes to a halt at this temperature. This is connected with the fact that only a small number of specialized bacteria species are capable of nitrification. The decomposition of organic matter is performed by a very large number of species, including species that are adapted to low temperature environments. Considering this, nitrification is formulated as follows:

$$F_{am,nit} = k0_{nit} + k1_{nit} \cdot f_{ox,nit} \cdot C_{am} \qquad (6.9)$$

$$k1_{nit} = k1_{nit20} \cdot kt_{nit}^{(T-20)} \qquad (6.10)$$

$$k1_{nit} = 0.0 \qquad \text{if } T < Tc_{nit} \text{ or } C_{ox} / p < Cc_{ox,nit}$$

$$k0_{nit} = 0.0 \qquad \text{if } T < Tc_{nit} \text{ or } C_{ox} / p \geq Cc_{ox,nit} \text{ or } C_{ox} / p < Cm_{ox,nit} \qquad (6.11)$$

$$f_{ox,nit} = C_{ox} / (K_{nit} + C_{ox}) \qquad \text{if } C_{ox} \geq 0.0 \qquad (6.12)$$

$$f_{ox,nit} = 0.0 \qquad \text{if } C_{ox} < 0.0$$

in which:
C_{am} = concentration of ammonium ($gN.m^{-3}$)
C_{ox} = concentration of dissolved oxygen ($gO_2.m^{-3}$)
$Cc_{ox,nit}$ = critical concentration of dissolved oxygen for nitrification ($gO_2.m^{-3} \geq 0.0$)
$Cm_{ox,nit}$ = minimal concentration of dissolved oxygen for nitrification ($gO_2.m^{-3}$)
$F_{am,nit}$ = nitrification flux ($gN.m^{-3}.day^{-1}$)
$f_{ox,nit}$ = oxygen dependent limiting function for nitrification (-)
K_{nit} = half saturation constant for nitrification ($gO_2.m^{-3}$)
$k0_{nit}$ = zero order nitrification rate ($gN.m^{-3}.day^{-1}$)
$k1_{nit}$ = pseudo first order nitrification rate (day^{-1})
$k1_{nit20}$ = nitrification rate constant at 20 °C (day^{-1})
kt_{nit} = nitrification temperature coefficient (-)
p = porosity (-)
T = temperature (°C)
Tc_{nit} = critical temperature for nitrification (°C)

The zero order nitrification rate takes over when the dissolved oxygen concentration drops below the critical value. This rate will be equal to its default value zero in most applications, especially for sediment. Notice however, that this rate can be used to have nitrification when the compartment average dissolved oxygen concentration is zero or even negative. In this way it can be taken into account that the water column may not be homogeneously mixed in reality, and a surface layer with positive oxygen concentrations persists (see chapter 7 for an the explanation of negative oxygen concentrations).

Care must be taken that the zero order rate is given the appropriate value in order to prevent negative ammonium concentrations. It should not be higher than the average first order nitrification flux at the critical oxygen concentration. The minimal oxygen concentration should be given a value equal or smaller than the critical oxygen concentration, just low enough to cause the required nitrification in a partially anoxic water column.

6.2.3 Denitrification

Denitrification is the microbial, stepwise reduction of nitrate into elemental nitrogen. Intermediate products do usually not accumulate. Denitrification can only proceed at almost complete absence of dissolved oxygen. Just like nitrification and for a similar reason, denitrification is highly sensitive to temperature. The process is formulated according to:

$$F_{ni,den} = k0_{den} + k1_{den} \cdot f_{ox,den} \cdot C_{ni} \tag{6.13}$$

$$k1_{den} = k1_{den20} \cdot kt_{den}^{(T-20)} \tag{6.14}$$

$$k1_{den} = 0.0 \qquad \text{if } T < Tc_{den} \text{ or } C_{ox} / p > Cc_{ox,den}$$

$$k0_{den} = 0.0 \qquad \text{if } T < Tc_{den} \text{ or } C_{ox} / p \leq Cc_{ox,den} \text{ or } C_{ox} / p > Cm_{ox,den} \tag{6.15}$$

$$f_{ox,den} = 1 - C_{ox} / (K_{den} + C_{ox}) \qquad \text{if } C_{ox} \geq 0.0 \tag{6.16}$$

$$f_{ox,den} = 1.0 \qquad \text{if } C_{ox} < 0.0$$

in which:

C_{ni} = concentration of nitrate ($gN.m^{-3}$)
$Cc_{ox,den}$ = critical concentration of diss. oxygen for denitrification ($gO_2.m^{-3}$, ≥ 0.0)
$Cm_{ox,den}$ = maximal concentration of dissolved oxygen for denitrification ($gO_2.m^{-3}$)
$F_{ni,den}$ = denitrification flux ($gN.m^{-3}.day^{-1}$)
$f_{ox,den}$ = oxygen dependent limiting function for denitrification (-)
K_{den} = half saturation constant for denitrification ($gO_2.m^{-3}$)
$k0_{den}$ = zero order denitrification rate ($gN.m^{-3}.day^{-1}$)
$k1_{den}$ = first order nitrification rate (day^{-1})
$k1_{den20}$ = denitrification rate constant at 20 °C (day^{-1})
kt_{den} = nitrification temperature coefficient (-)
Tc_{den} = critical temperature for denitrification (°C)

Denitrification has not been made dependent on the concentration of detritus, as it is thought that decomposable organic matter will always be relatively abundantly available.

The zero order rate takes over at dissolved oxygen concentrations higher than the critical value. This rate will be equal to its default value in most applications, especially for the water column. It can be used, however, to have denitrification when the compartment average dissolved oxygen concentration is positive, taking into account that a compartment is not homogeneously mixed in reality. For instance, this is case when:

- a bottom layer depleted with respect to oxygen persists in the water column;
- denitrification persists within (sizeable) suspended sediment particles or organisms; or
- vertical concentration gradients occur in sediment layers.

Care must be taken that the zero order rate is given the appropriate value in order to prevent negative nitrate concentrations. It should not be higher than the average first order denitrification flux at the critical oxygen concentration. The maximal oxygen concentration should be given a value equal or higher than the critical oxygen concentration, just high enough to produce the required denitrification in the partially aerobic compartment.

6.2.4 Net uptake by phytoplankton and microphytobenthos

Algae prefer ammonium over nitrate. Consequently, ammonium may be depleted before algae start to consume nitrate. The net uptake of nutrient nitrogen by primary producers follows from gross primary production, respiration, excretion and autolysis. The latter accompanies mortality. Therefore, the total net uptake of nitrogen is equal to the sum of the carbon fluxes for each of the algae species, which have been defined in chapter 3, multiplied with stoichiometric constants. The mortality flux must also be multiplied with the fraction of ammonium, which is autolysed at the death of algae. In case of microphytobenthos or when phytoplankton is simulated with BLOOM, the following flux formulations are used:

$$F'_{am,up} = \Sigma_i \left(a_{algni} \cdot \left(F_{algi,gp} - F_{algi,res} - F_{algi,exc} - b_{algni} \cdot F_{algi,mor}\right)\right) \qquad (6.17)$$

$$F_{am,up} = F'_{am,up} - F_{ni,up}$$

$$F_{ni,up} = 0.0 \qquad \text{if ammonium is amply available} \qquad (6.18)$$

$$F_{ni,up} = -\left(C_{am} - \Delta t . F'_{am,up}\right) \qquad \text{if not enough ammonium is available}$$

in which:

a_{algni} = stoichiometric constant of nitrogen in species i ($gN.gC^{-1}$)
b_{algni} = fraction of nitrogen released as ammonium at mortality of species i (-)
$F'_{am,up}$ = net ammonium uptake resulting from primary production, uncorrected for nitrate uptake ($gN.m^{-3}.day^{-1}$)
$F_{am,up}$ = net ammonium uptake resulting from primary production, corrected for nitrate uptake ($gN.m^{-3}.day^{-1}$)
$F_{ni,up}$ = nitrate uptake resulting from primary production ($gN.m^{-3}.day^{-1}$)
$F_{algi,gp}$ = gross primary production by species i ($gC.m^{-3}.day^{-1}$)
$F_{algi,res}$ = respiration by species i ($gC.m^{-3}.day^{-1}$)
$F_{algi,exc}$ = excretion by species i ($gC.m^{-3}.day^{-1}$)
$F_{algi,mor}$ = mortality flux of species i ($gC.m^{-3}.day^{-1}$)
Δt = time step of the numerical integration (day)

Consequently, if insufficient ammonium is available to support the primary production, nitrate is used to fill up the gap. The primary production module takes care that the production is not larger than allowed by the total amount of available nutrient (chapter 3).

In case of the Monod-module for phytoplankton, a smoother change-over from the uptake of ammonium to the uptake of nitrate applies:

$$F_{am,up} = \Sigma_i \left(a_{algni} \,.\, (fr_{algi,am} \,.\, F_{algi,gp} - F_{algi,res} - F_{algi,exc} - b_{algni} \,.\, F_{algi,mor})\right) \tag{6.19}$$

$$F_{ni,up} = \Sigma_i (a_{algni} \,.\, ((1-fr_{algi,am}) \,.\, F_{algi,gp} \tag{6.20}$$

$$fr_{algi,am} = f_{algi,am} / f_{algi,nut} \tag{6.21}$$

in which:

$f_{algi,am}$ = species ammonium based limitation function (-, see section 3.2.1)
$f_{algi,nut}$ = species nutrient limitation function (-, see section 3.2.1)
$fr_{algi,am}$ = fraction of nitrogen taken up as ammonium (-)

When necessary, a similar correction on these fluxes is made as for the BLOOM-approach in order to avoid negative ammonium concentrations.

6.2.5 Release from grazing

Grazers like zooplankton and filter feeders consume organic nutrients, which they decompose in gut and body tissue (see chapter 4). A part of the nutrients are stored in the organic matter of the tissue during net growth. Undigested organic nutrients are released in faecal pellets (see chapter 5). The excess of nitrogen is excreted as ammonium, delivering the following overall flux in GEM:

$$F_{am,exgr} = \Sigma_j \left(\Sigma_i (a_{algni} \,.\, F_{algi,csgrj}) + F_{dnf,csgrj} + F_{dns,csgrj} - F_{dnf,exgrj} - a_{grnj} \,.\, F_{grj,st}\right) \tag{6.22}$$

$$F_{dnf,csgrj} = F_{dcf,csgrj} \,.\, (C_{dnf} / C_{dcf}) \tag{6.23}$$

$$F_{dns,csgrj} = F_{dcs,csgrj} \,.\, (C_{dns} / C_{dcs}) \tag{6.24}$$

$$F_{dnf,exgrj} = F_{dcf,exgrj} \,.\, (C_{dnf} / C_{dcf}) \tag{6.25}$$

in which:

a_{grnj} = stoichiometric constant of nitrogen in grazer species j ($gN.gC^{-1}$)
C_{dcf} = concentration of fast decomposing detritus carbon ($gC.m^{-3}$)
C_{dcs} = concentration of slow decomposing detritus carbon ($gC.m^{-3}$)
C_{dnf} = concentration of fast decomposing detritus nitrogen ($gN.m^{-3}$)
C_{dns} = concentration of slow decomposing detritus nitrogen ($gN.m^{-3}$)
$F_{am,exgr}$ = ammonium excreted by grazers ($gN.m^{-3}.day^{-1}$)
$F_{algi,csgrj}$ = consumption of algae i by grazer j ($gC.m^{-3}.day^{-1}$)
$F_{dnf,csgrj}$ = consumption of fast decomposing detritus nitrogen by grazer j ($gN.m^{-3}.day^{-1}$)
$F_{dcf,csgrj}$ = consumption of fast decomposing detritus carbon by grazer j ($gC.m^{-3}.day^{-1}$)
$F_{dns,csgrj}$ = consumption of slow decomposing detritus nitrogen by grazer j ($gN.m^{-3}.day^{-1}$)

$F_{dcs,csgrj}$ = consumption of slow decomposing detritus carbon by grazer j ($gC.m^{-3}.day^{-1}$)
$F_{dnf,exgrj}$ = excretion of fast decomposing detritus nitrogen by grazer j ($gN.m^{-3}.day^{-1}$)
$F_{dcf,exgrj}$ = consumption of fast decomposing detritus carbon by grazer j ($gC.m^{-3}.day^{-1}$)
$F_{grj,st}$ = net storage of organic carbon in grazer j ($gC.m^{-3}.day^{-1}$)

6.2.6 Vertical dispersion

Dissolved ammonium and nitrate disperse along vertical concentration gradients in the sediment and across the sediment-water interface. The dispersion may simply reduce to molecular diffusion, when organisms are absent and laminar flow conditions exist just above the sediment. However, organisms are almost always present and turbulence in the overlying water may frequently disturb the top sediment. Organisms actively transport water by movement and ingestion. The resulting enhanced dispersion is called bio-irrigation. The concurrent ammonium dispersion flux is formulated as the discrete form of Fick's law:

$$F_{am,dis} = p_{ij} \cdot (D_{amm} + D_{ir}) \cdot (C_{amj} - C_{ami}) / (L_{ij} \cdot L_i) \qquad (6.26)$$

$$D_{amm} = D_{amm20} \cdot Dt_{am}^{(T-20)} \qquad (6.27)$$

$$D_{ir} = D_{ir20} \cdot Dt_{ir}^{(T-20)} \qquad (6.28)$$

$$L_{ij} = 0.5\,(L_i + L_j) \qquad (6.29)$$

in which:
C_{ami} = ammonium concentration in layer i ($gN.m^{-3}$)
C_{amj} = ammonium concentration in adjacent layer j ($gN.m^{-3}$)
D_{amm} = molecular diffusion of ammonium in water ($m^2.day$)
D_{amm20} = molecular diffusion of ammonium in water 20 °C ($m^2.day$)
Dt_{amm} = temperature coefficient for molecular diffusion of ammonium in water (-)
D_{ir} = bio-irrigation dispersion coefficient ($m^2.day$)
D_{ir20} = bio-irrigation dispersion coefficient at 20 °C ($m^2.day$)
Dt_{ir} = temperature coefficient for bio-irrigation (-)
$F_{am,dis}$ = vertical dispersion flux ($gN.m^{-3}.day^{-1}$)
L_i = thickness of layer i (m)
L_j = thickness of adjacent layer j (m)
L_{ij} = mixing distance for layers i and j (m)
p_{ij} = smallest porosity of adjacent layers i and j (-)
T = temperature (°C)

The formulation for the dispersion flux $F_{ni,dis}$ of nitrate differs only in the sense that a substance specific diffusion coefficient is used. The sign of the dispersion flux is either positive or negative dependent on the sign of the concentration gradient. The above equation is valid for layer i. Notice that L_i at the back is replaced with L_j in the equation for layer j.

The bio-irrigation factor b varies with temperature, as the activity of organisms has a rather strong relation with temperature and is consequently dependent on the season. Tortuosity has to be taken into account in the input value of the molecular diffusion coefficient. The mixing distance in the water column is not taken as half the water depth, but as a constant provided in the input of GEM.

6.3 Phosphate components

6.3.1 Mineralization of detritus

Analogous to ammonification, dissolved phosphate is produced from four detritus components. The total production of dissolved phosphate is consequently the sum of the decomposition fluxes:

$$F_{pho,min} = F_{dpf,dec} + F_{dps,dec} + F_{dppr,dec} + F_{dpdr,dec} \qquad (6.30)$$

in which:

$F_{pho,min}$ = phosphate release resulting from mineralization of detritus ($gP.m^{-3}.day^{-1}$)
$F_{dpf,dec}$ = decomposition of fast decomposing detritus phosphorus ($gP.m^{-3}.day^{-1}$)
$F_{dps,dec}$ = decomposition of slow decomposing detritus phosphorus ($gP.m^{-3}.day^{-1}$)
$F_{dppr,dec}$ = decomposition of particulate refractory detritus phosphorus ($gP.m^{-3}.day^{-1}$)
$F_{dpdr,dec}$ = decomposition of dissolved refractory detritus phosphorus ($gP.m^{-3}.day^{-1}$)

See section 5.3 for formulation of the decomposition fluxes.

6.3.2 Sorption

Dissolved phosphate adsorbs onto suspended sediment, in particular to the hydrous iron oxides in sediment particles. Other active components are aluminum hydroxides and silicates, manganese oxides and organic matter. Sorption of phosphate onto the sediment is highly pH dependent, adsorption decreases with increasing pH. Moreover, the process is relatively weakly dependent on temperature and ionic strength (salinity). The effect of the latter has not been quantified very well and is therefore ignored in GEM.

Sorption is also sensitive to low dissolved oxygen concentrations. Iron gets reduced when the dissolved oxygen concentration has become zero and anaerobic decomposition of detritus continues. As a result iron dissolves together with sorbed substances. Consequently, the sorption capacity of reducing sediment is relatively small. The sorption capacity of the oxidized top layer of the sediment may be relatively large, as oxidized iron tends to accumulate in this layer.

Adsorption is a fast process, desorption is somewhat slower. Nevertheless, equilibrium is usually established within a few hours. Although process rates are high, the sorption process is formulated kinetically for practical reasons. The net sorption flux follows from:

$$F_{phoa,sor} = k_{sor} \cdot (C_{phoa,eqs} - C_{phoa}) \; / \; p \tag{6.31}$$

$$F_{pho,sor} = F_{phoa,sor} \tag{6.32}$$

$$C_{phoa,eqs} = (C_{phoa} + C_{pho}) \cdot (1 - 1 / (K_{sor} \cdot A \cdot OH^{-a} + 1) \tag{6.33}$$

$$K_{sor} = K_{sor20} \cdot {Kt_{sor}}^{(T-20)} \tag{6.34}$$

$$A = A_{tot} - C_{phoa} / 31 \tag{6.35}$$

$$A_{tot} = f_{ox,sor} \cdot fr_{Fe} \cdot C_{ss} / (56 \; 10^3 \; p) \tag{6.36}$$

$$f_{ox,sor} = 1 \qquad \text{if } C_{ox} \geq Cc_{ox,sor} \tag{6.37}$$

$$f_{ox,sor} = fr_{Feox} \qquad \text{if } C_{ox} < Cc_{ox,sor}$$

$$OH = 10^{-(14-pH)} \tag{6.38}$$

in which:

A = concentration of free adsorption sites (mole.l^{-1})

A_{tot} = total concentration adsorption sites (mole.l^{-1})

C_{phoa} = concentration of adsorbed phosphate (gP.m^{-3})

$C_{phoa,eqs}$ = equilibrium concentration of adsorbed phosphate (gP.m^{-3})

C_{ox} = concentration of dissolved oxygen (gO_2.m^{-3})

$Cc_{ox,sor}$ = critical concentration of dissolved oxygen for sorption (gO_2.m^{-3})

C_{ss} = (suspended) sediment concentration (gO_2.m^{-3})

$F_{pho,sor}$ = sorption flux for dissolved phosphate (gP.m^{-3}.day^{-1})

$F_{phoa,sor}$ = sorption flux for adsorbed phosphate (gP.m^{-3}.day^{-1})

$f_{ox,sor}$ = oxygen dependent function for reduction of the sorption capacity (-)

fr_{Fe} = weight fraction of reactive iron in sediment (gFe/gDW)

fr_{Feox} = oxidized iron fraction of total iron in sediment (gFe/gDW)

K_{sor} = equilibrium constant ($mole^{a-1}$.l^{a-1})

K_{sor20} = equilibrium constant 20 °C ($mole^{a-1}$.l^{a-1})

Kt_{sor} = temperature coefficient of sorption (-)

k_{sor} = pseudo first order sorption rate (day^{-1})

OH = hydroxyl concentration (mole.l^{-1})

pH = acidity (-)

p = porosity (-)

T = temperature (°C)

The equation of the equilibrium concentration is derived as follows. The sorption equilibrium according to Langmuir can be described on a mole per m^3 water basis with:

$$Ads(OH)_a + P <=> AdsP + a\ OH^-$$

$$K_{sor} = ([AdsP] . [OH^-]^a) / ([Ads(OH)_a] . [P]) \qquad (6.33a)$$

in which:

$AdsP$ = adsorbed phosphate = adsorption sites occupied by phosphate
$Ads(OH)_a$ = adsorption sites occupied by hydroxyl groups
P = dissolved phosphate

Equation 6.33a can be converted into equation 6.33, when [P] and [AdsP] are replaced by fractions of $(C_{pho}+C_{phoa})$ and when $[OH^-]$ and $[Ads(OH)_a]$ are written as OH and A. Notice that correction for the volumetric quantity of the adsorbent in sediment can be ignored because it is rather small compared to the volume of pore water.

Using data of Stumm and Morgan (1981), the values of equilibrium constant K_{sor} and stoichiometric constant are estimated respectively at 3.8 and 0.2 for fresh water. They relate to sorption onto α-FeOOH at pH range of 6 to 9 and approximately 20 °C.

6.3.3 Precipitation and dissolution

Precipitation of phosphate occurs under reducing conditions in the form of vivianite, if the solution is supersaturated with respect to $(Fe_3[PO_4]_2)$. Usually, these conditions are only met in the sediment. Precipitation is not only temperature dependent, but also pH dependent, due to the acid-base equilibria to which dissolved phosphate is subjected. However, this effect does not have to be taken into account in the flux formulation as the pH is very constant in the sediment.

As iron(II) gets oxidized into iron(III) in the presence of oxygen, vivianite dissolves in the oxygen containing top sediment layer, to where it is transported by bioturbation. The kinetics of oxidative dissolution of vivianite are not straight forward. The oxidation with dissolved oxygen seems to be a temperature dependent surface reaction mainly, due to low solubility and slow dissolution of the mineral (Santchi et al, 1990). The pH dependency of the surface reaction is rather weak and therefore ignored.

Precipitation and dissolution have been formulated in GEM as follows:

$$F_{phop,pr} = f_{ox,pr} \cdot k_{phop,pr} \cdot (C_{pho} / p - C_{pho,eqp}) \qquad (6.39)$$

$$F_{pho,pr} = F_{phop,pr} \qquad (6.40)$$

$$f_{ox,pr} = 1 \qquad \text{if } C_{ox} / p < Cc_{ox,sor} \qquad (6.41)$$

$$f_{ox,pr} = 0 \quad \text{if } C_{ox} / p \geq Cc_{ox,sor}$$

$$k_{phop,pr} = k_{phop,pr20} \cdot kt_{phpr,sol}^{(T-20)} \qquad (6.42)$$

$$F_{phop,sol} = f_{ox,sol} \cdot k_{phop,sol} \cdot C_{phop} \cdot C_{ox} / p^2 \tag{6.43}$$

$$F_{pho,sol} = F_{phop,sol} \tag{6.44}$$

$$f_{ox,sol} = 1 \qquad \text{if } C_{ox} / p \geq Cc_{ox,sor} \tag{6.45}$$

$$f_{ox,sol} = 0 \qquad \text{if } C_{ox} / p < Cc_{ox,sor}$$

$$k_{phop,sol} = k_{phop,sol20} \cdot kt_{phop,sol}^{(T-20)} \tag{6.46}$$

in which:

C_{phop} = concentration of precipitated phosphate (gP.m^{-3})
$C_{pho,eqs}$ = equilibrium concentration of dissolved phosphate (gP.m^{-3}water)
$F_{pho,pr}$ = precipitation flux for dissolved phosphate (gP.m^{-3}.day^{-1})
$F_{phop,pr}$ = precipitation flux for precipitated phosphate (gP.m^{-3}.day^{-1})
$F_{pho,sol}$ = dissolution flux for dissolved phosphate (gP.m^{-3}.day^{-1})
$F_{phop,sol}$ = dissolution flux for precipitated phosphate (gP.m^{-3}.day^{-1})
$f_{ox,pr}$ = oxygen dependent function for inhibition of precipitation (-)
$f_{ox,sol}$ = oxygen dependent function for inhibition of dissolution (-)
$k_{phop,pr}$ = pseudo first order precipitation rate (day^{-1})
$k_{phop,pr20}$ = pseudo first order precipitation rate at 20 °C (day^{-1})
$kt_{phop,pr}$ = temperature coefficient of precipitation (-)
$k_{phop,sol}$ = second order dissolution/oxidationrate (g^{-1}.m^{3}.day^{-1})
$k_{phop,sol20}$ = second order dissolution/oxidationrate at 20 °C (g^{-1}.m^{3}.day^{-1})
$kt_{phop,sol}$ = temperature coefficient of dissolution/oxidation(-)

The equilibrium dissolved phosphate concentration follows from the solubility product of vivianite, the dissolved iron(II) concentration, two acid-base constants for phosphate and the pH. However, the solubility-product determined for crystalline vivianite in a laboratory provides an underestimate of the equilibrium dissolved phosphate concentration at field conditions. Reasons are to be found in the presence of impure, amorphous vivianite and the coating of minerals.

The same critical dissolved oxygen concentration has been taken as for sorption, as this process is also triggered by the oxidation state of iron. Moreover, notice that no link has been made between vivianite oxidation and dissolved oxygen consumption. The chemical oxygen demand of sediment is fully covered by the introduction of negative oxygen equivalents, which represent the reduced substances including iron that arise from the decomposition of organic matter (see chapter 7). There are indications that other phosphate minerals more stable than vivianite form in natural sediments. However, their nature has not been resolved.

6.3.4 Net uptake by phytoplankton and microphytobenthos

The net uptake of phosphate by primary producers is described in a way similar to that for ammonium (section 6.2.4). Consequently, the total net uptake of phosphate is equal to the sum of the carbon fluxes for each of the algal species (see chapter 3), multiplied with stoichiometric constants. For all phytoplankton and microphytobenthos species, the total net uptake flux is:

$$F_{pho,up} = \Sigma_i \, (a_{algpi} \, . \, (F_{algi,gp} - F_{algi,res} - F_{algi,exc} - b_{algpi} \, . \, F_{algi,mor})) \qquad (6.47)$$

in which:

a_{algpi} = stoichiometric constant of phosphorus in species i ($gP.gC^{-1}$)
b_{algni} = fraction of phosphorus released at mortality of species i (-)
$F_{pho,up}$ = net phosphate uptake resulting from primary production ($gP.m^{-3}.day^{-1}$)
$F_{algi,gp}$ = gross primary production by species i ($gC.m^{-3}.day^{-1}$)
$F_{algi,res}$ = respiration by species i ($gC.m^{-3}.day^{-1}$)
$F_{algi,exc}$ = excretion by species i ($gC.m^{-3}.day^{-1}$)
$F_{algi,mor}$ = mortality flux of species i ($gC.m^{-3}.day^{-1}$)

6.3.5 Release from grazing

The net release of phosphate by grazers is described in the same way as for ammonium (section 6.3.5). The consumption and excretion fluxes of grazers have been formulated in chapters 4 and 5 respectively. Excess inorganic phosphate is excreted according to:

$$F_{pho,exgr} = \Sigma_j \, (\Sigma_i \, (a_{algpi} \, . \, F_{algi,csgrj}) + F_{dpf,csgrj} + F_{dps,csgrj} - F_{dpf,exgrj} - a_{grpj} \, . \, F_{grj,st}) \qquad (6.48)$$

$$F_{dpf,csgrj} = F_{dcf,csgrj} \, . \, (C_{dpf} \, / \, C_{dcf}) \qquad (6.49)$$

$$F_{dps,csgrj} = F_{dcs,csgrj} \, . \, (C_{dps} \, / \, C_{dcs}) \qquad (6.50)$$

$$F_{dpf,exgrj} = F_{dcf,exgrj} \, . \, (C_{dpf} \, / \, C_{dcf}) \qquad (6.51)$$

in which:

a_{grpj} = stoichiometric constant of phosphorus in grazer species j ($gP.gC^{-1}$)
C_{dcf} = concentration of fast decomposing detritus carbon ($gC.m^{-3}$)
C_{dcs} = concentration of slow decomposing detritus carbon ($gC.m^{-3}$)
C_{dpf} = concentration of fast decomposing detritus phosphorus ($gP.m^{-3}$)
C_{dps} = concentration of slow decomposing detritus phosphorus ($gP.m^{-3}$)
$F_{pho,exgr}$ = phosphate excreted by grazers ($gP.m^{-3}.day^{-1}$)
$F_{algi,csgrj}$ = consumption of algae i by grazer j ($gC.m^{-3}.day^{-1}$)
$F_{dpf,csgrj}$ = consumption of fast decomposing detritus phosphorus by grazer j ($gP.m^{-3}.day^{-1}$)
$F_{dcf,csgrj}$ = consumption of fast decomposing detritus carbon by grazer j ($gC.m^{-3}.day^{-1}$)
$F_{dps,csgrj}$ = consumption slow decomposing detritus phosphorus by grazer j ($gP.m^{-3}.day^{-1}$)
$F_{dcs,csgrj}$ = consumption of slow decomposing detritus carbon by grazer j ($gC.m^{-3}.day^{-1}$)
$F_{dpf,exgrj}$ = excretion of fast decomposing detritus phosphorus by grazer j ($gP.m^{-3}.day^{-1}$)
$F_{dcf,exgrj}$ = consumption of fast decomposing detritus carbon by grazer j ($gC.m^{-3}.day^{-1}$)
$F_{grj,st}$ = net storage of organic carbon in grazer j ($gC.m^{-3}.day^{-1}$)

6.3.6 Settling and resuspension

Settling and resuspension of inorganic phosphate are proportional to the settling and resuspension of sediment, onto which it is adsorbed (section 6.3.2):

$$F_{phoa,set} = F_{ss,set} \cdot (C_{phoa} / C_{ss}) \tag{6.52}$$

$$F_{phoa,res} = F_{ss,res} \cdot (C_{phoa} / C_{ss}) \tag{6.53}$$

in which:

$F_{phoa,res}$ = adsorbed phosphate resuspension flux ($gP.m^{-3}.day^{-1}$)
$F_{phoa,set}$ = adsorbed phosphate settling flux ($gP.m^{-3}.day^{-1}$)
$F_{ss,res}$ = sediment resuspension flux ($gDW.m^{-3}.day^{-1}$)
$F_{ss,set}$ = sediment settling flux ($gDW.m^{-3}.day^{-1}$)

The formulation of the settling and resuspension fluxes $F_{phop,set}$ and $F_{phop,res}$ of precipitated phosphate are similar. The fluxes of (suspended) sediment are described in sections 8.2 and 8.3.

6.3.7 Vertical dispersion

Vertical dispersion of dissolved phosphate is described in the same way as for ammonium. Details on temperature dependency and mixing distance are given in section 6.2.6. The flux including molecular diffusion and bio-irrigation is:

$$F_{pho,dis} = p_{ij} \cdot (D_{phom} + D_{ir}) \cdot (C_{phoj} - C_{phoi}) / (L_{ij} \cdot L_i) \tag{6.54}$$

in which:

C_{phoi} = dissolved phosphate concentration in layer i ($gP.m^{-3}$)
C_{phoj} = dissolved phosphate concentration in adjacent layer j ($gP.m^{-3}$)
D_{phom} = molecular diffusion of phosphate in water ($m^2.day$)
$F_{pho,dis}$ = vertical dispersion flux ($gP.m^{-3}.day^{-1}$)
L_i = thickness of layer i (m)
L_{ij} = mixing distance for layers i and j (m)
p_{ij} = smallest porosity of adjacent layers i and j (-)

Dispersion of particulate inorganic phosphate in sediment layers is caused by bioturbation, the mixing of sediment by organisms through movement and ingestion. The bioturbation flux for adsorbed phosphate is formulated on the basis of the discrete version of Fick's law:

$$F_{phoa,dis} = D_b \cdot (C_{phoaj} - C_{phoai}) / (L_{ij} \cdot L_i) \tag{6.55}$$

$$D_b = D_{b20} \cdot Dt_b^{(T-20)} \tag{6.56}$$

in which:

C_{phoai} = adsorbed phosphate concentration in layer i ($gP.m^{-3}$)
C_{phoaj} = adsorbed phosphate concentration in adjacent layer j ($gP.m^{-3}$)

D_b = bioturbation dispersion coefficient (m^2.day)
D_{b20} = bioturbation dispersion coefficient at 20 °C (m^2.day)
Dt_b = temperature coefficient for bioturbation (-)
$F_{phop,dis}$ = vertical dispersion flux ($gP.m^{-3}.day^{-1}$)

The dispersion flux $F_{phop,dis}$ for precipitated phosphate is formulated in a similar way.

6.3.8 Burial and digging

Burial is the consequence of sediment accretion due to the net settling of sediment. In GEM it leads to the removal of particulate phosphate from the lower sediment layer to underlying sediment. Digging is the reverse process, the consequence of net erosion.

Burial and digging fluxes of adsorbed phosphate for a sediment layer are formulated as being proportional to sediment accretion and erosion:

$$F_{phoa,bur} = F_{ss,ac} \cdot (C_{phoa} / C_{ss}) \tag{6.57}$$

$$F_{phoa,dig} = F_{ss,er} \cdot (C_{phoa} / C_{ss}) \tag{6.58}$$

in which:
$F_{phoa,bur}$ = adsorbed phosphate burial flux ($gP.m^{-3}.day^{-1}$)
$F_{phoa,dig}$ = adsorbed phosphate digging flux ($gP.m^{-3}.day^{-1}$)
$F_{ss,ac}$ = sediment accretion flux ($gDW.m^{-3}.day^{-1}$)
$F_{ss,er}$ = sediment erosion flux ($gDW.m^{-3}.day^{-1}$)

The fluxes for precipitated phosphate $F_{phop,bur}$ and $F_{phop,dig}$ are similar. See section 8.4 for the formulation of the sediment fluxes.

6.4 Silicate components

6.4.1 Mortality of pelagic and benthic diatoms

Opal silicate frustules are released after mortality of diatoms (chapter 3). The total release flux is the sum of the contributions of various pelagic and benthic diatom species:

$$F_{sip,mor} = \Sigma_i \, (a_{algsii} \cdot F_{algi,mor}) \tag{6.59}$$

in which:
a_{algsii} = stoichiometric constant for silicate in diatoms ($gSi.gC^{-1}$)
$F_{sip,mor}$ = release flux of opal silicate ($gSi.m^{-3}.day^{-1}$)
$F_{algi,mor}$ = mortality flux of diatom species i ($gC.m^{-3}.day^{-1}$)

6.4.2 Dissolution

Opal silicate starts to dissolve when the solution is undersaturated with respect to silicate. The dissolution rate is only weakly affected by temperature, but much stronger by surface coating of hydrous metal oxides and organic matter (Schink and Guinasso, 1978). Adsorbed iron and aluminum in particular retard dissolution significantly. The effect is much more pronounced in the sediment than in the water column, as these substances are only abundantly available in sediment. The dissolution is formulated as a second order process according to:

$$F_{si,sol} = k_{sol} \cdot (C_{sip} / p) \cdot (C_{si,sat} - C_{si} / p) \qquad (6.60)$$

$$k_{si,ol} = k_{si,sol20} \cdot kt_{si,sol}^{(T-20)} \qquad (6.61)$$

in which:

C_{si} = concentration of dissolved silicate (gSi.m^{-3})
$C_{si,sat}$ = saturation concentration of dissolved silicate (gSi.m^{-3})
C_{sip} = concentration of opal silicate (gSi.m^{-3})
$F_{si,sol}$ = silicate dissolution flux (gSi.m^{-3}.day^{-1})
$k_{si,sol}$ = silicate dissolution rate (gSi^{-1}.m^{3}.day^{-1})
$k_{si,sol20}$ = dissolution rate constant at 20 °C (gSi^{-1}.m^{3}.day^{-1})
$kt_{si,sol}$ = dissolution temperature coefficient (-)
p = porosity (-)
T = temperature (°C)

The rate constant should be given different values for the water column and the sediment layers, in order to account for the greater extent of coating of opal silicate in the sediment.

6.4.3 Net uptake by pelagic and benthic diatoms

The net uptake of silicate by diatoms is described in a way similar to that for ammonium (section 6.2.4). However, respiration, excretion and autolysis are neglectable for silicate and therefore ignored here. Consequently, the total net uptake of silicate is simply equal to the sum of the gross uptake fluxes (see chapter 3) according to:

$$F_{si,up} = \Sigma_i \left(a_{algsii} \cdot F_{algi,gp}\right) \qquad (6.62)$$

in which:

$F_{si,up}$ = net silicate uptake resulting from primary production (gSi.m^{-3}.day^{-1})
$F_{algi,gp}$ = gross primary production by species i (gSi.m^{-3}.day^{-1})

6.4.4 Settling and resuspension

Settling and resuspension of opal silicate are proportional to the settling and resuspension of sediment, as these substances have similar physical properties and opal silicate becomes incorporated in sediment particles once it has entered the sediment (sections 8.2 and 8.3). Consequently, these processes are formulated according to:

$$F_{sip,set} = F_{ss,set} \cdot (C_{sip} / C_{ss}) \qquad (6.63)$$

$$F_{sip,res} = F_{ss,res} \cdot (C_{sip} / C_{ss}) \qquad (6.64)$$

in which:

C_{ss} = (suspended) sediment concentration ($\mathrm{gDW.m^{-3}}$)

$F_{sip,res}$ = opal silicate resuspension flux ($\mathrm{gSi.m^{-3}.day^{-1}}$)

$F_{sip,set}$ = opal silicate settling flux ($\mathrm{gSi.m^{-3}.day^{-1}}$)

$F_{ss,res}$ = sediment resuspension flux ($\mathrm{gDW.m^{-3}.day^{-1}}$)

$F_{ss,set}$ = sediment settling flux ($\mathrm{gDW.m^{-3}.day^{-1}}$)

6.4.5 Vertical dispersion

The vertical dispersion of dissolved and opal silicate is described in the same way as for phosphate (section 6.3.7). More details on temperature dependency and mixing distance are also given in section 6.2.6. The flux including molecular diffusion and bio-irrigation is:

$$F_{si,dis} = p_{ij} \cdot (D_{sim} + D_{ir}) \cdot (C_{sij} - C_{sii}) / (L_{ij} \cdot L_i) \qquad (6.65)$$

in which:

C_{sii} = dissolved silicate concentration in layer i ($\mathrm{gSi.m^{-3}}$)

C_{sij} = dissolved silicate concentration in adjacent layer j ($\mathrm{gSi.m^{-3}}$)

D_{sim} = molecular diffusion of silicate in water at 10 °C ($\mathrm{m^2.day}$)

$F_{si,dis}$ = vertical dispersion flux ($\mathrm{gSi.m^{-3}.day^{-1}}$)

L_i = thickness of layer i (m)

L_{ij} = mixing distance for layers i and j (m)

p_{ij} = smallest porosity of adjacent layers i and j (-)

Dispersion of opal silicate in sediment layers caused by bioturbation is described with:

$$F_{sip,dis} = D_b \cdot (C_{sipj} - C_{sipi}) / (L_{ij} \cdot L_i) \qquad (6.66)$$

in which:

C_{sipi} = opal silicate concentration in layer i ($\mathrm{gSi.m^{-3}}$)

C_{sipj} = opal silicate concentration in adjacent layer j ($\mathrm{gSi.m^{-3}}$)

D_b = bioturbation dispersion coefficient ($\mathrm{m^2.day}$)

$F_{sip,dis}$ = vertical dispersion flux ($\mathrm{gSi.m^{-3}.day^{-1}}$)

6.4.6 Burial and digging

Burial and digging of opal silicate are formulated similarly as for phosphate (section 6.3.8). The fluxes are respectively:

$$F_{sip,bur} = F_{ss,ac} \cdot (C_{sip} / C_{ss}) \tag{6.67}$$

$$F_{sip,dig} = F_{ss,er} \cdot (C_{sip} / C_{ss}) \tag{6.68}$$

in which:

$F_{sip,bur}$ = opal silicate burial flux ($gSi.m^{-3}.day^{-1}$)
$F_{sip,dig}$ = opal silicate digging flux ($gSi.m^{-3}.day^{-1}$)
$F_{ss,ac}$ = sediment accretion flux ($gDW.m^{-3}.day^{-1}$)
$F_{ss,er}$ = sediment erosion flux ($gDW.m^{-3}.day^{-1}$)

See section 8.4 for formulation of the sediment fluxes.

6.5 Sediment-water interaction according to GEMSED

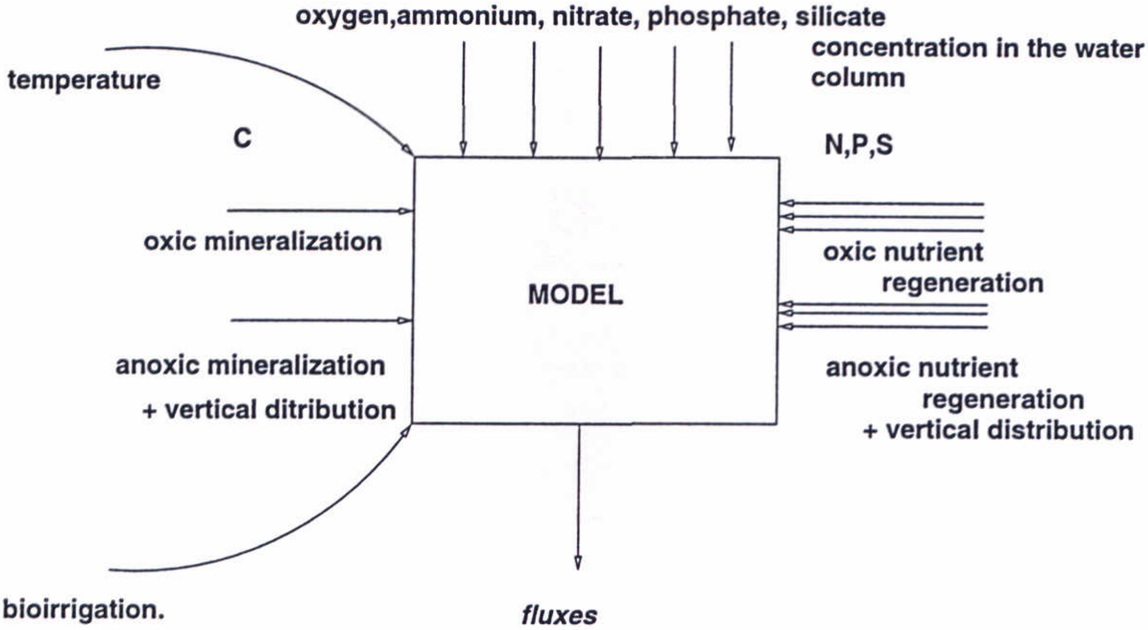

Fig. 1. The input/output information stream into/from the model.

6.5.1 Introduction

The benthic nutrient model GEMSED was originally developed for the ERSEM-model (Baretta *et al.*, 1995), with which include all major cycli of all important macronutrients (C,N,P,SI) The present approach concerns a conceptual model with a low number of state variables and parameters, in which only a limited amount of *a priori* knowledge of the processes dominating the benthic system is incorporated. In summary the original aim of this this was twofold:

- to construct nutrient models for the sediments including all important early diagenetic processes for the whole North Sea and describing the direct and indirect effects of the deposition of particulate organic matter on the nutrient cycles in space and time;
- to develop and test a computationally efficient method to model the dynamical behaviour of nutrient pore-water profiles but especially nutrient fluxes.

The input to this submodel is summarized in Fig. 1. The submodel needs in order for the calculation of the profiles the actual values of the mineralizations fluxes (oxic and anoxic), the regeneration fluxes (oxic and anoxic) and N, P and Si. Also it needs a value which describes the vertical exponential distribution of the anoxic mineralizations and regenerations. The model itself calculate only fluxes with which each time step the state variables are updated.

6.5.2 The coupling of GEMSED to GEM

The coupling og GEMSED to GEM is a complicated task. In the first place about 30 values representing state variables, fluxes and forcing are needed to describe the exchange of information between GEM and GEMSED and in the second place an auxilarly submodel, also orginating from

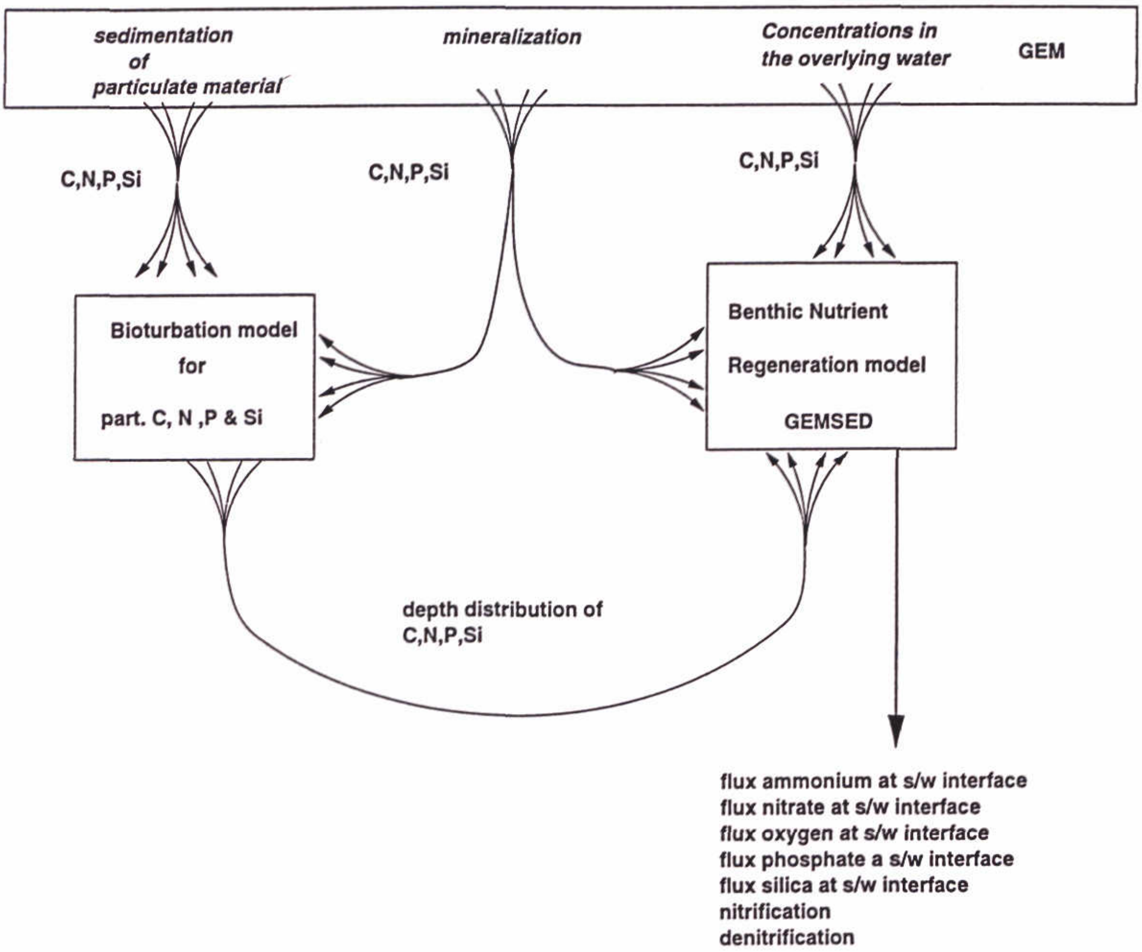

Fig. 2. The detailed representation of coupling between GEM and GEMSED

the ERSEM had to be included describing the transport and reworking of the particulate material by macrobenthos. The necessity for such inclusion follows from the way on which the anoxic mineralization of detritus is formulated in the orignal ERSEM-model In that model the assumption is made that the vertical distribution of the particulate detritus in the sediment is negative exponential. With the (ERSEM-)bioturbation model the variable representing the negative exponent is dynamically modelled for all particulate constituents seperately.

In Fig. 2 the coupling is visualized in tables 1 and 2 detailed lists are given of input and output variables to and from the GEMSED model. With the sedimentation rate in the bioturbation model the depth distribution can be corrected. The same is valid for the mineralization rates, however there the "average" depth where the mineralization take place has to be given as additional information in order to correct the depth distribution in a correct way. Be aware that NOT the concentration of detritus is modelled in the bioturbation model; this one is already present in the GEM model.

Table 1. I/O to/from Benthic nutrient regeneration model

I/O	Type		GEM Name	unit
Input	segment-dependent parameters			
	porosity		Poros	-
	phosphate adsorp. coef.		KdPO4AAP	-
Input-rates	oxic mineralization	C	dMinPOCox	$gC\ m^{-2}\ d^{-1}$
		N	dMinPONox	$gN\ m^{-2}\ d^{-1}$
		P	dMinPOPox	$gP\ m^{-2}d^{-1}$
	anoxic mineralization	C	dMinPOCred	$gC\ m^{-2}\ d^{-1}$
		N	dMinPONred	$gN\ m^{-2}\ d^{-1}$
		P	dMinPOPred	$gP\ m^{-2}\ d^{-1}$
Input state variables	concentration in the overlying water	O_2	OXY	gO_2m^{-3}
		NH_4^+	NH4	$gN\ m^{-3}$
		NO_3^-	NO3	$gN\ m^{-3}$
		PO_4^{3-}	PO4	$gP\ m^{-3}$
Input forcing	temperature			°C
	depth distribution of	C	*See table 2*	m
	(calculated in	N	*See table 2*	m
	(bioturbation model)	P	*See table 2*	m
Output rates	nitrification			$gN\ m^{-2}\ d^{-1}$
	denitrification			$gN\ m^{-2}\ d^{-1}$
	flux at water/sediment interface	at		
		O_2	FGSOX	$gO_2m^{-2}\ d^{-1}$
		NH_4^+	FGSNH4	$gN\ m^{-2}\ d^{-1}$
		NO_3^-	FGSNO3	$gN\ m^{-2}\ d^{-1}$
		PO_4^{3-}	FGSPO4	$gP\ m^{-2}\ d^{-1}$
	nett rate of change in pore water in the oxic layer	O_2	GSOXY	$gO_2m^{-2}\ d^{-1}$
		NH_4^+	GSNH4OX	$gN\ m^{-2}\ d^{-1}$
		PO_4^{3-}	GSPO4OX	$gP\ m^{-2}\ d^{-1}$
	nett rate of change in pore water in the anoxic layer	NH_4^+	GSNH4RED	$gN\ m^{-2}\ d^{-1}$
		PO_4^{3-}	GSNH4RED	$gP\ m^{-2}\ d^{-1}$
	nett rate of change in pore water in the sediment	reduc. equiv.	GSRED	$gS\ m^{-2}\ d^{-1}$
		NO_3^-	GSNO3	$gN\ m^{-2}\ d^{-1}$
	nett rate of change of O_2 -penetration depth.		GSDOM	md^{-1}

6.5.3 Basic concepts

The basis for our models is the general diagenetic equation developed in Berner (1980). For any component dissolved in the pore water this equation takes the form:

$$\frac{\partial \phi C}{\partial t} = \frac{\partial(\phi D \frac{\partial C}{\partial z})}{\partial z} - \frac{\partial(\phi \omega C)}{\partial z} + \phi \Sigma R \qquad (1)$$

where

C: Concentration of the component dissolved in the pore water ($mmol{\cdot}m^{-3}$).

Table 2. I/O to/from Bioturbation model (auxilary model)

I/O	Type	Depth	GEM Name	unit
Input	particulate sedimentation flux C	0		gC $m^{-2}d^{-1}$
	N	0		gN m^{-2} d^{-1}
	P	0		gP m^{-2} d^{-1}
	oxic mineralization C	average	dMinPOCox	gC $m^{-2}d^{-1}$
	N	of the oxic layer	dMinPONox	gN $m^{-2}d^{-1}$
	P		dMinPOPox	gP $m^{-2}d^{-1}$
	anoxic mineralization C	average	dMinPOCred	gC $m^{-2}d^{-1}$
	N	of the anoxic layer	dMinPONred	gN $m^{-2}d^{-1}$
	P		dMinPOPred	gP $m^{-2}d^{-1}$
	transport of oxic C	Δ (depth)		gC $m^{-2}d^{-1}$
	to anoxici layer N			gN $m^{-2}d^{-1}$
	P			gP $m^{-2}d^{-1}$
Output	total rate of change of C		GSDCM	m
	state variable representing N		GSDNM	m
	depth distribution of P		GSDPM	m

t: time (day).

z: depth in the sediment, zero at the sediment-water interface (m).

ϕ: volumetric porosity (-).

D: whole sediment diffusion coefficient ($m^2 \cdot d^{-1}$).

ω: whole sediment advection constant ($m \cdot d^{-1}$).

ΣR: the sum of all reactions and transformations affecting C ($mmol \cdot m^{-3} \cdot d^{-1}$).

All parameters of eq. (1) may vary with depth and can be a function of other components. This implies that eq. (1) represents a set of equations coupled through the parameters. To give an example, NO_3^- production through nitrification is directly coupled to both O_2 and NH_4^+. The vertical variability of the parameters is covered in the models by schematizing the sediment into a limited number of layers. Our main objective is to adequately describe fluxes at the sediment-water interface, rather than to simulate vertical concentration profiles in great detail. Thus we refrain from using a large number of thin layers, but restrict the schematization to three functional layers: 1- the oxic layer, in which O_2 serves as main electron acceptor; 2- the denitrification layer, in which nitrate is reduced; 3- the sulphide layer, in which Mn(IV), Fe(III) and sulphate are reduced through mineralization of organic matter. In each of these layers eq. (1) is applied with depth invariant parameters. The layers are linked by stating continuity in both concentrations and fluxes at the boundaries. The other simplifications are:

- all loss processes are modelled as first-order reactions, productions are assumed to have zero-order kinetics;

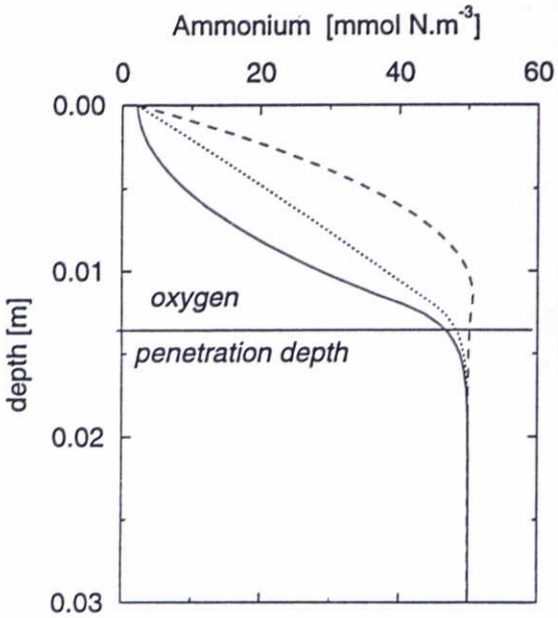

Fig. 3. An example of an initial profile P_{in} (solid line)obtained from the preceding time step, a steady state profile P_{eq} (dashed line) and a transient profile P_{tr} (dotted line) for ammonium. See text for further explanation .

- fast adsorption is included as an instantaneous equilibrium reaction (Berner, 1976);
- advection is ignored as relatively unimportant in comparison to diffusion and the other processes concerned.

Now for each of the layers the basic equation becomes:

$$(p+1)\frac{\partial C}{\partial t} = D\frac{\partial^2 C}{\partial z^2} - kC + M \qquad (2)$$

in which:

k: first-order loss rate constant (d^{-1}).

M: zero-order production rate constant (mmol·m^{-3}·d^{-1}).

p: dimensionless distribution coefficient defined as the proportion between the concentration of the adsorbed and dissolved constituent, respectively.

6.5.4 Simulation of fluxes and gradients

The model is based on analytical solutions of eq. (2). Obviously, full dynamic solutions of eq. (2) cannot always be found and the approach would then lead to serious mathematical problems. Instead we approximate the dynamical behaviour starting from steady-state solutions of eq. (2). Subsequently we make corrections to account for the effect of changing fluxes and profiles within a time-step. This sequence (steady state, corrections) is performed every time-step of a simulation run. The steady-state solutions are obtained by standard numerical techniques (Press *et al.*, 1986) after introduction of the time-step dependent boundary conditions and parameter values. The need for correction is based on the consideration that it takes some time to reach a new steady state and that steady-state fluxes and profiles may not be established within a single time step. Consequently the steady-state fluxes do not represent time-step averaged fluxes, even when steady-state actually is reached within a time step. The average profiles and hence the time-step dependent fluxes depend also on the initial profiles. To account for this we distinguish three concentration profiles for each layer (Fig. 3): 1. the initial profile (P_{in}) obtained from the preceding time step; 2. the equilibrium profile (P_{eq}) finally to be obtained at steady-state conditions and 3. the transient profile (P_{tr}) defined as the time averaged profile underway from P_{in} towards P_{eq}. The correction thus consists of calculating P_{tr} and its associated fluxes.

The calculation is done in an indirect way. The associated depth averaged concentrations $\overline{C_{in}}$ and $\overline{C_{eq}}$ are determined from P_{in} and P_{eq}, respectively, and are used to calculate $\overline{C_{tr}}$ according to:

$$\overline{C_{tr}} = \overline{C_{eq}} + (\overline{C_{in}} - \overline{C_{eq}}) \cdot (1 - e^{-\frac{\Delta t}{t_a}}) \cdot \frac{t_a}{\Delta t} \tag{3}$$

in which Δt is the time step and t_a the adaptation time.

From the analytical solution of the general dynamical equation (Carslaw & Jaeger, 1946) the adaptation time (t_a) is derived and is defined as (Ruardij & van Raaphorst, 1995):

$$t_a = \frac{p + 1}{k + \pi^2 D/H^2} \tag{4}$$

in which D is the diffusion coefficient in the layer and H is the thickness of the layer in which C is defined Subsequently, P_{tr} is calculated under the constraint that the average value of C is $\overline{C_{tr}}$.

To calculate P_{tr} we assume that changes from time step to time step are small in the deeper layers and that the shapes of the profiles within the individual layers are close to their steady state. In other words, we expect 'pseudo steady state' in the layers, however, without 'equilibrium' between the layers. Thus P_{tr} is calculated from the steady-state solutions of eq. (2), creating a fictitious mineralization term to match $\overline{C_{tr}}$ in the upper layer and P_{in} in both lower layers. From P_{tr} the concentration gradients at the interfaces and associated fluxes are calculated, as well as all first-order loss processes. Subtracting the fluxes and losses from the original and true mineralization yields the total change $\overline{\Delta C}$ in the layers. This value is transferred to the integration subroutine of the simulation package for the calculation of the next $\overline{C_{in}}$ after Δt.

The applied calculation scheme is robust, but gives only acceptable results when the changes ΔC during a time step are not too large. This is extensively tested with the ERSEM-model which make use use of an adaptive time-step algorithm that minimizes the step sizes at large values of ΔC (Ruardij & van Raaphorst, 1995).

Especially in cases of thin layers changes of the input fluxes to the submodel (mineralization fluxes), are directly taken in account by correcting the vertical profile and hence all output fluxes (especially vertical fluxes) are directly adapted to the input.

6.5.5 The submodels

Below we describe the submodules for ammonium, nitrate, phosphate and silica. The interrelations between the different submodules are given in Fig. 4. As mentioned in the introduction, the sediment is divided into three functional layers (oxic layer, denitrification layer and sulphide layer). The depths of the interfaces between these layers are dynamically modelled and are coupled to the

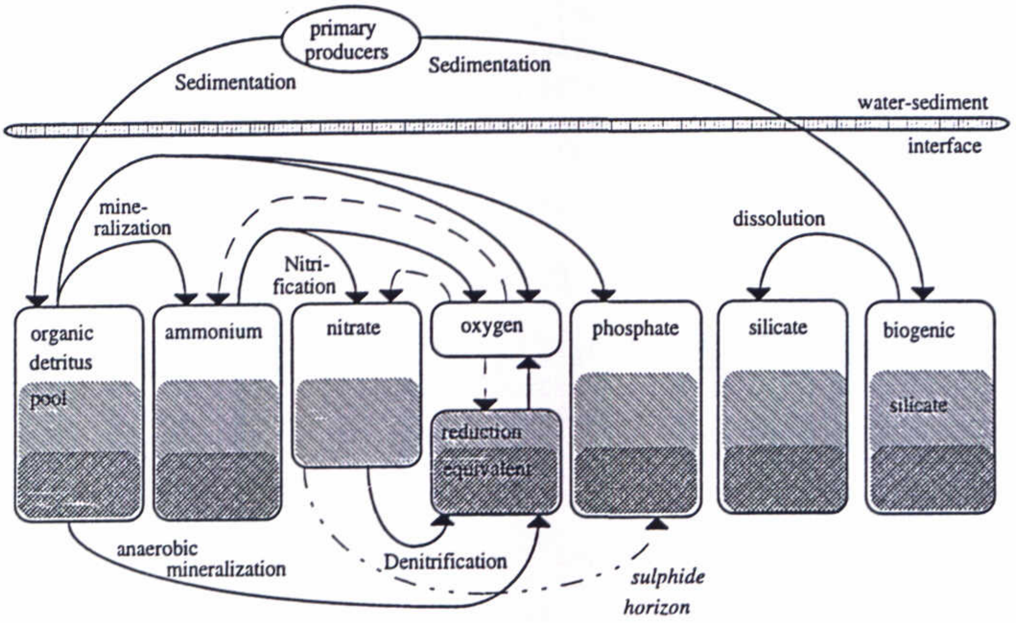

Fig. 4. The interrelations ('arrows') between the different submodules. The input to the benthic system is controlled by the settling of remains of phytoplankton. This input arrives in the benthic organic pool (particulate carbon including N and P) or in the biogenic silica pool. The main driving and controlling force of the benthic nutrient processes is mineralization: phosphate, ammonium, oxygen and reduction equivalents are directly affected. Nitrate is coupled to mineralization through nitrification. The oxygen consumption by mineralization, nitrification and oxidation of reduction equivalents determines the interstitial oxygen concentration and the oxygen penetration depth. The oxygen penetration (dashed lines) modifies the nutrient dynamics considerably. The sulphide horizon depth (dotted- dotted line), derived from the nitrate module controls the adsorption properties of phosphate. Silicate is the only nutrient which is not affected by one of the other variables.

diagenetic redox processes. The upper interface is the oxygen penetration depth (z_{ox}). The second interface, the sulphide horizon (z_{an}) is the depth at which sulphate reduction becomes dominant. In between these surfaces nitrate is assumed to be the main oxidant. Manganese and iron are assumed to occur in their oxidized forms in the upper two layers and in their reduced forms below the second interface. Particularly the reduction of Fe(III) to Fe(II) is important to describe different sorption properties of phosphate in the upper two and in the lower layers. The reduction of electron acceptors and the production of ammonium and phosphate are related to the decomposition of organic matter. Decomposition fluxes are obtained from the decompoition module of GEM (See chapter 6) Other variables directly related to the activity of benthic organisms, such as bioirrigation and bioturbation, are calculated also available in GEM. Burial of organic matter and nutrients is not incorporated in the present GEMSED submodel. In the GEMSED-version of this regeneration model silica is not included. The lack of knowledge about the diagenetic silica processes has lead to the conclusion that the application of this model concept is not useful. Moreover because silica uptake of benthic diatoms is not included (until now) in the orginal ERSEM-version.

BOX 1 *Set of equations in the ammonium and nitrate model*

$$
\begin{aligned}
(p+1)\frac{\partial A(z)}{\partial t} &= D_A \frac{\partial^2 A(z)}{\partial z^2} - kA(z) + M_A && (0 \le z \le z_{oz}) \\
\frac{\partial N(z)}{\partial t} &= D_N \frac{\partial^2 N(z)}{\partial z^2} \quad + kA(z) && (0 \le z \le z_{oz}) \\
(p+1)\frac{\partial A(z)}{\partial t} &= D_A \frac{\partial^2 A(z)}{\partial z^2} \quad + M_A e^{-\alpha\zeta} && (z > z_{oz}) \\
\frac{\partial N(z)}{\partial t} &= D_N \frac{\partial^2 N(z)}{\partial z^2} \quad - d_N N(z) && (z > z_{oz})
\end{aligned}
$$

where:

$A(z)$: ammonium concentration in the pore-water (mmol $N \cdot m^{-3}$).
$N(z)$: nitrate concentration in the pore-water (mmol $N \cdot m^{-3}$).
z_{oz}: oxygen penetration depth (m).
$\zeta = z - z_{oz}$ (m).
D_A: whole sediment diffusion constant of ammonium ($m^2 \cdot d^{-1}$).
D_N: whole sediment diffusion constant of nitrate ($m^2 \cdot d^{-1}$).
k: specific nitrification rate (d^{-1}).
d_N: specific denitrification rate (d^{-1}).
M_A: ammonium production through mineralization in the oxic layer (mmol $N \cdot m^{-3} \cdot d^{-1}$).
α: constant, describing the exponential decrease of mineralization with depth (m^{-1}).
p: adsorption distribution coefficient of ammonium (-).

The equations for each nutrient are linked by stating continuity in the concentration and the flux at $z = z_{oz}$. The boundary conditions are for $z = 0$: $A = A(0)$ and $N = N(0)$ and for $z \to \infty$: $\partial A / \partial z = 0$ and $N(z) \to 0$.

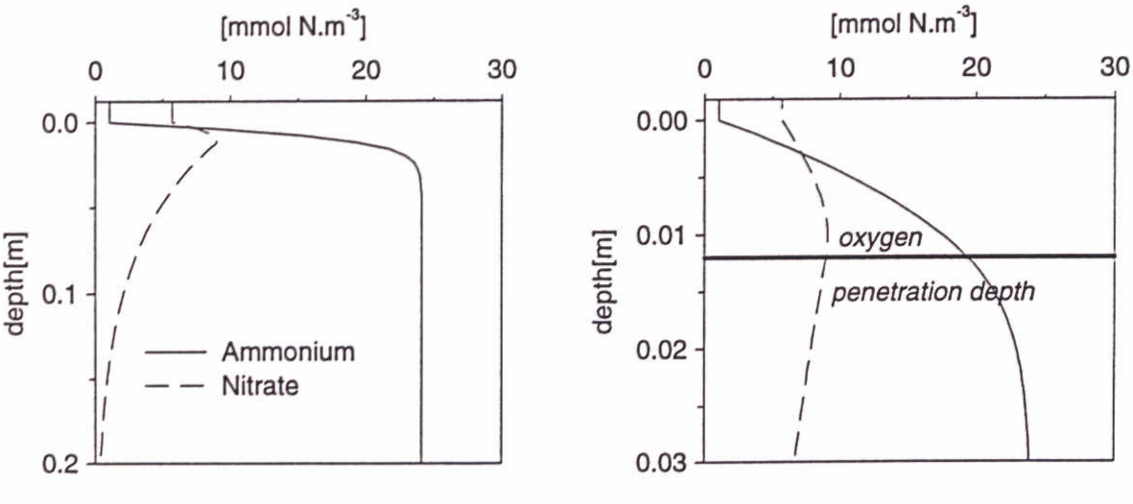

Fig. 5. Steady-state profiles for ammonium and nitrate in the upper 20 cm and upper 3 cm of the sediment obtained from the equations listed in Table 1.

AMMONIUM

Mineralization is the main process controlling ammonium dynamics. Other processes are nitrification, adsorption and of course vertical transport. We apply the steady state model described by Van

BOX 2 *Set of partial differential equations applied for phosphate.*

$$
\begin{aligned}
(p_{oz}+1)\frac{\partial P(z)}{\partial t} &= D_P\frac{\partial^2 P(z)}{\partial z^2} + M_P & (0 \le z \le z_{oz})\\
(p_{oz}+1)\frac{\partial P(z)}{\partial t} &= D_P\frac{\partial^2 P(z)}{\partial z^2} + M_P e^{-\alpha\zeta} & (z_{oz} < z \le z_{an})\\
(p_{an}+1)\frac{\partial P(z)}{\partial t} &= D_P\frac{\partial^2 P(z)}{\partial z^2} + M_P e^{-\alpha\zeta} & (z > z_{an})
\end{aligned}
$$

In these equations:

$P(z)$: phosphate concentration in the pore-water (mmol P·m^{-3} pw).
z_{oz}: oxygen penetration depth (m).
z_{an}: sulphide horizon (m).
$\zeta = z - z_{oz}$ (m).
D_P: whole sediment diffusion constant for phosphate (m^2·d^{-1}).
M_P: phosphate production through mineralization in the oxic layer (mmol P·m^{-3}·d^{-1}).
α: constant, describing the exponential decrease of mineralization with depth (m^{-1}).
p_{oz}: adsorption distribution coefficient of phosphate in the oxic and denitrification layer (-).
p_{an}: adsorption distribution coefficient of phosphate in the sulphide layer (-).

The 3 equations are linked by stating continuity in the concentration and the flux at the interfaces between the 3 layers. The boundary conditions are $z = 0 : P = P(0)$ and $z \to \infty$: $\partial P(z)/\partial z \to 0$.

Raaphorst *et al.* (1990) that in turn is a modification of the models of Vanderborght & Billen (1975) and Vanderborght *et al.* (1977). In their nitrate models Goloway & Bender (1982) and Jahnke *et al.* (1982) assumed that ammonium released during oxidation of organic matter is immediately converted into nitrate when sufficient oxygen is present, without any build-up of reaction intermediates. When describing both nitrate and ammonium, such a rapid conversion is best formulated as a first-order nitrification rate. This approach is further justified by the expected ammonium concentrations in the oxic few upper mm of the sediment in most of the ERSEM-segments (< 25 mmol N·m^{-3}), which are low compared to the half saturation constant for ammonium oxidation (Henriksen & Kemp, 1988). The adsorption of ammonium onto sediment particles by ion exchange reactions is considered a fast process and consequently the ammonium distribution between the solvent (pore water) and the sorbent phase (sediment particles) is assumed to be in equilibrium. The equilibrium distribution is mostly characterized by a linear distribution coefficient (Mackin & Aller, 1984) and is implemented in the model as a reduction of the apparent rate parameters (*e.g.* mineralization, nitrification and diffusion) (Berner, 1976). Following Vanderborght & Billen (1975) the sediments are partitioned in two layers: a nitrification zone extending from $z = 0$ at the sediment surface to the oxygen penetration depth (z_{oz}), and a zone below where nitrification is absent. The ammonium production is described by a zero-order reaction in the upper layer and with a declining exponential term in the lower layer. The set of partial differential equations for ammonium is given in box 1. In Fig. 5 an example of a steady-state ammonium profile is given.

NITRATE

Nitrate is coupled to ammonium through nitrification in the oxic layer. Denitrification is described as a first-order loss process. Steady state models to describe nitrification and denitrification including vertical transports are well-established (Vanderborght & Billen, 1975; Vanderborght *et al.*, 1977;

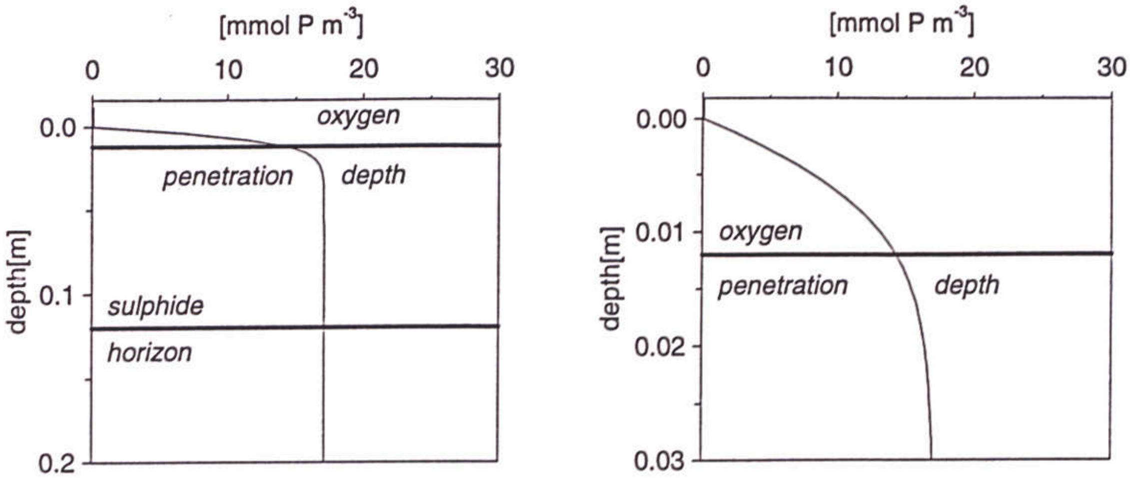

Fig. 6. The steady state profiles for phosphate in first 20 cm and first 3 cm of the sediment.

Van Raaphorst *et al.*, 1990).

The general set of partial differential equations is given in box 1. Fig. 5 gives an example of a steady-state nitrate profile obtained with this set of equations.

PHOSPHATE

Adsorption is an important process in sedimentary phosphate dynamics (Van Raaphorst *et al.*, 1988; Sundby *et al.*, 1992). It is assumed that reduction of Fe(III) concurrently mobilizes Fe(II) and adsorbed phosphate in the sulphide layer. We expect that the nitrate concentration remains sufficiently high in the denitrification layer to inhibit the reduction of Fe(III). Thus it is assumed that the proportion between adsorbed and dissolved phosphate is considerably less (2:1, Krom & Berner, 1980) in the sulphide layer than in the upper two layers (250 to 400:1, see section 6.8.). Sorption of phosphate is considered as a fast process and consequently the phosphate concentration in the solvent phase (pore water) and the sorbent phase (sediment particles) are in equilibrium. The phosphate production in the oxic layer is described as a zero-order reaction declining exponentially below $z = z_{ox}$ and is stoichometrically coupled to the carbon and ammonium mineralization. The set of equations applied in the phosphate submodels is presented in box 2. An example of steady state phosphate profiles obtained with this set of equations is given in Fig. 6.

6.5.6 Reduction equivalents

In the North Sea the oxygen penetration in sediments varies from a few mm in coastal to a few cm in off-shore areas (Lohse *et al.*, 1993). Nitrate may penetrate much deeper than oxygen (Jørgensen, 1989; Van Raaphorst *et al.*, 1990). In the reduced sediment below, sulphate reduction mostly is the dominant process in the degradation of organic matter (Froelich *et al.*, 1979). Modelling of the anaerobic oxidation reactions is important for two reasons. First, it is necessary to maintain mass conservation. Second, ions reduced by anaerobic mineralization can substantially add to oxygen

BOX 3 *Set of partial differential equations applied for reduction equivalents.*

$$\frac{\partial R(z)}{\partial t} = D_S \frac{\partial^2 R(z)}{\partial z^2} - M_r \qquad (0 \leq z \leq z_{ox})$$

$$\frac{\partial R(z)}{\partial t} = D_S \frac{\partial^2 R(z)}{\partial z^2} + M_o e^{-\alpha\zeta} - \xi_d d N(z) \qquad (z > z_{ox})$$

In these equations:

$R(z)$: reduction equivalent concentration in the pore-water(mmol $O_2 \cdot m^{-3}$).
= (- O_2concentration in the pore water)
$N(z)$: nitrate concentration in the pore water (mmol $N \cdot m^{-3}$).
z_{ox}: oxygen penetration depth (m).
$\zeta =$ $z - z_{ox}$ (m).
D_S: diffusion coefficient of sulphide ($m^2 \cdot d^{-1}$).
M_o: formation of reduction equivalents through anoxic carbon mineralization (mmol $O_2 \cdot m^{-3} \cdot d^{-1}$).
α: constant, describing the exponential decrease of mineralization with depth (m^{-1}).
M_r: zero-order coefficient describing the oxidation of reduction equivalents by O_2 (mmol $O_2{}^{2-} \cdot m^{-3} \cdot d^{-1}$).
d: first-order denitrification rate for oxidation of organic carbon by nitrate (d^{-1}).
ξ_d: denitrification stoichiometric factor (= 0.3 mmol $O_2 \cdot$ (mmol N)$^{-1}$).

M_r is unknown and calculated from the steady-state solution. The two equations are linked by stating continuity in the concentration and the flux at $z = z_{ox}$. The boundary conditions are $z = 0$: $R = 0$ and $\partial R/\partial z = 0$ and $z \rightarrow \infty$: $\partial R/\partial z \rightarrow 0$.

BOX 4 *Set of partial differential equations for oxygen.*

$$0 = D_{Ox} \frac{\partial^2 Ox(z)}{\partial z^2} - M - \eta_r M_r - M_n \qquad (0 \leq z \leq z_{ox})$$

$$z_{ox} = \sqrt{\frac{2DOx_0}{M + \eta_r M_o + M_n}}$$

$$z_{an} = \log 0.10/\sqrt{d/D_N} + z_{ox}$$

in which:

Ox: O_2 (mmol $O_2 \cdot m^{-3}$).
z_{ox}: O_2 penetration depth (m).
z_{an}: sulphide horizon (m).
D_{Ox}: diffusion constant of oxygen ($m^2 \cdot d^{-1}$).
D_N: diffusion constant of nitrate ($m^2 \cdot d^{-1}$).
M: zero-order O_2 consumption rate (mmol $O_2 \cdot m^{-3} \cdot d^{-1}$).
M_r: zero-order oxidation rate of reduction equivalents (mmol $S^{2-} \cdot m^{-3} \cdot d^{-1}$).
η_r: O_2:S^{2-}conversion factor (=2 (mmol O_2)$\cdot$(mmol S)$^{-1}$).
d: denitrification constant (d^{-1}).
M_n: average nitrification rate (mmol $O_2 \cdot m^{-3} \cdot d^{-1}$). Defined as:

$$M_n = \frac{\xi_k k}{z_{ox}} \int_{z=0}^{z_{ox}} A(z) dz$$

k: nitrification constant (d^{-1}).
ξ_k: nitrification stoichiometric factor (= 2 mmol $O_2 \cdot$(mmol N)$^{-1}$).
$A(z)$: NH_4^+ concentration (mmol $N \cdot m^{-3}$).

The boundary condition for the equation are $z = 0$: $Ox = Ox(0)$ and $z \geq z_{ox}$: $Ox(z) = 0$.

demands in the oxic sediment layer and thus influence the oxygen penetration depth (Billen, 1982). Oxidation of reduced components as Fe(II), Mn(II) or HS^- may even dominate oxygen consumption rates at specific locations during certain periods in the seasonal cycle (Canfield *et al.*, 1993).

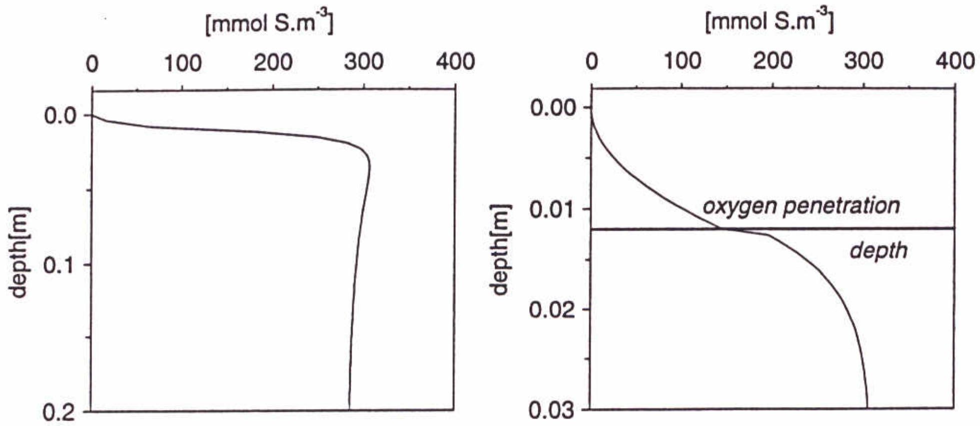

Fig. 7. Steady-state profile for reduction equivalents in the upper 20 cm and upper 3 cm of the sediment.

Modelling of all the redox elements explicitly is not necessary, however, for our purpose. Instead we make use of the negative oxygen concentration as modelled in GEM representing all reduced components except nitrate generated in the denitrification and sulphide layer. This negative concentration can be considered as a pool of reduced ions with the properties of the most common one, sulphide (*e.g.* diffusion coefficient). The reduction equivalents diffuse upward towards the oxic layer where they are oxidized by O_2, we assume that they are not oxidized by NO_3^-. The oxidation rate M_r is determined from the additional boundary condition $\partial R/\partial z = 0$ at $z = 0$. The general set of partial differential equations applied to reduction equivalents is given in box 3. Examples of steady-state profiles obtained with this set of equations are given in Fig. 7.

6.5.7 Oxygen penetration depth and sulphid horizon

The oxygen penetration depth (z_{ox}) and the depth at which the sulphate reduction starts (z_{an}) have to be known before the nutrient equations can be solved. Mineralization of organic matter is the main O_2-consuming process, but nitrification and oxidation of reduced ions can enhance the O_2 consumption considerably. We apply the model of Bouldin (1968) to calculate the O_2 profiles and penetration depths (box 4). In contrast to Bouldin (1968), however, we included zero-order consumption rates to take nitrification and oxidation of reduction equivalents into account. The interface between the denitrification layer and the sulphide layer (z_{an}), called the sulphide horizon, is derived from the nitrate submodel. The nitrate gradient shows an exponential decrease with depth due to denitrification below z_{ox} (Fig. 5). Following the criterion of Van Raaphorst *et al.* (1990) we defined the sulphide horizon (z_{an}) as the depth at which denitrification has decreased to 10% of its initial value at the oxygen penetration depth (box 4).

Each detritus component in the ERSEM model on which this GEMSED model is based is described by the mass but also by a state variable which describes the vertical distribution. This vertical distribution is assumed to be exponential and hence the state variable describes the mean intrusion

Table 3.
Overview of the input variables into the benthic nutrient model.

variable	*variable type*	*calculated in submodel*
P-mineralization	rate	benthic biology model
N-mineralization	rate	benthic biology model
O_2-mineralization	rate	benthic biology model
temperature	forcing function	
bioirrigation	environmental variable	benthic biology model
porosity	environmental variable	parameter

depth of component into the sediment. The main purpose in ERSEM however was the modelling in a simple way of the bioturbation. In this way microbiological activity and nutrient production by decomposition will depend on detritus density and composition at different depths. The GEMSED-version of this (bioturbation) submodel in the GEM-environment aims only to estimate the intrinsic depth from the particulate transport dynamics in the sediment as modelled in GEM. Therefore in the GEM-model on all places where rates are calculated modifying the concentration of particulate marerial an extra rate definition has to be defined with which the total change of the intrinsic depth can be derived:

$$\Delta D_i = (d - D_i)\frac{f}{\Sigma Q} \tag{5}$$

in which:

D_Q: the intrinsic depth of particulate constituent Q (m)

ΔD_Q: Rate of change of D_Q (m d^{-1})

d: Everage depth at which change in Q take place (m).

f: Rate of change of Q (mg $m^{-2}d^{-1}$).

ΣQ: Total amount of Q present in the sediment(mg m^{-2}).

6.5.8 External forcing

The forcing parameters are divided in 2 groups. The first group consists of parameters which are calculated outside the nutrient submodels and from there are introduced into the benthic nutrient submodels (Table 3). All mineralization rates are within this group of external parameters. The second group of parameters is specified in the benthic nutrient submodels. These parameters may be corrected for temperature, bioirrigation and porosity of the sediments. The latter three variables are either taken as forcing functions from outside the ERSEM model, or are calculated in the benthic biology model (Ebenhöh *et al.*, 1995).

The main source of organic matter to the benthic system is detritus, generated in the pelagic system and deposited on the sea floor or filtered by suspension feeders. Subsequently the detritus is redistributed in the sediment by particulate transport and bioturbation and decomposed by benthic organisms. All these processes are described in the benthic biology model. In our model it is assumed that the detritus is exponentially distributed with depth. The steepness of this exponential distribution is recalculated from the output of the benthic biology model. The decomposition of organic matter in the benthic biology model is effectuated by bacteria and macro benthos which consume detritus for their growth. In the benthic biology model it is assumed that all benthic organisms live in the oxic layer. For the thickness of this layer the value of z_{ox} from the previous time step is used. The total mineralization in the oxic layer is derived from the sum of all respirations (O_2) and all excretions (N and P) of the benthic organisms in this layer. In the other layers the mineralization is caused by the activity of anaerobic bacteria. These mineralizations are the main input to the benthic nutrient model. The parameter α is calculated from the difference between the oxic and anoxic mineralizations (see Boxes 1, 2 & 3):

$$M = \frac{\overline{\mathcal{M}}}{\alpha \cdot H}(1 - e^{-\alpha H}) \tag{6}$$

where M is the average mineralization in the oxic layer (mmol·m^{-3}·d^{-1}), $\overline{\mathcal{M}}$ is the depth-averaged mineralization in the in the layers below $z = z_{ox}$ (mmol·m^{-3}·d^{-1}) and H (=0.3$-z_{ox}$) is the thickness of the 2 lower layers (m).

The physical characteristics of the sediments in the GEMSED segments are important factors for the diagenetic processes in the sediments. In table 1 two parameters can be found which are segment dependent: the porosoty (fraction of water in the sediment) and the adsorption capacity of the sediment for phosphate to iorn. Pororsity and sedimentary contents of reactive components as *e.g.* Fe are in field observations often correlated with grain size distribution (Mackin & Aller, 1984; Wiesner *et al.*, 1990). If not values are availble for these parameters for all segments in the ERSEM the values for these parameters were derived from observations on the weight fraction of particles with the grain size smaller than 63 μm in the sediment:

$$\phi = 0.38662 + 0.0425 p_s \tag{7}$$

$$k_d = 4.031 p_s \tag{8}$$

$$p_p = k_d \frac{(1-\phi)}{\phi} \rho \tag{9}$$

in which

p_s: fraction of sediment with grain szie $< 63\mu$m

ϕ: porosity

k_d: adsorption coefficient (ml/mg)

p_p: adsorption distribution coefficient (-)
(=dimensionless adsorption coefficient)

ρ: density of sediment particles (g m^{-3})

These correlations were found in a large dataset collected in the sediments of the North Sea.

Acknowledgements.— This research was partly funded by the European Community under MAST contract number CT90-0021. Additional funds were supplied by BEON (proj. nr. NIOZ 92 E 03). Most field data were obtained from two BELS-cruises financially supported by the Netherlands Marin Research Foundation (grant 39104). We thank Leo Maas for mathematical advice during the devolpment of the model.

REFERENCES

BARETTA, J. W., W. EBENHÖH & P. RUARDIJ, 1995. The European Regional Ecocsystems Model, a complex marine ecosystem model. – Neth. J. Sea Res. **33**, 233–246.

BERNER, R. A., 1976. Inclusion of adsorption in the modelling of early diagenesis. – Earth Planet. Sci. Letters **29**, 333–340.

BERNER, R. A., 1980. Early diagenesis: A theoretical approach. Princeton Univ. Press, Princeton.

BILLEN, G., 1982. An idealized model of nitrogen recycling in marine sediments. – Am. J. Sci. **282**, 512–514.

BOULDIN, D. R., 1968. Models for describing the diffusion of oxygen and other mobile constituents across the mud-water interface. – J. Ecol. **56**, 77–87.

CANFIELD, D. E., B. B. JØRGENSEN, H. FOSSING, R. GLUD, J. GUNDERSEN, N. B. RAMSING, J. W. HANSEN, L. P. NIELSEN & P. O. J. HALL, 1993. Pathways of organic carbon oxidation in three continental margin sediments. – Mar. Geol. **113**, 27–40.

CARSLAW, H. S. & J. C. JAEGER, 1946. Conduction of heat in solids. Oxford University Press, London. 1-510.

EBENHÖH, W., C. KOHLMEIER & P. RADFORD, 1995. The benthic biological submodel in the European Regional Seas Ecosystem model. – Neth. J. Sea Res. **3/4**, 423–452.

FROELICH, P. N., G. P. KLINKHAMMER, M. L. BENDER, N. A. LUEDTKE, G. R. HEATH, D. CULLEN, P. DAUPHIN, D. HAMMOND, B. HARTMAN & V. MAYNARD, 1979. Early oxidation of organic matter in pelagic sediments of the eastern equatorial Atlantic: suboxic diagenesis. – Geochim. cosmochim. Acta **43**, 1075–1090.

GOLOWAY, F. & M. BENDER, 1982. Diagenetic models of interstitial nitrate profiles in deep sea sediments. – Limnol. Oceanogr. **27**, 624–638.

HENRIKSEN, K. & W. M. KEMP, 1988. Nitrification in estuarine and coastal marine environments. In T. H. Blackburn & J. Sørensen (Eds.), Nitrogen cycling in coastal marine environments, Volume 33 of *SCOPE*, pp. 207–249. Wiley & Sons, New York.

JAHNKE, R. A., S. R. EMERSON & J. W. MURRAY, 1982. A model of oxygen reduction, denitrification and organic matter mineralization in marine sediments. – Limnol. Oceanogr. **27**, 610–623.

JØRGENSEN, B. B., 1989. Sulphate Reduction in marine sediments from the Baltic Sea-North Sea transition. – Ophelia **31**, 1–15.

KROM, M. D. & R. A. BERNER, 1980. The diagenesis of phosphorus in a nearshore marine sediment. – Geochim. cosmochim. Acta **45**, 207–216.

LOHSE, L., J. F. P. MALSCHAERT, C. P. SLOMP, W. HELDER & W. VAN RAAPHORST, 1993. Nitrogen cycling in North Sea sediments: interaction of denitrification and nitrification in offshore and coastal areas. – Mar. Ecol. Prog. Ser. **101**, 283–296.

MACKIN, J. E. & R. C. ALLER, 1984. Ammonium adsorption in marine sediments. – Limnol. Oceanogr. **29**, 250–257.

PRESS, W. H., B. P. FLANNERY, S. A. TEUKOLSKY & W. T. VETTERLING, 1986. Numerical recipes. The art of Scientific Computing. Cambridge University Press, Cambridge.

RUARDIJ, P. & W. VAN RAAPHORST, 1995. Benthic nutrient regeneration in the ERSEM ecosystem model of the North Sea. – Neth. J. Sea Res. **3/4**, 453–483.

SUNDBY, B., V. GOBEIL, N. SILVERBERG & A. MUCCU, 1992. The phosphorus cycle in coastal marine sediments. – Limnol. Oceanogr. **37**, 1129–1145.

VAN RAAPHORST, W., H. T. KLOOSTERHUIS, A. CRAMER & K. J. M. BAKKER, 1990. Nutrient early diagenesis in the sandy sediments of the Dogger Bank area, North Sea: pore water results. – Neth. J. Sea Res. **26**, 25–52.

VAN RAAPHORST, W., P. RUARDIJ & A. G. BRINKMAN, 1988. The assessment of benthic phosphorus regeneration in an estuarine ecosystem model. – Neth. J. Sea Res. **22**, 23–36.

VANDERBORGHT, J.-P. & G. BILLEN, 1975. Vertical distribution of nitrate concentration in interstitial water of marine sediments with nitrification and denitrification. – Limnol. Oceanogr. **20**, 953–961.

VANDERBORGHT, J.-P., R. WOLLAST & G. BILLEN, 1977. Kinetic models of diagenesis in disturbed sediments. Part 2. Nitrogen diagenesis. – Limnol. Oceanogr. **22**, 794–803.

WIESNER, M. G., B. HAAKE & H. WIRTH, 1990. Organic facies of surface sediments in the North Sea. – Org. Geochem. **15**, 419–432.

6.6 Sediment-water interaction according to SWITCH

6.6.1 Introduction

SWITCH was developed as a submodel of the surface water eutrophication model DBS for the prediction of the nutrient fluxes across the sediment-water interface (DELFT HYDRAULICS, 1992). SWITCH distinguishes four sediment layers and calculates the thicknesses of the aerobic and denitrifying layers on the basis of a steady state approach. The concentrations of detritus, ammonium, nitrate, phosphate and silicate in the sediment and the pore water are simulated dynamically using mass balance equations. Details with respect to background, objectives, starting-points and formulations of SWITCH have been described in DELFT HYDRAULICS (1991a and 1994a). The first version of SWITCH and the application for Lake Veluwe have also been described by Smits and Van der Molen (1993).

The link between GEM and SWITCH is formed by the sediment-water exchange fluxes of dissolved oxygen, nutrients and organic matter. The net settling and resuspension fluxes of the particulate detritus components and adsorbed phosphate is input, whereas SWITCH delivers the oxygen and dissolved nutrient fluxes as output. Sediment layers are not present in GEM, when SWITCH is active. SWITCH acts directly on the water column, just like any other process routine.

6.6.2 Spatial schematization and processes

Figure 6.1 depicts the vertical schematization of the 'active' sediment layer in SWITCH. An overview of the processes included in SWITCH is given in Figure 6.2. The 'active' sediment layer has a constant thickness (d), and is divided in 4 sublayers. An upper layer (dh) and a lower layer ($dl=d_4$) have been defined in order to account for vertical characteristics such as decomposition of organic matter, dispersion and porosity. These layers are also fixed. A second partition follows from chemical differences. A thin toplayer (do) is oxidized, the remaining part ($dh-do = d_3$, > minimal value) of the upper layer is reduced. The oxidized layer is divided in an oxygen containing layer d_1 and a denitrifying layer d_2. Both d_1 and d_2 are variable, and are deduced from steady-state solutions of the mass balance equations for dissolved oxygen and nitrate. In order to avoid numerical problems neither do nor d_1 may become infinitely thin, a minimal thickness (do_m) has therefore been defined. However, the denitrifying layer disappears entirely, when the nitrate concentration drops below a critical value (Cn_c).

Additionally, a very thin meta-stable boundary layer has been defined, which receives the detritus settled from the overlying water and produced from microphytobenthos. From this layer detritus is incorporated in the sediment as the consequence of bioturbation. Nutrients produced from decomposition of detritus in the boundary layer or consumed in primary production by microphytobenthos are attributed or withdrawn from the oxygen containing layer. The same goes for the dissolved oxygen fluxes pertaining to these processes. The boundary layer does not affect the dispersion of dissolved substances across the sediment-water interface.

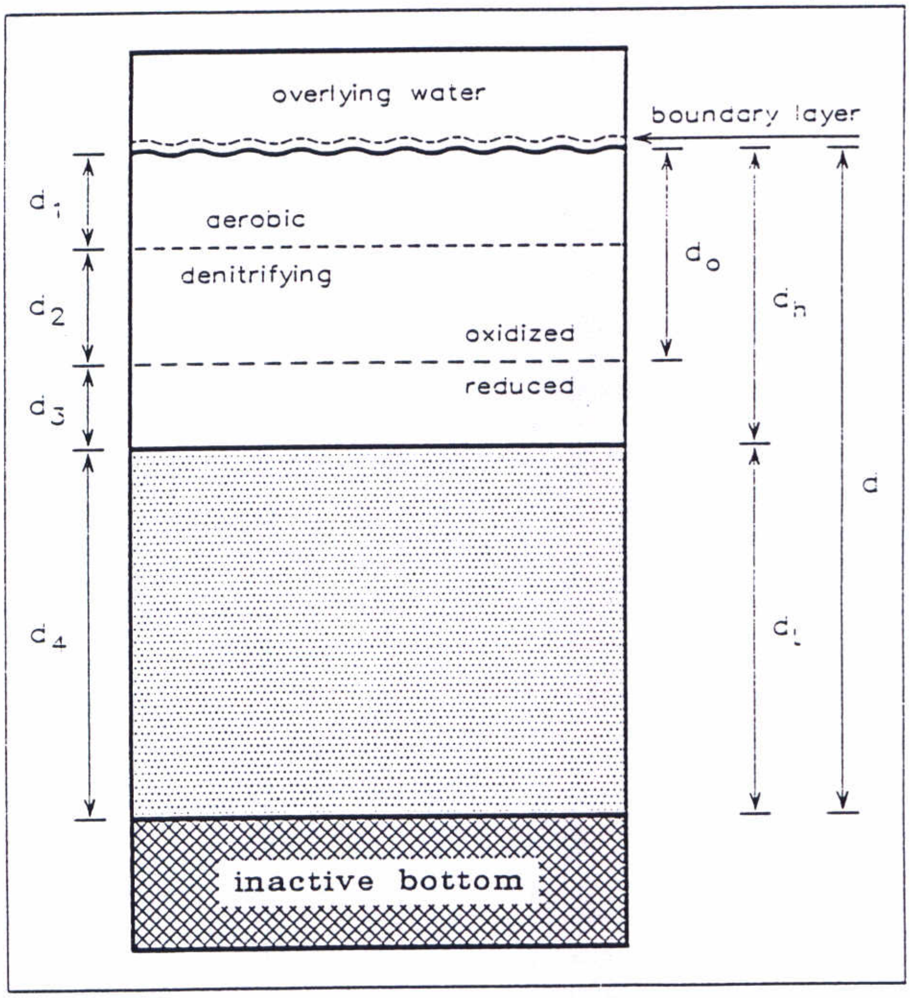

Figure 6.1 The schematization of the sediment layer in SWITCH.

6.6.3 The aerobic layer and the sediment oxygen demand

The thickness of the aerobic layer is dependent on the oxygen consumption rate according to the following steady-state equation:

$$d_1 = \sqrt{(2\, p_1.D.fo.Co_0 / Ro)} \qquad (6.6.1)$$

$$d_1 = do_m \text{ if } d_1 < do_m$$

in which:

Co_0 = oxygen concentration in the overlying water (g m^{-3})
do_m = minimal thickness of the oxidized layer (m)
D = dispersion coefficient ($m^2\ d^{-1}$)
fo = ratio of the oxygen concentrations at the upper and lower sides of the water boundary layer (-)
p = porosity (-)
Ro = oxygen consumption rate (g m^3 bottom d^{-1})
A subscript figure indicates a layer number or an interface number!

The introduction of ratio fo relates to the existence of a relatively stagnant boundary layer in the overlying water, which contains a part of the oxygen gradient at the sediment-water interface. The oxygen concentration at the interface is a certain fraction of the average oxygen concentration in the water column.

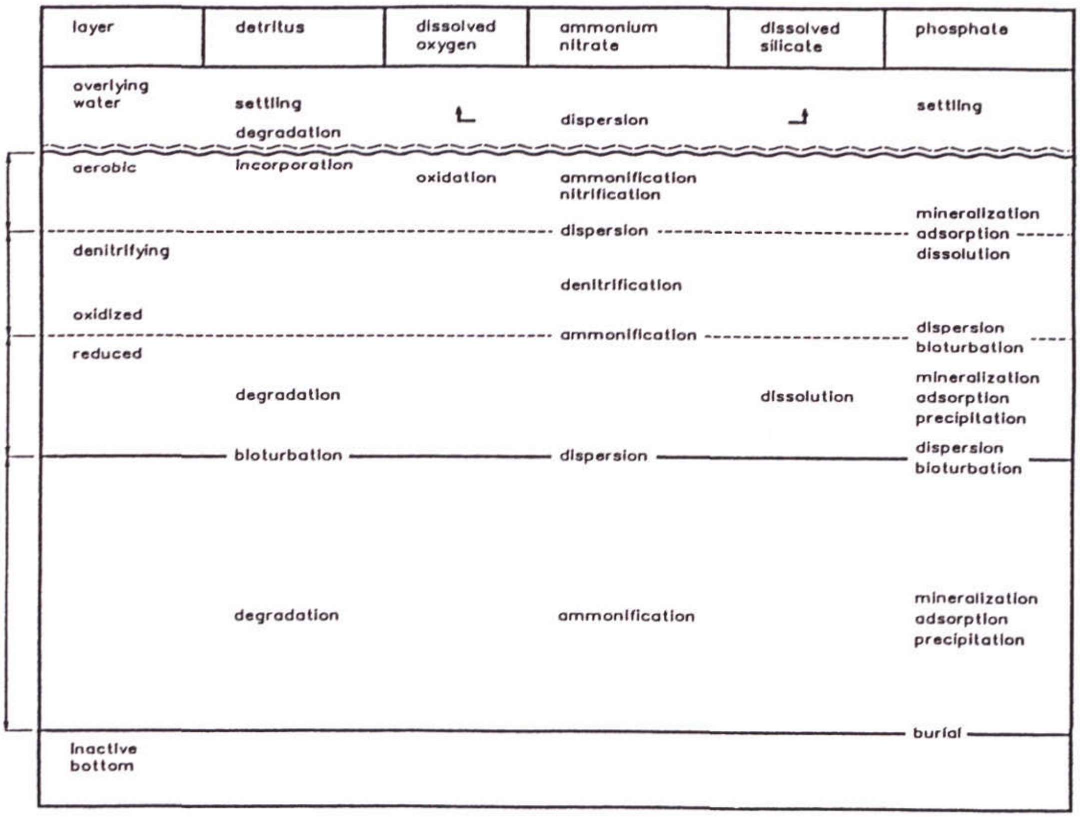

Figure 6.2 Overview of the processes included in SWITCH. Oxygen is consumed in the degradation of detritus in the boundary layer (complex-detritus in the terminology of DBS) and of detritus in the aerobic layer, in the nitrification and in the chemical oxidation. The oxygen consumption rate Ro is formulated as follows:

$$Ro \quad = Fo_b \,/\, d_1 + ac.kc_1.Cd_1 + p_1.an.kn.Ca_1 + Fo_c \,/\, d_1 \qquad (6.6.2)$$

in which:

ac = stoichiometric constant ($gO_2\ gC^{-1}$)

an = stoichiometric constant ($gO_2\ gN^{-1}$)

Cd_1 = detritus concentration in the upper layer ($gC\ m^{-3}B$)

Ca_1 = ammonium concentration in the aerobic layer ($gN\ m^{-3}PW$)

Fo_b = oxygen consumption in the boundary layer ($gO_2\ m^{-2}\ d^{-1}$)

Fo_c = chemical oxygen demand ($gO_2\ m^{-2}\ d^{-1}$)

kc_1 = degradation rate of detritus in the upper layer (d^{-1})

kn = nitrification rate (d^{-1}), equal to zero if $Co_0 = 0.0$

The oxygen consumption in the boundary layer is connected with the degradation of detritus on top of the sediments and is equal to:

$$Fo_b = ac.kc_b\ .\ Cd_b \qquad (6.6.3)$$

in which:

Cd_b = amount of complex-detritus in the boundary layer (gC m^2)

kc_b = degradation rate of complex-detritus in the boundary layer (d^{-1})

The chemical oxygen demand concerns the oxidation of reduced substances, such as iron(II), manganese(II), sulphide and methane originating from the degradation of detritus in the anaerobic part of the 'active' bottom. However, the reduced substances will not be oxidized completely. A part of the sulphide resulting from sulphate reduction precipitates with iron and may accumulate in the reduced part of the sediments. Methane may escape from the sediments in gasbubbles. Consequently, the actual chemical oxygen demand is formulated as a fraction of the potential chemical oxygen demand:

$$Fo_c = (1\text{-}fro).ac.(kc_1.Cd_1.(d_2+d_3) + kc_4.Cd_4.d_4) \qquad (6.6.4)$$

in which:

fro = fraction reduced substances permanently removed or fixed (-)

kc_4 = degradation rate of detritus in the lower layer (d^{-1})

Note that the degradation of detritus in the denitrifying layer has been included entirely in the chemical oxygen demand. This is not correct as such, since the elementary nitrogen produced by denitrification is chemically inert. It is not oxidized, but escapes from the bottom. A correction for the amount of nitrate consumed by denitrification can be made with fro. No correction was made in the second version of SWITCH.

The sediment oxygen demand is quantified with:

$$Fo = Fo_b + (ac.kc_1.Cd_1 + p_1.an.kn.Ca_1).d_1 + Fo_c \qquad (6.6.5)$$

Maintaining a bottom oxygen demand under anaerobic conditions in the water column (kn = 0.0 !) leads to a negative oxygen concentration in the water quality model representing the surplus of reduced substances.

6.6.4 The denitrifying layer and nitrate

Nitrate is formed from ammonium through nitrification in the aerobic toplayer. It is subjected to vertical transport and denitrification in the zone just below this layer (Vanderborght et al., 1977b). The thickness of the denitrifying layer follows from the (approximate) steady-state solution of the differential equation for nitrate in this layer:

$$d_2 = 2\,(Cn_l - Cn_c) / Cn_l . \sqrt{(D/kd)} \qquad (6.6.6)$$

$$d_2 = 0.0 \quad \text{if } Cn_l \leq Cn_c$$

in which:

kd = first order denitrifcation rate (d^{-1})

Cn_l = nitrate concentration in the toplayer ($gN.m^{-3}$)

Cn_c = critical nitrate concentration ($gN.m^{-3}$)

The critical nitrate concentration is the maximal concentration at which sulphate reduction is possible, about 0.1 $gN.m^{-3}$.

The nitrate concentration in the aerobic and denitrifying layers follow from:

$$\frac{dCn_l}{dt} = (Fn_b - Fn_0 + Fn_l) / (p_1.d_1) + kn.Ca_l \qquad (6.6.7)$$

with:

$$Fn_0 = 2\,p_1.D.(Cn_l - Cn_0) / (l + d_1)$$

$$Fn_l = -\,p_1.kd.Cn_2.d_2$$

$$Cn_2 = Cn_2 / 2$$

in which:

Ca_l = ammonium concentration in the toplayer ($gN.m^{-3}$)

Fn_b = flux from the boundary layer ($gN\ m^{-2}\ d^{-1}$)

Fn_0 = dispersive return flux to the overlying water ($gN\ m^{-2}\ d^{-1}$)

Fn_l = flux to the denitrifying layer ($gN\ m^{-2}\ d^{-1}$)

l = thickness of the water boundary layer (m)

6.6.5 Detritus

Organic carbon

All organic matter, which settles on the sediments is considered as detritus, regardless of its origin. GEM distinguishes:

- live phytoplankton, which enters the complex-detritus pool in the boundary layer due to settling;
- dead microphytobenthos, which enters the complex-detritus pool in the boundary layer due to mortality;
- fast decomposing detritus and slow decomposing detritus, that enter the complex-detritus pool in the boundary layer as the net result of settling and resuspension; and
- refractory detritus, which enters the slow decomposing detritus pool in the lower layer due to settling.

SWITCH transfers the complex-detritus to the relatively fast decomposing sediment-detritus pool. Resuspension (if occurring) leads to reincorporation of the detritus into the water column as fast decomposing detritus. The model converts a fraction of the sediment-detritus into refractory humic matter, which is stored in the sediment.

Summarizing, detritus is subjected to settling, resuspension, incorporation from the boundary layer into the sediment, degradation, humification and burial (Berner, 1974). The degradation rate decreases while the organic matter is transported downwards in the sediment. The concentrations of detritus in the boundary layer and the bottom layers are described with the following differential equations:

$$\frac{dCd_b}{dt} = Fd_s - Fd_b - kc_b . Cd_b \qquad (6.6.8)$$

$$\frac{dCd_1}{dt} = (Fd_b - Fb_3 . Cd_1 + Fd_3)/dh - kc_1 . Cd_1 \qquad (6.6.9)$$

$$\frac{dCd_4}{dt} = (Fxd_s + Fb_3 . Cd_1 - Fd_3)/d_4 - (1+frf) . kc_4 . Cd_4 \qquad (6.6.10)$$

with:

$Fd_s = sc . Cd_0$

$Fd_b = rc . Cd_b$

$Fb_3 = Fs - Fr \geq 0.0$

$Fb_4 \quad = Fb_3.(1-p_1)/(1-p_4)$

$Fd_3 \quad = 2\ Db.(Cd_4/(1-p_4) - Cd_1/(1-p_1)) / (dh+d_4)$

$Fxd_s \quad = sc.Cxd_0$

in which:

Cd_0	= detritus concentration in the overlying water (gC m^{-3})
Cd_b	= amount of detritus in the boundary layer (gC m^{-2})
Cd_1	= detritus concentration in the upper layer (gC m^{-3}B)
Cd_4	= detritus concentration in the lower layer (gC m^{-3}B)
Cxd_0	= refractory detritus concentration in the overlying water (g m^{-3})
Db	= bioturbation dispersion coefficient (m^2 d^{-1})
frf	= factor for the conversion of detritus into refractory organic matter (-)
Fb	= burial flux based on displaced bottom volume (m^{3}B m^{-2} d^{-1})
Fd	= bioturbation flux (gC m^{-2} d^{-1})
Fd_b	= flux of detritus incorporated in the upper layer (gC m^{-2} d^{-1})
Fd_s	= flux of detritus settled from the overlying water (gC m^{-2} d^{-1})
Fr	= resuspension flux based on displaced bottom volume (m^{3}B m^{-2} d^{-1})
Fs	= sedimentation flux based on displaced bottom volume (m^{3}B m^{-2} d^{-1})
kc_b	= degradation rate of detritus in the boundary layer (d^{-1})
rc	= rate of incorporation in the upper layer (d^{-1})
sc	= sedimentation rate for detritus (m d^{-1})
Fxd_s	= flux of refractory detritus incorporated in the sediment (gC m^{-2} d^{-1})

The amount of detritus in the boundary layer (Cd_b) is not calculated in SWITCH but in the microphytobenthos module of GEM.

Notice that the conversion of detritus into refractory organic matter has been formulated as a process that is proportional and additive to decomposition at the same time. frf can be seen as an amplification factor. frf/(1-frf) delivers the fraction of the degradable organic matter that is converted into refractory organic matter.

SWITCH has only one input parameter with respect to settling and resuspension. This parameter is equal to Fs-Fr and is in fact the net sedimentation/erosion rate or the burial rate in case of a positive value. Notice that the formulations in SWITCH are only valid for burial. Moreover, it is assumed that all detritus has been degraded or converted before it arrives at the lower boundary of the 'active' bottom layer, so that burial does not remove degradable detritus from the lower layer.

Only the 'average' concentration of the refractory organic matter is calculated for the 'active' bottom. The concentration is derived from:

$$\frac{dCrd_l}{dt} = (-Fb_4.Crd_l + frf.kc_4.Cd_4.d_4) \,/\, (dh+d_4) \qquad (6.6.11)$$

Organic nitrogen

Similar equations have been formulated for organic nitrogen. The decomposable organic nitrogen in detritus is converted into ammonium and into refractory organic nitrogen in the following way:

$$\frac{dCnd_b}{dt} = Fnd_s - Fnd_b - knd_b.Cnd_b \qquad (6.6.12)$$

$$\frac{dCnd_l}{dt} = (Fnd_b - Fb_3.Cnd_l + Fnd_3)/dh - (1+fa_l).kc_1.Cnd_l \qquad (6.6.13)$$

$$\frac{dCnd_4}{dt} = (Fxn_s + Fb_3.Cnd_l - Fnd_3)/d_4 - (1+fa_4+frf).kc_4.Cnd_4 \qquad (6.6.14)$$

with:

$fa_l = (Cnd_l/Cd_l - aa) \,/\, aa$

$fa_4 = (Cnd_4/Cd_4 - aa) \,/\, aa$

$Fnd_s = sc.Cnd_0$

$Fnd_b = rc.Cnd_b$

$Fnd_3 = 2\ Db.(Cnd_4/(1-p_4) - Cnd_l/(1-p_l)) \,/\, (dh+d_4)$

$Fxn_s = sc.Cxn_0$

in which:

aa = stoichiometric constant for nitrogen in refractory detritus (gN gC^{-1})
Cnd_0 = detritus nitrogen concentration in the overlying water (gN m^{-3})
Cnd_b = amount of detritus nitrogen in the boundary layer (gN m^{-2})
Cnd_l = detritus nitrogen concentration in the upper layer (gN m^{-3}B)
Cnd_4 = detritus nitrogen concentration in the lower layer (gN m^{-3}B)
Cxn_0 = slow decomposing detritus nitrogen (OON) concentration in overlying water (gN m^{-3})
fa = correction factor for organic nitrogen degradation rate (-)

Fnd = bioturbation flux ($gN\ m^{-2}\ d^{-1}$)
Fnd_b = flux of detritus nitrogen incorporated in the upper layer ($gN\ m^{-2}\ d^{-1}$)
Fnd_s = flux of detritus nitrogen settled from the overlying water ($gN\ m^{-2}\ d^{-1}$)
Fxn_s = flux of slow decomposing detritus nitrogen (OON) incorp. in sediment ($gN\ m^{-2}\ d^{-1}$)
knd_b = degradation rate of detritus nitrogen in the boundary layer (d^{-1})

The amount of detritus nitrogen in the boundary layer (Cnd_b) is not calculated in SWITCH but in the complex-module of GEM.

The degradation rates of organic nitrogen are adjusted in such a way that the organic matter is gradually stripped from nitrogen in excess of the nitrogen in refractory organic matter.

The 'sediment-average' concentration of the refractory organic nitrogen follows from:

$$\frac{dCrn_1}{dt} = (-Fb_4.Crn_1 + frf.kc_4.Cnd_4.d_4) / (dh+d_4) \qquad (6.6.15)$$

Organic phosphorus

The following equations describe the organic phosphorus in accordance with the above:

$$\frac{dCpd_b}{dt} = Fpd_s - Fpd_b - kpd_b.Cpd_b \qquad (6.6.16)$$

$$\frac{dCpd_1}{dt} = (Fpd_b - Fb_3.Cpd_1 + Fnd_3)/dh - (1+fp_1).kc_1.Cpd_1 \qquad (6.6.17)$$

$$\frac{dCpd_4}{dt} = (Fxp_s + Fb_3.Cpd_1 - Fnd_3)/d_4 - (1+fp_4+frf).kc_4.Cpd_4 \qquad (6.6.18)$$

with:

fp_1 = $(Cpd_1/Cd_1 - ap) / ap$

fp_4 = $(Cpd_4/Cd_4 - ap) / ap$

Fpd_s = $sc.Cpd_0$

Fpd_b = $rc.Cpd_b$

$Fpd_3 = 2\ Db.(Cpd_4/(1-p_4) - Cpd_1/(1-p_1)) / (dh+d_4)$

$Fxp_s = sc.Cxp_0$

in which:
ap = stoichiometric constant for phosphorus in refractory detritus (gP gC^{-1})
Cpd_0 = detritus phosphorus concentration in the overlying water (gP m^{-3})
Cpd_b = amount of detritus phosphorus in the boundary layer (gP m^{-2})
Cpd_1 = detritus phosphorus concentration in the upper layer (gP m^{-3}B)
Cpd_4 = detritus phosphorus concentration in the lower layer (gP m^{-3}B)
Cxp_0 = slow decomposing detritus phosphorus (OOP) concentration overlying water (gP m^{-3})
fp = correction factor for organic phosphorus degradation rate (-)
Fpd = bioturbation flux (gP m^{-2} d^{-1})
Fpd_b = flux of detritus phosphorus incorporated in the upper layer (gP m^{-2} d^{-1})
Fpd_s = flux of detritus phosphorus settled from the overlying water (gP m^{-2} d^{-1})
Fxp_s = flux of slow decomp. detritus phosphorus (OOP) incorp. in sediment (gP m^{-2} d^{-1})
kpd_b = degradation rate of detritus phosphorus in the boundary layer (d^{-1})

The amount of detritus phosphorus in the boundary layer (Cpd_b) is not calculated in SWITCH but in the complex-module of GEM.

The 'sediment-average' concentration of the refractory organic phosphorus follows from:

$$\frac{dCrp_1}{dt} = (-Fb_4.Crp_1 + frf.kc_4.Cpd_4.d_4) / (dh+d_4) \qquad (6.6.19)$$

6.6.6 Ammonium

Ammonium is released the degradation of detritus and is nitrified by bacteria under aerobic conditions (Berner, 1974; Vanderborght et al., 1977b). Ammonium adsorbs to a certain extent to clays in the sediments. The adsorption equilibrium is pH dependent. It is estimated that about 25 to 50 % of the ammonium present in silty sediments may be adsorbed (partition coefficient ≈ 1). This is a relatively small quantity compared to the high turn-over rates of ammonium in sediments. Thus, the adsorption offers only a small buffering capacity, which implies that no large mass fluxes are involved in the adsorption of ammonium. A change of ammonification is quickly followed by a proportional change of the ammonium concentration in the pore water. It is therefore justified to ignore the adsorption of ammonium in SWITCH.

The ammonium concentrations in the aerobic toplayer, the remaining part of the upper layer (d_2+d_3) and the lower reduced layer (dl) are described with:

$$\frac{dCa_1}{dt} = (Fa_b - Fa_0 + Fa_1 + Fas_0 - Fas_1)/(p_1.d_1) + (1+fa_1).kc_1.Cnd_1/p_1 - kn.Ca_1 \tag{6.6.20}$$

$$\frac{dCa_2}{dt} = (- Fa_1 + Fa_3 + Fas_1 - Fas_3)/(p_1.(d_2+d_3)) + (1+fa_1).kc_1.Cnd_1/p_1 \tag{6.6.21}$$

$$\frac{dCa_4}{dt} = (-Fa_3 + Fas_3 - Fas_4)/(p_4.d_4) + (1+fa_4).kc_4.Cnd_4/p_4 \tag{6.6.22}$$

with:

$Fa_b = knd_b.Cd_b$

$Fa_0 = 2\ p_1.D.(Ca_1-Ca_0)\ /\ (l+d_1)$

$Fa_1 = 2\ p_1.D.(Ca_2-Ca_1)\ /\ do$

$Fa_3 = (p_1+p_4).D.(Ca_4-Ca_2)\ /\ (d-d_1)$

$Fas_0 = -\ vs.Ca_0$ if $vs < 0.0$
$Fas_1 = -\ vs.Ca_1$
$Fas_3 = -\ vs.Ca_2$
$Fas_0 = -\ vs.Ca_1$ if $vs > 0.0$
$Fas_1 = -\ vs.Ca_2$
$Fas_3 = -\ vs.Ca_4$
$Fas_4 = -\ vs.Ca_4$

in which:
Fa_b = flux from degradation detritus in boundary layer (gN m^{-2} d^{-1})
Fa_0 = dispersive return flux to the overlying water (gN m^{-2} d^{-1})
Fa_{1-3} = dispersive flux between two adjacent layers (gN m^{-2} d^{-1})
Fas_0 = seepage flux at the sediment-water interface (gN m^{-2} d^{-1})
Fas_{1-3} = seepage flux between two adjacent layers (gN m^{-2} d^{-1})
Fas_4 = seepage flux at the lower boundary (gN m^{-2} d^{-1})
knd_b = degradation rate of detritus nitrogen in the boundary layer (d^{-1})
vs = seepage velocity (m d^{-1})

It is assumed that no dispersive transport occurs across the interface of the 'active' and 'inactive' parts of the bottom. The assumption implies that the concentration of a dissolved substance is the same at both sides of the lower boundary of the bottom in the model. It is a reasonable assumption when seasonal variations in the concentration of a dissolved substance is small at the lower boundary. Moreover, a long-term shift in the ammonium concentration in the 'inactive' bottom does hardly affect the sediment-water exchange fluxes.

SWITCH stops nitrification (kn=0.0) when the dissolved oxygen concentration in the water column is equal to or less than 0.0.

6.6.7 Phosphate

Bacterial activity liberates phosphate from organic matter just like ammonium. In contrast with ammonium, phosphate adsorbs strongly to several components of the sediments, the hydroxides of iron(III) and aluminum in particular. Iron(III) hydroxide is present in a relatively high concentration in the oxidized layer, where it is stable. The concentration declines at the interface of the oxidized and reduced layers and goes down further in the reduced layer under the influence of reduction processes. Consequently, the adsorption is much stronger in the oxidized layer than in the reduced layer (Van Raaphorst et al., 1988; Brinkman and Van Raaphorst, 1986; Lyklema, 1980; Berner, 1974).

Phosphate also precipitates in minerals, the identity of which has not been determined unequivocally (DELFT HYDRAULICS, 1994b). Vivianite (iron(II)phosphate) is being mentioned as the main mineral, but vivianite is not stable under oxidized conditions. Apatite (calcium phosphate) may be present as a stable mineral in marine water sediments. Coprecipitation with several carbonates and sulphides is also possible.

SWITCH assumes equilibrium for the adsorption process, whereas precipitation and dissolution are formulated as slow processes. The assumption of equilibrium has the advantage, that only inorganic phosphate and precipitated phosphate need to be calculated explicitly on the basis of mass balances. The dissolved and adsorbed phosphate concentrations follow from the equilibrium condition for adsorption. The following four fractions are distinguished:

$$\begin{aligned} Cpp &= fpp.Cp \\ Cmp &= fmp.Cp \\ Cdp &= fdp.Cp/p \\ Cap &= fap.Cp \end{aligned} \qquad (6.6.23)$$

$$fap + fdp + fpp + fmp = 1$$

in which:

Cp = total inorganic phosphate concentration (gP m^{-3}B)
Cap = adsorbed phosphate concentration (gP m^{-3}B)
Cdp = dissolved phosphate concentration (gP m^{-3}PW)
Cmp = concentration of phosphate in a stable mineral (gP m^{-3}B)
Cpp = concentration of phosphate in vivianite (gP m^{-3}B)

fap = adsorbed fraction (-)
fdp = dissolved fraction (-)
fmp = stable mineral fraction (-)
fpp = vivianite fraction (-)

These fractions are relevant for the mass balance equation for total inorganic phosphate, because the processes affect only one or two of the fractions.

The mineral phosphate fractions can be determined after solution of the mass balance equations for these components. The precipitation process is formulated with first order kinetics. The driving force is the difference between the actual concentration and the saturation concentration of ortho-phosphate dissolved in the pore water. In principle, the latter may be determined from the solubility product of the phosphate mineral, when its identity has been established. No distinction was made between the precipitation rates and the saturation concentrations of vivianite and the stable mineral, as the in-situ properties of these minerals are unknown. The precipitation rate is a function of the driving force, the nature of which depends on the rate limiting mechanism. The function is linear when diffusion to the surface of the mineral is the rate limiting process. In case that the surface reaction is rate limiting, the function may be non-linear. However, the assumption of simple first order reaction kinetics ignoring the role of coprecipitants seems reasonable in this stage, considering that the precipitation rate has not yet been determined accurately and that the dissolved iron concentration is not simulated.
The development of the concentrations of the stable mineral phosphate is described with:

$$\frac{dCmp_1}{dt} = + p_1.fm.kp.\,(fdp_1.Cp_1/p_1 - Cdp_s) + \qquad (6.6.24)$$
$$(-Fr.fmp_1.Cp_1 - Fb_2.fmp_1.Cp_1) / do +$$
$$2\,Db.\,(fmp_3.Cp_3 - fmp_1.Cp_1) / (1-p_1) / (do+d_3) / do$$

$$\frac{dCmp_3}{dt} = + p_1.fm.kp.\,(fdp_3.Cp_3/p_1 - Cdp_s) + \qquad (6.6.25)$$
$$(Fb_2.fmp_1.Cp_1 - Fb_3.fmp_3.Cp_3) / d_3 -$$
$$2\,Db.\,(fmp_3.Cp_3 - fmp_1.Cp_1) / (1-p_1) / (do+d_3) / d_3 +$$
$$2\,Db.\,(fmp_4.Cp_4/(1-p_4) - fmp_3.Cp_3/(1-p_1)) / (d_3+d_4) / d_3$$

$$\frac{dCmp_4}{dt} = + p_4.fm.kp.\,(fdp_4.Cp_4/p_4 - Cdp_s) + \qquad (6.6.26)$$
$$(Fb_3.fmp_3.Cp_3 - Fb_4.fmp_4.Cp_4) / d_4 -$$
$$2\,Db.\,(fmp_4.Cp_4/(1-p_4) - fmp_3.Cp_3/(1-p_1)) / (d_3+d_4) / d_4$$

in which:

Cdp_s = saturation concentration for dissolved ortho-phosphate ($gP\ m^{-3}PW$)

fm = fraction of precipitated phosphorus stored in the stable mineral (-)

Fr = resuspension flux based on bottom volume ($m^3\ m^{-2}\ d^{-1}$)

kp = precipitation rate (d^{-1})

Vivianite forms in the reduced parts of the sediments. It dissolves gradually when transported into the oxidized layer by means of bioturbation of the sediments. This hypothesis can be justified as follows:

- Vivianite (iron(II) phosphate) is unstable under oxidized conditions (Lijklema, 1980).
- The concentration of dissolved Fe(II), and in some parts also the concentration of dissolved ortho-phosphate, is much higher in the reduced layer than in the oxidized layer. The solubility product is probably only exceeded in the reduced layer.

The formulation of the dissolution process is not straight forward. The dissolution is probably characterized by two steps: a) the oxidation of dissolved Fe^{2+}, b) the dissolution of vivianite at a very low dissolved Fe^{2+}-concentration. The driving force may therefore be the difference between the Fe^{2+}-concentration near the vivianite crystals and the average dissolved Fe^{2+}-concentration. The latter may approximately be equal to zero, due to oxidation. The dissolution rate may then be formulated as follows:

$$Rdis = kdis.Cpp.Cfe \qquad (6.6.27)$$

in which:

Cfe = the dissolved Fe2+-concentration near the surface of vivianite crystals ($gFe\ m^{-3}$)

kdis = the (second order) dissolution rate constant ($m^3\ gFe^{-1}\ d^{-1}$)

Rdis = the dissolution rate ($gP\ m^{-3}\ d^{-1}$)

The dissolved Fe^{2+}-concentration near the surface of the crystals is calculated from the solubility product (equilibrium constant) and the dissolved phosphate concentration with:

$$Cfe = (L_s / Cdp^2)^{0.33} \qquad (6.6.28)$$

in which:

L_s = solubility product of vivianite

Equations 6.6.27-28 have been combined to make the dissolution rate dependent on the dissolved phosphate concentration (power -0.67). The solubility product becomes an implicit part of the dissolution rate constant. The resulting formulation meets the demand that the dissolution process slows down when the dissolved phosphate concentration increases.

The mass balances for phosphate in vivianite in three layers are:

$$\frac{dCpp_1}{dt} = - kdp.fpp_1.Cp_1.\,(fdp_1.Cp_1/p_1)^{-0.67} + \tag{6.6.29}$$
$$(-Fr.fpp_1.Cp_1 - Fb_2.fpp_1.Cp_1)\,/\,do +$$
$$2\,Db.\,(fpp_3.Cp_3 - fpp_1.Cp_1)\,/\,(1-p_1)\,/\,(do+d_3)\,/\,do$$

$$\frac{dCpp_3}{dt} = + p_1.kp.\,(fdp_3.Cp_3/p_1 - Cdp_s) + \tag{6.6.30}$$
$$(Fb_2.fpp_1.Cp_1 - Fb_3.fpp_3.Cp_3)\,/\,d_3 -$$
$$2\,Db.\,(fpp_3.Cp_3 - fpp_1.Cp_1)\,/\,(1-p_1)\,/\,(do+d_3)\,/\,d_3 +$$
$$2\,Db.\,(fpp_4.Cp_4/(1-p_4) - fpp_3.Cp_3/(1-p_1))\,/\,(d_3+d_4)\,/\,d_3$$

$$\frac{dCpp_4}{dt} = + p_4.kp.\,(fdp_4.Cp_4/p_4 - Cdp_s) + \tag{6.6.31}$$
$$(Fb_3.fpp_3.Cp_3 - Fb_4.fpp_4.Cp_4)\,/\,d_4 -$$
$$2\,Db.\,(fpp_4.Cp_4/(1-p_4) - fpp_3.Cp_3/(1-p_1))\,/\,(d_3+d_4)\,/\,d_4$$

in which:

kdp = dissolution rate ($m^{-2.01}\ gP^{0.67}\ d^{-1}$)

The dissolved fraction can be derived from the following Langmuir adsorption isoterm:

$$Cap = Cam.Cdp\,/\,(Ks+Cdp) \tag{6.6.32}$$

$$Cam = Cac.(1-p).Ws$$

in which:

Cac = adsorption capacity (gP kg^{-1}DM)

Cam = maximal concentration of adsorbed phosphate (gP m^{-3}B)

Ks = half saturation concentration (gP m^{-3}PW)

Ws = specific weight of the sediments (kg m^{-3})

The adsorption capacity depends on the oxidized iron (III) and aluminum contents of the sediments. This sediment property is different for the oxidized layer and the reduced layer. The oxidized iron content and (therefore) the adsorption capacity decrease in a downward direction. Iron(III) is reduced to iron(II) in connection with the degradation of organic matter. The oxidized iron gradient is smoothed by bioturbation of the sediment, which results in upward transport of iron(II) formed in the reduced layer and in downward transport of iron(III) formed in the oxidized layer. Moreover, the adsorption capacities change in time due to changes of the temperature dependent rates of degradation of organic matter and bioturbation. Both processes affect the position of the interface between the layers and the amounts of oxidized iron present in the layers. This is taken into account in SWITCH, whereas the dependency on pH and salinity of the adsorption parameters is not considered explicitly.

Tentative simulations with the complex chemical model HADES showed that the iron(III) contents of the oxidized layer and the reduced layer are related to the thickness of the oxidized layer (DELFT HYDRAULICS, 1991b). The adsorption capacity increases with increasing thickness of the oxidized layer. However, it has not been possible yet to formulate this relation deterministically. Empirical relations, determined by means of model calibration for Lake Veluwe, have been introduced in SWITCH in stead. The relations used in SWITCH are:

$$\begin{aligned} Cam_1 &= fac_1.Cac.(1-p_1).Ws \qquad (6.6.33) \\ Cam_3 &= fac_1.fac_3.Cac.(1-p_1).Ws \\ Cam_4 &= 0.5\ fac_4.Cac.(1-p_4).Ws \end{aligned}$$

$$\begin{aligned} fac_1 &= ((d_1+d_2) / 0.005)^{0.25} \\ fac_3 &= ((d_1+d_2) / dh)^{0.25} \\ fac_4 &= dh / (dh+d_4) \end{aligned}$$

in which:

Cam_1 = maximal concentration of adsorbed phosphate in the oxidized layer ($gP\ m^{-3}B$)
Cam_3 = maximal concentration of adsorbed phosphate in the upper reduced layer ($gP\ m^{-3}B$)
Cam_4 = maximal concentration of adsorbed phosphate in the lower reduced layer ($gP\ m^{-3}B$)
Cac = time average adsorption capacity of the oxidized layer ($gP\ kg^{-1}DM$)
fac = empirical factor linking up the ads. capacity with layer thickness (-)

The adsorption capacity of the oxidized layer becomes bigger than the 'average' capacity (Cac) when the thickness of the oxidized layer becomes bigger than 0.005 m, which is about half the maximal thickness of the oxidized layer. The adsorption capacities of the reduced layers depend also on the values of dh and d_4 (input parameters for SWITCH). The thicker the reduced layers are, the smaller their depth average adsorption capacities are. This is logical considering the fact that the capacity decreases with depth.

An earlier approach, which defined the adsorption capacities of reduced layers as constant fractions of the adsorption capacity of the oxidized layer, is also available in SWITCH as an alternative option. A quadratic equation in fdp is obtained when equation 6.6.32 is substituted in equations 6.6.23. The positive root is:

$$\begin{aligned} fdp = {} & [\,(1-fmp-fpp).Cp - p.Ks - Cam + \\ & \sqrt{\{((1-fmp-fpp).Cp - p.Ks - Cam)^2 +} \\ & 4\,(1-fmp-fpp).Cp.p.Ks\}\,]\,/\,(2\,Cp) \end{aligned} \tag{6.6.34}$$

Having defined al four phosphate fractions, the mass balances for total inorganic phosphate in the oxidized layer, the upper reduced layer and the lower reduced layer have been formulated as follows:

$$\begin{aligned} \frac{dCp_1}{dt} = {} & (Fp_b + Fp_s - Fp_0 + Fp_2 + Fps_0 - Fps_2 - \\ & Fr.Cp_1 + Fpd_2 - Fb_2.Cp_1)\,/\,do + \\ & (1+fp_1).kc_1.Cpd_1 \end{aligned} \tag{6.6.35}$$

$$\begin{aligned} \frac{dCp_3}{dt} = {} & (-\,Fp_2 + Fp_3 + Fps_2 - Fps_3 - \\ & Fpd_2 + Fpd_3 + Fb_2.Cp_1 - Fb_3.Cp_3)\,/\,d_3 + \\ & (1+fp_1).kc_1.Cpd_1 \end{aligned} \tag{6.6.36}$$

$$\begin{aligned} \frac{dCp_4}{dt} = {} & (-\,Fp_3 + Fps_3 - Fps_4 - \\ & Fpd_3 + Fb_3.Cp_3 - Fb_4.Cp_4)\,/\,d_4 + \\ & (1+fp_4).kc_4.Cpd_4 \end{aligned} \tag{6.6.37}$$

with:

$$Fp_b = kpd_b.Cpd_b$$

$$Fp_0 = 2\,p_1.D.\,(fdp_1.Cp_1/p_1 - fdp_0.Cp_0)\,/\,(l+do)$$

$$Fp_2 = 2\,D.\,(fdp_3.Cp_3 - fdp_1.Cp_1)\,/\,(do+d_3)$$

$$Fp_3 = (p_1+p_4).D.\,(fdp_4.Cp_4/p_4 - fdp_3.Cp_3/p_1)\,/\,(d_3+d_4)$$

$Fpd_2 = 2\ Db.\ ((fpp_3+fap_3).Cp_3-fap_1.Cp_1) / (1-p_1) / (do+d_3)$

$Fpd_3 = 2\ Db.\ ((fpp_4+fap_4).Cp_4/(1-p_4)-(fpp_3+fap_3).Cp_3/(1-p_1)) / (d_3+d_4)$

$Fps_0 = -\ vs.fdp_0.Cp_0/p_1$ if $vs < 0.0$
$Fps_2 = -\ vs.fdp_1.Cp_1/p_1$
$Fps_3 = -\ vs.fdp_3.Cp_3/p_1$

$Fps_0 = -\ vs.fdp_1.Cp_1/p_1$ if $vs > 0.0$
$Fps_2 = -\ vs.fdp_3.Cp_3/p_1$
$Fps_3 = -\ vs.fdp_4.Cp_4/p_4$

$Fps_4 = -\ vs.fdp_4.Cp_4/p_4$

in which:
Fb = burial flux based on bottom volume ($m^3\ m^{-2}\ d^{-1}$)
Fr = resuspension flux based on bottom volume ($m^3\ m^{-2}\ d^{-1}$)
Fp_b = flux from degradation detritus in boundary layer (gP $m^{-2}\ d^{-1}$)
Fp_s = sedimentation flux of adsorbed phosphate (gP $m^{-2}\ d^{-1}$)
Fp_0 = dispersive return flux to the overlying water (gP $m^{-2}\ d^{-1}$)
Fp_{2-3} = dispersive flux between two adjacent layers (gP $m^{-2}\ d^{-1}$)
Fpd_{2-3} = bioturbation flux between two adjacent layers (gP $m^{-2}\ d^{-1}$)
Fps_0 = seepage flux at the sediment-water interface (gP $m^{-2}\ d^{-1}$)
Fps_{2-3} = seepage flux between two adjacent layers (gP $m^{-2}\ d^{-1}$)
Fps_4 = seepage flux at the lower boundary (gP $m^{-2}\ d^{-1}$)

The resuspension of phosphate is taken into account explicitly, because of the importance for the phosphate budget in the overlying water. Phosphate adsorbed to resuspended sediments may desorb in the water column.

6.6.8 Silicate

Reactive silicate enters the sediment primarily in the form of opal silicate, the remains of diatom skeletons. Opal silicate dissolves gradually, because pore water is undersaturated with respect to silicate. The process is retarded by coating of the particles with minerals of iron and aluminum. Dissolved silicate may adsorb onto aluminum silicates and may precipitate in stable minerals (Berner, 1974; Vanderborght et al., 1977a; Schink and Guinasso, 1978). Because all these processes are very slow and poorly understood, it was decided to include in SWITCH only the dissolution process.

Furthermore it is assumed that opal silicate is present in abundance in estuarine sediment. This seems a reasonable assumption considering the high productivity of diatoms and the slowness of the dissolution process. The rate is than only dependent on the difference between the saturation concentration and the actual dissolved concentration of silicate.

Sublayers are not distinguished with respect to silicate. The mass balance of dissolved silicate in the pore water of the sediment is:

$$\frac{dCs_l}{dt} = (Fs_b - Fs_0 + Fss_0 - Fss_4)/(pa.d) - ks.(Cs_l - Cs_s) \qquad (6.6.38)$$

with:

$$pa = (p_1.dh + p_4.dl)/d$$

$$Fs_0 = 2\ pa.D.(Cs_l - Cs_0)\ /\ (l+dh)$$

$$Fss_0 = -\ vs.Cs_0 \ \text{ if } \ vs < 0.0$$
$$ = -\ vs.Cs_l \ \text{ if } \ vs > 0.0$$

$$Fss_4 = -\ vs.Cs_l$$

in which:

Cs_l = dissolved silicate concentration (gSi.m^{-3})
Cs_s = saturation dissolved silicate concentration (gSi.m^{-3})
Fs_b = dissolution flux of opal silicate in the boundary layer (gSi m^{-2} d^{-1})
Fs_0 = dispersive return flux to the overlying water (gSi m^{-2} d^{-1})
Fss_0 = seepage flux at the sediment-water interface (gSi m^{-2} d^{-1})
Fss_4 = seepage flux at the lower boundary (gSi m^{-2} d^{-1})
ks = dissolution rate (d^{-1})
pa = average porosity (-)

6.6.9 Temperature dependency and dispersion

All process rates are temperature dependent according to:

$$k = k^{20}.kt^{(T-20)} \qquad (6.6.39)$$

in which:

k = first order process rate (d^{-1})
k^{20} = first order process rate at 20 °C (d^{-1})
kt = temperature coefficient (-)

Temperature coefficients vary between 1.04 and 1.09.

Dispersion in the pore water is the result of molecular diffusion and bio-irrigation. The dispersion coefficient is defined as:

$$D = Dm + (bt-1).Dm \qquad (6.6.40)$$

in which:

D = dispersion coefficient ($m^2.d^{-1}$)
Dm = molecular diffusion coefficient ($m^2.d^{-1}$)
bt = amplification factor for bio-irrigation (-)

The amplification factor can be provided to the model as a sinus function with a period of one year and a maximum in the summer. The dispersion coefficient for bioturbation (Db) can be assigned a similar function.

7 Process formulations for dissolved oxygen

7.1 Starting points and coherence

The concentration of dissolved oxygen (O_2 or DO) in the water column and in sediment layers is determined by a range of water quality processes next to horizontal transport (Figure 7.1). In turn, the oxygen concentration influences processes to which ammonium nitrate and phosphate are subjected, namely mineralization, nitrification, denitrification, sorption and precipitation (chapter 6).

Under reducing conditions negative oxygen concentrations will develop in GEM, usually only in sediment layers. Negative oxygen equivalents represent reductants that are not modelled explicitly, like methane, hydrogen sulphide and iron(II). Once in the presence of oxygen these equivalents are instantaneously neutralized with dissolved oxygen.

Most process fluxes for oxygen are derived from the kinetics of processes concerning other substances, such as decomposition of detritus or primary production of algae. Most of these processes are kinetically zeroth order with respect to oxygen. The processes considered explicitly for DO in GEM are primary production, consumption by grazers, consumption for detritus decomposition, nitrification, reaeration and vertical dispersion. The net process flux of DO is therefore composed as follows:

$$F_{ox,npf} = F_{ox,np} - F_{ox,csgr} - F_{ox,con} - F_{ox,nit} + F_{ox,rear} + F_{ox,dis} \qquad (7.1)$$

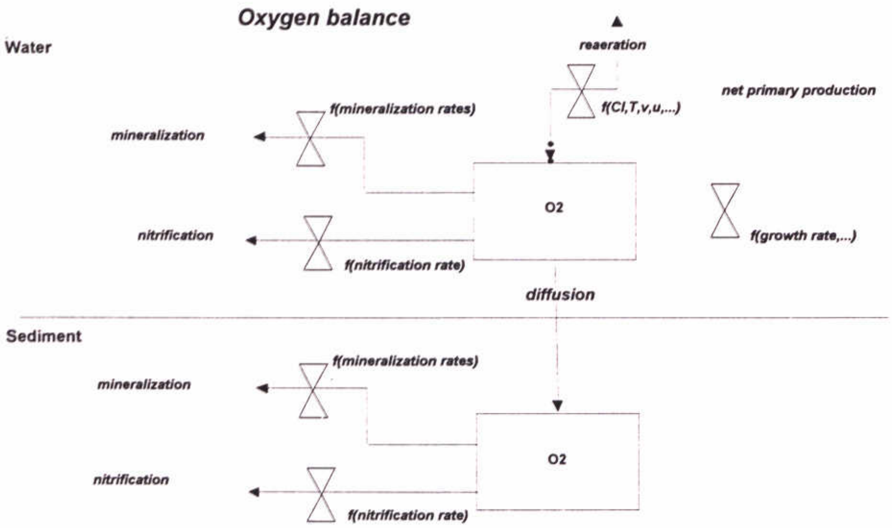

Figure 7.1 Processes for oxygen.

The net primary production flux of phytoplankton and microphytobenthos follows from the sum of gross primary production and respiration of all species (chapter 3):

$$F_{ox,np} = a_{ox,np} \cdot \Sigma_i \, (F_{algi,gp} - F_{algi,res}) \qquad (7.2)$$

in which:

$a_{ox,np}$ = quantity of DO produced relative to algae biomass (gO_2/gC)
$F_{alg,np}$ = total net primary production of algae species ($gC.m^{-3}.day^{-1}$)
$F_{algi,gp}$ = gross primary production by species i ($gC.m^{-3}.day^{-1}$)
$F_{algi,res}$ = respiration by species i ($gC.m^{-3}.day^{-1}$)

The average composition of biomass produced from CO_2 is approximately CH_2O. Hence each mole of biomass-C produced corresponds with one mole of O_2 produced. The stoichiometric constant for DO with respect to primary production $a_{ox,np}$ is consequently equal to 2.67 gO_2/gC.

7.2 Consumption by decomposition of detritus

As appears from chapter 5, detritus is present in four components. The total consumption flux of dissolved oxygen is proportional to the sum of the decomposition fluxes of these components (see section 5.3):

$$F_{ox,con} = a_{ox,con} \cdot (F_{dcf,dec} + F_{dcs,dec} + F_{dcpr,dec} + F_{dcdr,dec}) \qquad (7.3)$$

in which:

$a_{ox,con}$ = quantity of DO consumed per quantity of detritus decomposed (gO_2/gC)
$F_{ox,con}$ = oxygen consumption flux ($gO_2.m^{-3}.day^{-1}$)
$F_{dcf,dec}$ = decomposition of fast decomposing detritus ($gC.m^{-3}.day^{-1}$)
$F_{dcs,dec}$ = decomposition of slow decomposing detritus ($gC.m^{-3}.day^{-1}$)
$F_{dcpr,dec}$ = decomposition of particulate refractory detritus nitrogen ($gC.m^{-3}.day^{-1}$)
$F_{dcdr,dec}$ = decomposition of dissolved refractory detritus nitrogen ($gC.m^{-3}.day^{-1}$)

The oxygen content of organic matter gets lower during the gradual conversion of organic matter into humic substances. Notice however, that only one stoichiometric constant is used for all detritus components, because oxygen in organic matter is not modelled. Consequently, the stoichiometric constant for oxygen consumption at the decomposition of detritus must be equal to the constant $a_{ox,np}$ for primary production.

7.3 Release from grazing

Grazers like zooplankton and filter feeders consume algal biomass and detrital organic matter (chapter 4). A substantial part of the organic matter is oxidized into CO_2 in this process. The concurrent overall oxygen consumption flux is:

$$F_{ox,csgr} = b_{ox,csgr} \cdot a_{ox,csgr} \cdot (\Sigma_j \, (\Sigma_i(F_{algi,csgrj}) + F_{dcf,csgrj} + F_{dcs,csgrj}) \qquad (7.4)$$

in which:

$a_{ox,csgr}$ = quantity oxygen consumed per quantity organic matter consumed ($gO_2.gC^{-1}$)

$b_{ox,csgr}$ = fraction of ingested biomass and organic matter which is oxidized (-)
$F_{ox,csgr}$ = grazer consumption flux ($gO_2.m^{-3}.day^{-1}$)
$F_{algi,csgrj}$ = consumption of algae i by grazer j ($gC.m^{-3}.day^{-1}$)
$F_{dcf,csgrj}$ = consumption of fast decomposing detritus by grazer j ($gC.m^{-3}.day^{-1}$)
$F_{dcs,csgrj}$ = consumption of slow decomposing detritus by grazer j ($gC.m^{-3}.day^{-1}$)

The constant $a_{ox,csgr}$ is to be equal to the stoichiometric constant $a_{ox,np}$ for primary production.

7.4 Nitrification

Nitrification occurs both in the water column and the sediment under aerobic conditions. Below a critical oxygen level inhibition occurs. Details on the formulation of this inhibition and the temperature dependency are given in section 6.2.2. The oxygen consumption flux is:

$$F_{ox,nit} = a_{ox,nit} \cdot F_{am,nit} \tag{7.5}$$

in which:

$a_{ox,nit}$ = quantity of oxygen consumed per quantity of ammonium oxidized (gO_2/gN)
$F_{ox,nit}$ = oxygen flux consumed in nitrification ($gO_2.m^{-3}.day^{-1}$)
$F_{am,nit}$ = nitrification flux ($gN.m^{-3}.day^{-1}$)

Two molecules of O_2 are required to oxidize one molecule of $NH4^+$ into a nitrate molecule. Stoichiometric constant $a_{ox,nit}$ is therefore equal to 4.57 gO_2/gN.

7.5 Reaeration

Reaeration is the exchange of oxygen between water and atmosphere. The reaeration flux is driven by the difference between the DO saturation concentration an the actual DO concentration:

$$F_{ox,rear} = k_{rear} \cdot (C_{ox,sat} - C_{ox}) \tag{7.6}$$

$$k_{rear} = k_{rear20} \cdot kt_{rear}^{(T-20)} \tag{7.7}$$

in which:

$F_{ox,rear}$ = reaeration flux ($g.m^{-3}.day^{-1}$)
C_{ox} = dissolved oxygen concentration ($gO_2.m^{-3}$)
$C_{ox,sat}$ = saturation dissolved oxygen concentration ($gO_2.m^{-3}$)
k_{rear} = reaeration rate constant (day^{-1})
k_{rear20} = reaeration rate constant at 20 °C (day^{-1})
kt_{rear} = reaeration temperature coefficient (-)
T = water temperature (°C)

Several formulations are available to calculate the rate constant in delwaq. In GEM the formulation by Van Pagee (1978) and Delvigne (1980) is used, which relates the rate constant to stream velocity, wind velocity and water depth:

$$k_{rear} = (0.065\, v_{wind}^2 + 3.86\, (v_{stream}/h)^{0.5}) / h \tag{7.8}$$

in which:

v_{wind} = windspeed (m.sec^{-1})
v_{stream} = stream velocity (m.sec^{-1})
h = water depth (m)

The saturation concentration of oxygen is computed as a function of water temperature and chlorinity, according to Weiss (1970):

$$C_{sat,oxy} = (14.7 - 0.41\, T + 0.089\, T^2 - 0.043\, T^3).\, (1 - 10^{-5}\, C_{Cl}) \tag{7.9}$$

in which:

C_{Cl} = chloride concentration (gCl.m^{-3})

7.6 Vertical dispersion

Dissolved oxygen disperse along vertical concentration gradients into the sediment, due to microbial decomposition of organic matter accumulated in sediment. The formulation of dispersion of oxygen is similar to those of nutrients. Both molecular diffusion and bio-irrigation are considered. See for details on the temperature dependency and the mixing distance section 6.2.6.

The dispersion flux is:

$$F_{ox,dis} = p_{ij}.\, (D_{oxm} + D_{ir}).\, (C_{oxj} - C_{oxi}) / (L_{ij}.\, L_i) \tag{7.10}$$

in which:

C_{oxi} = dissolved oxygen concentration in layer i (gO$_2$.m^{-3})
C_{oxj} = dissolved oxygen concentration in adjacent layer j (gO$_2$.m^{-3})
D_{oxm} = molecular diffusion of oxygen in water °C (m^2.day)
D_{ir} = bio-irrigation dispersion coefficient (m^2.day)
$F_{ox,dis}$ = vertical dispersion flux (gO$_2$.m^{-3}.day^{-1})
L_i = thickness of layer i (m)
L_j = thickness of adjacent layer j (m)
L_{ij} = mixing distance for layers i and j (m)
p_{ij} = smallest porosity of adjacent layers i and j (-)

8 Process formulations for suspended sediment

8.1 Starting points and coherence

The sedimentation and erosion patterns of sediments in estuaries are often a complex function of hydrodynamics, sediment loadings and biological and anthropogenic factors. Besides cohesive sediment (mud) also non-cohesive sediment (sand) is important. Thus, modelling of the morphology of estuaries is complex.

However, the focus of GEM is on primary production and consumption. Prediction of morphological changes is not a target, so suspended sediment in GEM is only considered as a carrier for nutrients and as a light adsorbing substance (see chapter 6). Relatively simple model formulations were chosen to serve this purpose. Figure 8.1 depicts the main processes.

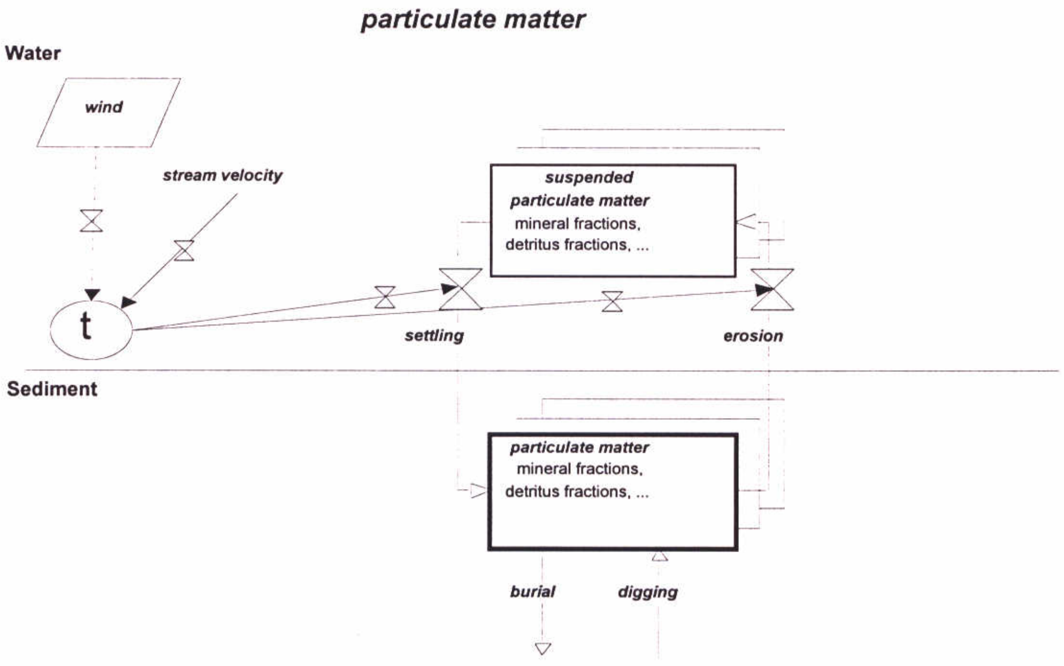

Figure 8.1 Processes for suspended matter.

The processes simulated in GEM for (suspended) sediment are settling, resuspension, accretion and erosion. The latter are the result of settling or resuspension and relate to the sediment layers. They are used to bury or dig up nutrients and organic matter (see chapter 6). Consequently, the net process fluxes in the respectively the water column and a sediment layer are:

$$F_{ss,npf} = - F_{ss,set} + F_{ss,res} \qquad (8.1)$$

$$F_{ss,npf} = + F_{ss,ac} - F_{ss,er}$$

The bottom shear stress (τ) controls the settling and resuspension fluxes. It depends on the flow velocity, wave action and the bottom roughness. It may be calculated by GEM, or be provided as an output parameter of a hydrodynamical model.

In the formulations several factors are not taken into account, such as the occurrence of a sand fraction in the sediment, fluid mud transport and biological influences (such as enhanced net sedimentation by filter feeders). The effect of flocculation is parameterized in a salinity dependent correction factor of the settling rate.

In GEM sediment layers may be simulated in two ways. Layers may be fixed and have a constant sediment quantity. In the second option, layers may also be expanded to a maximal thickness or be depleted. The fluxes of sediment accretion and erosion are used to this end. After depletion of the top layer, the next layer may be eroded. The effects of consolidation are ignored as such in the formulations. However, different values of the critical shear stress may be used for the sediment layers in order to account for differences in sediment cohesion.

8.2 Settling

Settling of suspended sediment is basically a first order process. The rate is a function of the shear stress (τ) at the sediment-water interface. Above the critical shear stress for settling ($\tau_{cr,s}$) no settling occurs, at values below $\tau c_{ss,set}$ the settling rate is a function of τ, according to the formulation of Krone (1962):

$$F_{ss,set} = (1/H) . (1 - \tau/\tau_{cr,s}) . (v0_{ss,set} + v1_{ss,set} . C_{ss}) \qquad \text{if } \tau \leq \tau c_{ss,set} \qquad (8.2)$$

$$F_{ss,set} = 0.0 \qquad \text{if } \tau > \tau c_{ss,set}$$

in which:

$F_{ss,set}$ = settling flux (gDW.m^{-3}.day^{-1})

C_{ss} = suspended sediment concentration (gDW.m^{-3})

H = water depth (m)

τ = shear stress at the sediment-water interface (Pa)

$\tau c_{ss,set}$ = critical shear stress for settling (Pa)

$v1_{ss,set}$ = settling velocity of suspended sediment (m.day^{-1})

$v0_{ss,set}$ = zeroth-order settling flux (gDW.m^{-2}.day^{-1})

The settling velocity depends on chlorinity ($\approx$ 0.5 salinity), temperature and on a flocculation function:

$$v1_{ss,set} = f_{cl,set} . v_{ss,set20} . vt_{ss,set}^{(T-20)} \qquad (8.3)$$

$$f_{cl,set} = f_{ss,floc} . (b_{cl,set} + 1)/2 - ((b_{cl,set} - 1)/2) . \cos(\pi . C_{cl}/Cm_{cl})) \qquad (8.4)$$

$$f_{cl,set} = f_{ss,floc} \cdot b_{cl,set} \qquad \text{if } C_{cl} > Cm_{cl}$$

$$f_{ss,floc} = (C_{ss}/Cc_{ss})^n \tag{8.5}$$

in which:

$b_{cl,set}$ = settling enhancement factor for chlorinity (of $v0_{ss,set}$ at $C_{cl} = Cm_{cl}$) (-)
$f_{ss,set}$ = function for settling enhancement by flocculation (-)
$f_{ss,floc}$ = function for the concentration effect on flocculation (-)
Cc_{ss} = critical concentration of suspended sediment for flocculation ($g.m^{-3}$)
C_{cl} = chloride concentration ($g.m^{-3}$)
Cm_{cl} = critical chloride concentration at which $f_{ss,set}$ is at its maximum ($g.m^{-3}$)
n = coefficient of flocculation function (-)
T = water temperature (°C)
$v1_{ss,set20}$ = fresh water settling velocity of suspended sediment at 20 °C ($m.day^{-1}$)
$vt_{ss,set}$ = temperature coefficient for settling (-)

In stead of using simulated chloride concentrations, the user may provide salinity in the input to overrule this. Internally, GEM converts chlorinity into salinity and vice versa.

8.3 Resuspension

Resuspension of sediment is basically a zeroth order process with respect to the concentration of particulate matter in the sediment. Like settling, the process depends on the shear stress at the sediment-water interface. Below a critical shear stress no resuspension occurs, above the critical value the resuspension flux depends on τ, according to the formulation of Partheniades (1962). The resuspension flux into the water column is described with:

$$F_{ss,res} = (\tau/\tau c_{ss,res} - 1).\,(k0_{ss,res} + (k1_{ss,res} \cdot C'_{ss,sed} \cdot H))/\,H \qquad \text{if } \tau \geq \tau c_{ss,res} \tag{8.6}$$

$$F_{ss,res} = 0 \qquad \text{if } \tau < \tau c_{ss,res}$$

in which:

$C'_{ss,sed}$ = concentration of sediment in the top sediment layer (g)
$F_{ss,res}$ = resuspension flux in the water column ($g.m^{-3}.day^{-1}$)
$k0_{ss,res}$ = zeroth order resuspension flux ($g.m^{-2}.day^{-1}$)
$k1_{ss,res}$ = first order resuspension rate constant ($1.day^{-1}$)
$\tau c_{ss,res}$ = critical shear stress for resuspension (Pa)

Notice that the water depth h is replaced by the thickness L of the top sediment layer, when the resuspension flux relates to this layer.

The first order resuspension rate is usually set to zero. Moreover, when several sediment layers are distinguished, different values for $\tau c_{ss,res}$ and $k0_{ss,res}$ can be provided to GEM for each of the layer.

8.4 Accretion and erosion

The accretion and erosion fluxes are derived from the settling and resuspension fluxes as follows in case of fixed sediment layers:

$$F_{ss,ac} = F_{ss,set} \tag{8.7}$$

$$F_{ss,er} = F_{ss,res} \tag{8.8}$$

in which:

$F_{ss,ac}$ = sediment accretion flux (gDW.m^{-3}.day^{-1})

$F_{ss,er}$ = sediment erosion flux (gDW.m^{-3}.day^{-1})

The accretion flux passes the interfaces of sediment layers in downward direction, the erosion flux passes the interfaces in upward direction.

When sediment layers may shrink until depletion or expand to a maximal thickness, the fluxes are formulated as follows:

for the top layer:

$$F_{ss,ac} = F_{ss,set} \tag{8.7a}$$

$$F_{ss,er} = F_{ss,res} \tag{8.8a}$$

for other layers:

$$F_{ss,ac} = F_{ss,set} \quad \text{if } L = Lm \tag{8.7b}$$

$$F_{ss,ac} = 0.0 \quad \text{if } L < Lm$$

$$F_{ss,er} = F_{ss,res} \quad \text{if } L = 0.0 \tag{8.7b}$$

$$F_{ss,er} = 0.0 \quad \text{if } L > 0.0$$

in which:

L = thickness of the overlying sediment layer (m)

9 Numerical algorithms

9.1 Interfacing BLOOM II with DELWAQ

BLOOM II is used in combination with DELWAQ a transportmodel based on differential equations. Integration of BLOOM II in such an environment is not trivial, however. This is because BLOOM is not a differential equation model, but an optimization model: BLOOM computes concentrations rather than derivatives and it allows changes, which are not possible in differential equation models. A derivative can be calculated rather easily, however. For example for each phytoplankton type k we take:

$$\frac{x_{k,t+\Delta t} - x_{k,t}}{\Delta t} \tag{9.1}$$

in which:

$x_{k,t+\Delta t}$	=	biomass of type k at the end of interval Δt	($gdry.m^{-3}$)
$x_{k,t}$	=	biomass of type k at the beginning of interval Δt	($gdry.m^{-3}$)
Δt	=	time interval	(day)

A similar procedure is adopted to compute other contributions to derivatives for example the uptake of dissolved nutrients.

The Linear Programming algorithm adopted in BLOOM II by itself can never generate negative numbers. However, without special precautions the resulting concentrations of phytoplankton types could become negative. Suppose all biomass of a particular species is present in the form of the energy type. Since there is a positive amount, DELWAQ (or any other interfacing program) will therefore determine that a positive amount will be subjected to processes not considered by BLOOM II notably transport. Suppose BLOOM decides it wants to reallocate **all** biomass of the energy type to the nitrogen type. So the biomass of the energy type will be 0 at Δt and the derivative due to processes considered by BLOOM is $-x_{k,t} / \Delta t$. This means that the **total** derivative due to phytoplankton processes and transport is $(-x_{k,t}$ - transport) / Δt which will result in a negative concentration at Δt. Notice that a reduction of the time-step reduces the possibility of this phenomenon, but it can never eliminate it under all possible conditions!

To solve this integration problem the 'fractional step' method is adopted which solves the equations for transport and processes not simultaneously but one after the other: transport acts upon **updated** concentrations and so if BLOOM wipes out a particular type, the concentration is put to zero before transport is computed hence there can be no transport. We will not go into further details here on the validity of this method, which is, however, a prerequisite for any model interfacing with BLOOM II.

9.2 GEMSED

The method for calculation of the profiles given in section 6.5 aims to estimate more precisely the vertical profiles of the nutrients. In doing so, the fluxes at the sediment water interface of ammonium, nitrate and phosphate can be calculated more accurately. This estimation is repeated every time step, based on the nutrient contents and boundary conditions for the benthic nutrient model GEMSED. For this estimation numerical techniques to solve a set of linear equations are used (matrix inversion). This fairly complicated way of calculation cannot lead to a numerical deficiency with respect to mass balance, because the estimated profiles are only used indirectly. Fluxes are derived from the concentration profiles (fluxes at the sediment-water water interface, nitrification and denitrification) to calculate the total rate of change of the state variables in GEMSED. These rates are given back to GEM/DELWAQ for integration.

9.3 SWITCH

The mass balances given in section 6.6 are given in the form of differential equations. Within SWITCH these equations are solved numerically with an algorithm that:

- discretises vertical distance according to explicit finite differences; and
- integrates over time according to a fractional step method.

The algorithm uses a maximal allowable timestep for SWITCH, which is evaluated each timestep of GEM-DELWAQ. A criterion for the maximal timestep mt was found in the maximal change of mass in a layer during a timestep, at which stability is maintained. The number of SWITCH-loops n taken every DELWAQ-timestep _t is equal to _t/mt. Generally, n is small when the layers are relatively thick and the concentration gradients are relatively weak. This happens in the winter half year. Computation on the basis of a variable optimal value of n in stead of a fixed value turned out to be very efficient in saving computer time.

A complication in the algorithm arises from the variability of the thickness of the layers d_1, d_2 and d_3. Violation of the mass conservation law will occur, if no corrective steps are taken to account for the change of layer thickness in the concentrations. In order to maintain mass conservation in the aerobic and oxidized layers, the following correction is carried out for the dissolved concentrations at the beginning of a timestep:

$$C = C' . d'/d \qquad (9.2)$$

The quote indicates the values from the previous timestep. Corrections like these are small, when the appropriate timestep is chosen.

This procedure is not applicable to inorganic phosphate, as the particulate phosphate quantity is simply too large. The artificial vertical mixing that arises from the procedure would be unacceptably strong. In stead, the phosphate concentrations are corrected by redistribution of phosphate among the layers, which involves adding and subtracting of the quantities present in the increments of the layers.

10 Pilot Application GEM: the Western Scheldt

10.1 Introduction

The objective of the pilot application was to get a first impression of the performance of the GEM formulations and to show that a technically working model can be built with the current version of GEM. For this first application the Western Scheldt has been selected. An extensively calibrated and validated DELWAQ-based model (SAWES) was available for this estuary. Hence, model input such as physical schematization, boundary concentrations and waste loads could be taken from the SAWES model. This enabled a rapid model set up of GEM-Western Scheldt, by incorporating the GEM substances, processes and process parameters in the SAWES modelling system. As the extensive calibration of GEM-Western Scheldt will be performed in a follow-up study, the current simulations should be regarded as tentative results.

10.2 Brief description of model set up

The SAWES (System Analysis of WEStern Scheldt) model was initiated in 1989 by the Dutch Ministry of Transportation and Public Works and DELFT HYDRAULICS, and was further developed in the LIFE Western Scheldt project, commissioned by the LIFE programme of the EC. The model is described in detail in DELFT HYDRAULICS, 1995c. A brief overview of the main features of the model is given below.

Physical schematization, hydrodynamics, sediment and simulation year

The SAWES model has been calibrated on data for 1987 and 1991 The model was verified with data for 1992. For the GEM application, 1987 is chosen as simulation year.

The schematization of the water quality model consists of 14 longitudinal segments, with additional 7 segments for the adjacent coastal zone (Figure 10.1). The water quality model uses output from a hydrodynamics and a mud transport model, which is based upon a spatial grid of 800 elements.

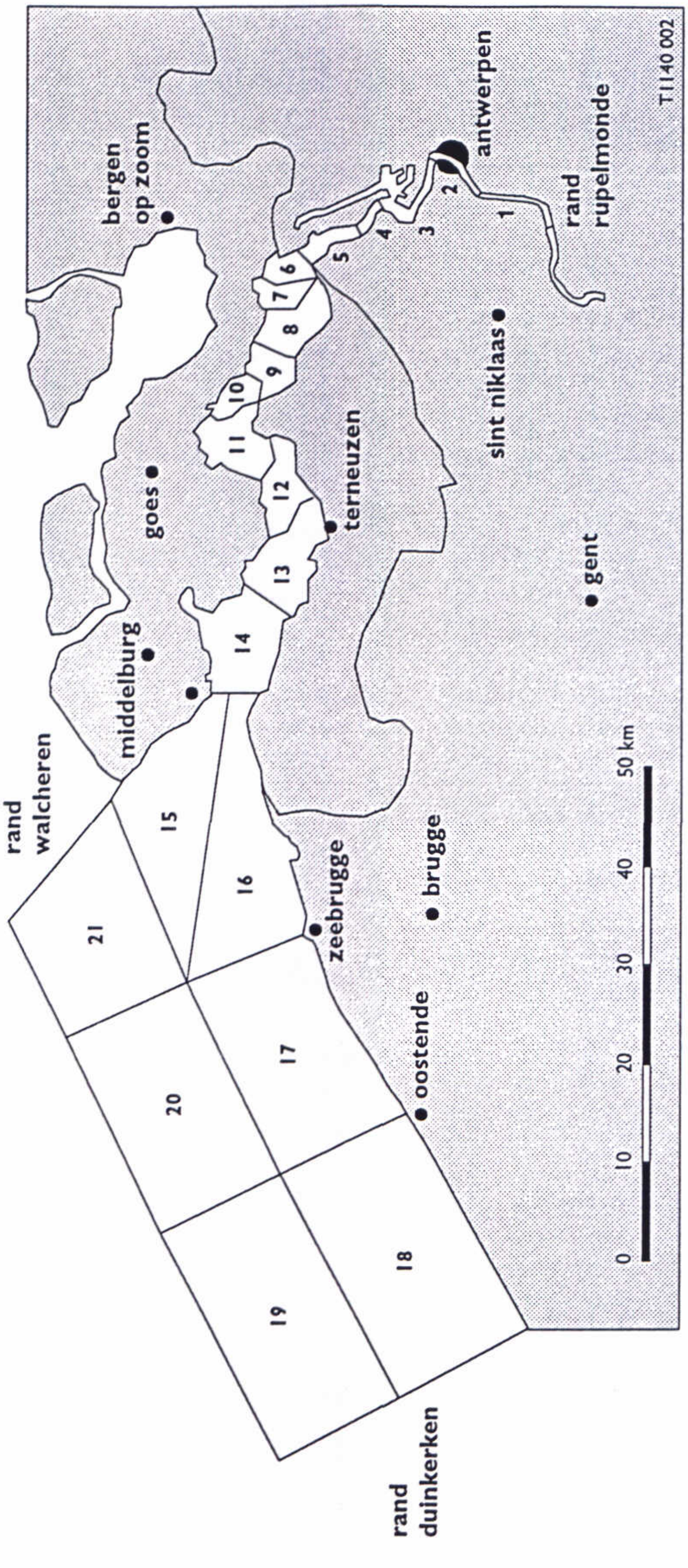

Figure 10.1 Spatial schematization of Western Scheldt (from Van Gils and Ouboter, 1995)

Waste loads, boundary conditions and forcing

The water quality model is an application of the general DELWAQ modelling framework. The waste loads are quantified with DELFT HYDRAULICS' Waste Load Model (WLM) (DELFT HYDRAULICS, 1995d), the boundary concentrations at the upstream and downstream boundaries of the estuary were derived from monitoring data (the SAWES project database, see also DELFT HYDRAULICS, 1995c). The SAWES light and temperature curves were applied.

Processes and parameters

The GEM model formulations were implemented by replacing the SAWES process library of DELWAQ by the GEM library, and by adapting the DELWAQ input files. The latter comprised the introduction of the GEM-specific substances and process parameters (see previous chapters) and the adaptation of boundary conditions and waste loads. The Monod-type phytoplankton module was used. Sediment-water interaction has not been included in the model.

10.3 Evaluation of model functioning

In the Western Scheldt application of the pilot GEM the Monod type phytoplankton module was used. This module includes some highly innovative formulations. It describes algal photosynsthesis in response to light intensity as a dynamic process and describes the additive effect of multiple nutrient limitation. These formulations are closely interrelated. For instance the gross primary production rate depends on the chlorophyll content (eq. 3.2.5), the chlorophyll content depends on the light limitation function (eq. 3.2.5) and the light limitation function depends on the gross primary production rate (eq. 3.2.12), thus making the circle round. Regarding the complexity of the formulations and the analysis of the first GEM simulations with default parameter settings it is concluded that much work has to be done to realize a calibrated and validated GEM application of the Western Scheldt. At the current stage the GEM-Western Scheldt must be regarded as tested and technically working.

10.4 Evaluation of the development procedure of GEM

The procedure aimed at making the formulations of GEM as generic as possible. Generic means with respect to GEM that:

- all relevant, available knowledge is taken into account in the formulations;
- a choice can be made from several formulations (alternatives, simplifications) in order to tailor the model to a specific case or ecosystem according to the insights of the modeler; and
- the model can be modified and extended in a simple way (modular structure).

To develop GEM a procedure was chosen, in which all Dutch institutes professionally involved in estuarine research contributed their expertise. Two workshops in an early stage of the development of GEM lead to the definition of functionality, the determination of starting points and design criteria, the selection of alternatives for certain process modules and the establishment of a task division with respect to model formulation. Before the actual model implementation took place, a full description of the formulations was realised.

This procedure would have to induce broad acceptance of GEM as an estuarine ecological model to support management and research. Now the first version of GEM has been made available, the following remarks can be made:

- GEM has been formulated with active contribution and consent of all institutes involved.
- The contributions of the institutes focused on those parts of science concerning aquatic ecological modelling, in which they have extensive expertise.
- These conditions in particular cause GEM to be well deliberated, broadly applicable and yet highly detailed in nature.
- Extensions and improvements are possible, but the opinions of the scientists involved largely coincide on what is needed.
- The pilot-GEM meets the above demands to a very high degree within the limitations imposed.
- The overall project is well manageable because the development procedure is systematic.
- The development of GEM is characterized by a strict division between formulation and documentation of the model and the actual implementation. This approach proved to be very efficient.

It may therefore be concluded that the procedure has been effective with respect to its goals. Next to this, the procedure stimulated the exchange of knowledge and expertise in the field of aquatic ecology among the institutes involved, thus creating new opportunities for co-operation.

11 Literature

Baretta, J., and P. Ruardij (eds), 1988.
Tidal flat estuaries.
Springer Verlag (Berlin) Ecological Studies 74, 353 pp.

Beon, 1994.
Comparison of model describing species composition of marine phytoplankton.

Berner, R.A., 1974.
Kinetic models for the early diagenesis of nitrogen, sulphur, phosphorus and silicon in anoxic marine sediments.
In: E.D. Goldberg (ed.), The Sea: Marine Chemistry, Vol. 5, John Wiley & Sons, New York, pp. 427-450.

Bouldin, D.R., 1968.
Models for describing the diffusion of oxygen and other mobile constituents across the mud-water interface.
J. Ecol. 56: 77-450.

Brinkman, A.G., 1993.
Estimation of length and weight growth parameters in populations with a discrete reproduction characteristic.
Institute for Forestry and Nature, Research report 93/6.

Brinkman, A.G., and W. van Raaphorst, 1986.
De fosfaathuishouding van het Veluwemeer (in Dutch).
Thesis, Twente University, The Netherlands.

Colijn, F., 1983.
Primary production in the Ems-Dollard Estuary.
Ph. D. Thesis, University of Groningen.

Danzig, G.B., 1963.
Linear programming and extentions.
Princeton University Press, Princeton, N.J.

DELFT HYDAULICS / WL, 1996a.
DELFT3D-flow, User Manual (version 0.1), release 2.48.

DELFT HYDRAULICS / WL, 1996b.
DIDO coupling program (version 3.2), User Manual, release 3.2.

DELFT HYDRAULICS / WL, 1995a.
Generiek Estuarium Model (GEM). Aanzet voor het functioneel ontwerp.
Rapport onderzoek T1058, March 1995 (in Dutch; RIKZ, NIOO-CEMO, IBN-DLO, NIOZ and WL).

DELFT HYDRAULICS / WL, 1995b.
Generiek Estuarium Model (GEM). Fase 2: Technisch Ontwerp.
Discussiedocument T1058, November 1995 (in Dutch; J.G.C. Smits, J.A. van Pagee, F.J. Los and P.M.A. Boderie).

DELFT HYDRAULICS, 1995d
Decision Support System for the management of water quality in the Scheldt Estuary and the adjacent coastal zone. Volume E: waste load model.
DELFT HYDRAULICS, report T1140.

DELFT HYDRAULICS / WL, 1995c.
Decision Support System for the management of water quality in the Scheldt Estuary and the adjacent coastal zone. Volume F: Water quality model.
Research report T1140 (J.A.G. van Gils and M.R.L. Ouboter).

DELFT HYDRAULICS / WL, 1995c.
DELWAQ 4.0. User's Manual.

DELFT HYDRAULICS / WL, 1995d.
DELWAQ 4.0. Technical Reference Manual.

DELFT HYDRAULICS / WL, 1994a.
Switch, a model for sediment-water exchange of nutrients; Part 3: Reformulation and recalibration for Lake Veluwe.
Research report T584. J.G.C. Smits.

DELFT HYDRAULICS / WL, 1994b.
Fosfaat mineralen in waterbodems: Literatuur studie en analyse van veldgegevens (in Dutch).
Research report T584. N.M. de Rooij and J.J.G. Zwolsman.

DELFT HYDRAULICS / WL, 1992.
Proces formuleringen DBS (in Dutch).
Documentatie rapport T542.

DELFT HYDRAULICS / WL, 1992.
Process formulations DBS (in Dutch)
Documentation report T542.

DELFT HYDRAULICS / WL, 1991a.
Switch, a model for sediment-water exchange of nutrients; Part 1: Formulation; Part 2: Calibration/Application for Lake Veluwe.
Research report T542/T584. J.G.C. Smits.

DELFT HYDRAULICS / WL, 1991b.
HADES; Ontwikkeling en verkennende berekeningen (in Dutch).
Research report T584, N.M. de Rooij.

DELFT HYDRAULICS / WL, 1988.
GREWAQ: an ecological model for Lake Grevelingen.
Documentation report T0215-03, Delft.

Delvigne, G.A.L., 1980
Natuurlijke beluchting van open water.
Verslag literatuuronderzoek R1149. Waterloopkundig Laboratorium (in Dutch).

Dienst Getijdewateren, 1993.
The impact of marine eutrophication on phytoplankton and benthic suspension feeders: results of a mesocosm pilot study.
Report DGW-93.039, NIOO/CEMO-654.

Droop, M.R., 1973.
Some thoughts on nutrient limitation in algae.
Journal of Phycology 9:264-272.

Eilers, P. & J.H.C. Peeters, 1988.
A model for the relationship between light intensity and the rate of photosynthesis in phytoplankton.
Ecological Modelling 42: 185-198.

Kamp-Nielsen, L., 1975.
A kinetic approach to the aerobic sediment-water exchange of phosphorus in Lake Esrom.
Ecol. Modelling 1: 153-160.

Klepper, O., M.W.M. van der Tol, H. Scholten and P.M.J. Herman, 1994.
SMOES: a simulation model for the Oosterschelde ecosystem. Part I: Description and uncertainty analysis.
Hydrobiologia 282/283: 437-451.

Krone, R.B., 1962.
Flume studies of the transport of sediment in estuarine shoaling processes.
Final Report, University of California, Hydraulic engineering and sanitary engineering laboratory, Berkeley (Cal), USA.

Kühl, M. and B.B. Jørgensen, 1994
The light field of microbenthic communities: radiance distribution and microscale optics of sandy coastal sediments.
Limnology and Oceanography 39: 1368-1398.

Kühl, M., C. Lassen and B.B. Jørgensen, 1994.
Light penetration and light intensity in sandy marine sediments measured with irradiance and scalar irradiance fiber-optic microprobes.
Marine Ecology Progress Series 105: 139-148.

Lampert, W., and U. Sommer, 1993.
Limno-oekologie.
Georg Thieme Verlag Stuttgart. 439 pp.

Lijklema, L., 1980.
Interaction of ortho-phosphate with iron(III) and aluminum hydroxides.
Envir. Sci. Technol. 14: pp. 537-541.

Los, F.J., 1991.
Mathematical simulation of algae blooms by the model BLOOM II. Version 2.
WL rapport T68.

Luning, K., 1981.
Light.
In: C.S. Lobban & M.J. Wynne. The biology of seaweeds. Botanical Monographs 17: 326-355.
Blackwell Scientific Publ., Oxford.

MacIntyre, H.L., and J.J. Cullen, 1995
Fine-scale vertical resolution of chlorophyll and photosynthetic parameters in shallow-water benthos.
Marine Ecology Progress Series 122: 227-237.

McCarthy, J.J., W.R. Taylor and J.L. Taft, 1977.
Nitrogenous nutrition of the plankton in the Chesapeake Bay. 1. Nutrient availability and phytoplankton preferences.
Limnology Oceanography 22: 996-1011.

NIOO/CEMO, 1993.
moses: Model of the Scheldt Estuary.
NIOO/CEMO. Yerseke.

O'Neill, R.V., D.L. DeAngelis, J.J. Pastor, B.J. Jackson and W.M. Post, 1989.
Multiple nutrient limitations in ecological models.
Ecological Modelling 46: 147-163.

Partheniades, E., 1962.
A study of erosion and deposition of cohesive soils in salt water.
PhD thesis, University of California (USA).

Pagee, J.A. van, 1978.
Natuurlijke beluchting van open water ten gevolge van wind.
Verslag onderzoek R1318-II. Waterloopkundig Laboratorium (in Dutch).

Pfeiffer, K. 1995.
Hydrographic measurements and numerical modelling.
Contributions compiled and issued by ZMK, University of Hamburg.
Unpublished MATURE report.

RIKZ, 1996.
User's guide WAQUA (version 8.21)
SIMONA rapport 92-10

RIKZ, 1993.
Generieke Ecologische Stofstroommodellering voor Estuaria; Programma van Eisen.
Werkdocument GWAO-93.151x (in Dutch; M.W.M. van der Tol and I. de Vries).

Schink, D.R., and N.L. Guinasso, 1978.
Effects of bioturbation on sediment seawater interaction.
Mar. Geology 23: 133-154.

Scholten, H. and M.W.M. van der Tol, 1994.
SMOES: a simulation model for the Oosterschelde ecosystem. Part II: Calibration and validation.
Hydrobiologia 282/283: 453-474.

Schnitzer, M., and S.U. Khan, 1972.
Humic substances in the environment.
Marcel Dekker, Inc. New York. 322 pp.

Schnitzer, M., and S.U. Khan, 1978.
Soil organic matter.
Elsevier Sci. Publ. Comp., Amsterdam.

Smits, J.G.C., and D.T. van der Molen, 1993.
Application of SWITCH, a model for sediment-water exchange of nutrients, to Lake Veluwe in the Netherlands.
Hydrobiologia 253: 281-300.

Steele, J.H., 1962.
Environmental control of photosynthesis in the sea.
Limnology Oceanography 7: 137-150.

Szeics, G., 1974.
Field measurements of energy in the 0.4 - 0.7 micron range II.
In: Light as an Ecological Factor. Brit. Ecol. Soc. Symp. No 16: 513-520. Blackwell Scientific Publ.

Santschi, P., P. Höhener, G. Benoit, and M. Buchholtz-ten Brink, 1990.
Chemical processes at the sediment water-interface.
Mar. Chem. 30: 269-315.

Vanderborght, J.P., R. Wollast and G. Billen, 1977a.
Kinetic models of diagenesis in disturbed sediments: PartI. Mass transfer properties and silica diagenesis. Limnol. Oceanogr. 22: 787-793.

Vanderborght, J.P., R. Wollast & G. Billen, 1977b.
Kinetic models of diagenesis in disturbed sediments, Part II; Nitrogen diagenesis.
Limnol. Oceanogr. 22: 794-803.

Van Raaphorst, W., P. Ruardij and A.G. Brinkman, 1988.
The assessment of benthic phosphorus regeneration in an estuarine ecosystem model. In: The Ecosystem of the Western Wadden Sea: Field Research and Mathematical modelling.
Netherlands Institute for Sea Research, Texel, pp. 23-36.

Webb, W.L., M. Newton and D. Starr, 1974.
Carbon dioxide exchange of Alnus rubra: a mathematical model.
Oecologia 17: 281-291.